

AN ATLAS OF THE CHOROICAL
ULTRASTRUCTURE WITH THE
HISTOCHEMICAL LOCALIZATION OF
CHOROICAL AND PSEUDOBANCHIAL
CARBONIC ANHYDRASE ACTIVITY
IN THE RAINBOW TROUT
(SALMO GAIRDNERI)

Thesis for the Degree of M. S.
MICHIGAN STATE UNIVERSITY
GRAIG E. ELDRED
1975

LIBRARY
Michigan State
University

BINDING BY
HOAG & SONS
BOOK BINDERY INC.
LIBRARY BINDERS
EAST LANSING, MICHIGAN

ABSTRACT

AN ATLAS OF THE CHOROIDAL ULTRASTRUCTURE
WITH THE HISTOCHEMICAL LOCALIZATION
OF CHOROIDAL AND PSEUDOBANCHIAL
CARBONIC ANHYDRASE ACTIVITY
IN THE RAINBOW TROUT
(SALMO GAIRDNERI)

By

Graig E. Eldred

A specific site of carbonic anhydrase activity within the efferent vessels of the choroidal rete mirabile had been speculated for the prevention of short-circuiting of the oxygen multiplication mechanism by the diffusion of carbon dioxide from the efferent to afferent retial vessels. It had further been speculated that the pseudobranch may secrete carbonic anhydrase for use at this site. With the development of a specific histochemical method for demonstration of carbonic anhydrase at an electron microscopic level, the localization of specific sites of carbonic anhydrase activity within the choroidal vasculature and pseudobranch of the rainbow trout, Salmo gairdneri, became feasible.

An atlas of choroidal vascular pattern and ultrastructure has been compiled and presented in Part I. In working with vascular tissues, particularly in fishes, special precautions must be taken in order to avoid clot formation. Specific examples from the existing literature in which this had been neglected are cited, and the importance of the tissue preparatory technique upon the appearance of

the ultrastructure is stressed.

The existence of a possible mechanism for the neural control of flow through the counter-current multiplier via the arterial manifold is identified.

The packing pattern of the retial vessels is cubic, such that there is an equal number of afferent and efferent vessels. At an ultrastructural level, the endothelial cells of the afferent and efferent retial vessels are structurally practically identical, yet the afferent vessels are clearly distinguishable as having associated pericytes, a distinct basement membrane, and a smaller lumenal diameter. No structural differences could be detected distinguishing distribution from collection vessels. The choriocapillaris region has three distinguishing features: 1) the endothelium is relatively free of fenestrae, 2) Bruch's membrane lacks the complexity seen in higher vertebrates, and 3) the pigment epithelium lacks a highly involuted basal border.

Light and electron microscopic carbonic anhydrase histochemistry was pursued in Part II. Problems with visualization of the cobalt sulfide reaction product were encountered on the electron microscopic level, but not on the light microscopic level.

The normal ultrastructure of the pseudobranch-type cell was found to be similar to those investigated elsewhere. Conclusions are drawn regarding the possibility

Graig E. Eldred

that pseudobranchial secretion of carbonic anhydrase may occur for subsequent usage in the choroidal counter-current oxygen multiplier.

Carbonic anhydrase activity within the choroidal rete mirabile is found to increase in intensity along the length of the afferent retial vessels and is seen to extend for some distance into the peripheral distribution vessels. These sites of activity are consistent with a short-circuit model for oxygen multiplication.

AN ATLAS OF THE CHOROIDAL ULTRASTRUCTURE
WITH THE HISTOCHEMICAL LOCALIZATION
OF CHOROIDAL AND PSEUDOBRANCHIAL
CARBONIC ANHYDRASE ACTIVITY
IN THE RAINBOW TROUT
(SALMO GAIRDNERI)

By

Graig E. Eldred

A THESIS

Submitted to
Michigan State University
in partial fulfillment of the requirements
for the degree of

MASTER OF SCIENCE

Department of Physiology

1975

DEDICATION

To my parents who from the start provided
the environment which made 'the acquisition
of knowledge a desire, not a task'.....

To the Vosses whose generosity permitted me to begin
when I did.....

To Barbara whose chronic case of epistemophilia
provided her with the strength and competitive-
ness which forced me to do and achieve where I
may not have otherwise.....

To one yet to become whose beginnings spurred me on to
completion.....

And, to me.....Why not?

ACKNOWLEDGMENTS

I wish to reiterate my feelings of gratitude to all those persons whose insistent assistance has taught me the pitfalls of total self-reliance and the real value of cooperative help. Included are:

Professors J.R. Hoffert, P.O. Fromm, and R.P. Pittman who served as members of my committee.

Jerry Friedman for help in the darkroom with the development of all photographs herein.

Professor P.O. Fromm for his alert perusal of the literature which frequently led me to papers which would otherwise have escaped my attention, and for his modest words of encouragement regarding the true value of electron microscopy as a research tool.

Esther Brenke for the feat of reading red ink handwriting and translating it into legible type.

Professor J.R. Hoffert, first, for the task of reading and evaluating the original manuscript, and second, for the awesome task of labelling 366 prints by hand. I am sure that this latter accomplishment will never be forgotten, for he will most certainly and deservedly offer continual reminders of the fact that I am forever indebted to him.

Additional thanks go to Esther and Jack for their labors of sectioning and staining ocular tissues for light microscopy at a time when I was supposed to be in bed with

infectious mononucleosis, but was caught in the act of sewing lace on a blouse for my wife with a friend.

Finally, acknowledgements are due the National Institutes of Health, Grant EY-00009 VIS, and the Barbara Jo Hoppe Eldred Support Foundation for their continued financial assistance through the 2.5 years of this ordeal.

TABLE OF CONTENTS

	Page
LIST OF FIGURES	vii
GENERAL INTRODUCTION	1
PART I	
INTRODUCTION	5
LITERATURE REVIEW	8
General Vascular Patterns	8
Choroidal and Retial Ultrastructure	10
Swimbladder Rete	10
Choroidal Rete	13
Choriocapillaris	16
Ultrastructure Summary	18
MATERIALS AND METHODS	20
RESULTS	23
Light Microscopic Choroidal Morphology	23
Electron Microscopic Fixation Techniques	25
Electron Microscopic Choroidal Morphology	26
DISCUSSION	31
Vascular Artifacts	31
Choroidal Ultrastructure and Function	36
CONCLUSIONS	50
PART II	
INTRODUCTION	52
LITERATURE REVIEW	57
The Historical Elucidation of Retial Function	57
The Rete Mirabile as an Exchanger	59
The Rete Mirabile as a Multiplier	61
The Role of Carbonic Anhydrase	62
Carbonic Anhydrase Histochemistry	67

	Page
MATERIALS AND METHODS	69
RESULTS	72
Light Microscopic Carbonic Anhydrase	
Histochemistry	72
Choroidal Electron Microscopic Carbonic	
Anhydrase Histochemistry	73
Electron Microscopic Pseudobranch	
Morphology	76
Pseudobranch Carbonic Anhydrase	
Histochemistry	78
DISCUSSION	80
Interpretation of Carbonic Anhydrase	
Histochemistry	80
Choroidal Carbonic Anhydrase	83
Functional Implications	84
SUMMARY AND CONCLUSIONS	89
COMBINED SUMMARY AND CONCLUSIONS	91
Techniques Findings	91
Morphological Findings	92
Carbonic Anhydrase Histochemistry	94
RECOMMENDATIONS	95
LITERATURE CITED	99
APPENDIX	107

LIST OF FIGURES

FIGURE	Page
1. Microfil casts of the afferent vessels of the choroidal vasculature.	108
2. Generalized diagram of the choroidal vascular pattern within the eye of <u>Salmo gairdneri</u>	110
3. Choroid rete mirabile (hematoxylin and eosin, 145X).	112
4. Parallel rete vessels (Masson's trichrome, 1,480X).	114
5. Central side of the rete mirabile (hematoxylin and eosin, 145X).	116
6. Central side of the rete mirabile (hematoxylin and eosin, 440X).	118
7. Central side of the rete mirabile (Masson's trichrome, 295X).	120
8. Central side of the rete mirabile (Masson's trichrome, 145X).	122
9. Peripheral side of the rete mirabile (hematoxylin and eosin, 145X).	124
10. Vessels of the peripheral region (hematoxylin and eosin, 145X).	126
11. Peripheral collection and distribution vessels (hematoxylin and eosin, 440X).	128
12. Choroidal rete mirabile cross-section (methylene blue, 925X).	130
13. Standard immersion-fixed rete in cross-section (18,975X).	132
14. Standard immersion-fixed rete: Areas with myeloid configurations in the lumen.	134
15. Standard immersion-fixed rete: Area with thin-walled vacuoles within the lumen (10,240X).	136

LIST OF FIGURES--Continued	Page
16. Myelinated and non-myelinated neural elements within the arterial manifold wall (26,250X). . . .	138
17. Smooth muscle layer underlying the endothelial border of the arterial manifold wall (27,190X). .	140
18. Arterial manifold wall displaying an association between pinocytotic activity within the endothelium and smooth muscle (26,250X).	142
19. Heparinized, immersion-fixed choroidal rete mirabile in cross-section (8,400X).	144
20. Afferent retial vessel in cross-section (20,755X).	146
21. Afferent versus efferent rete endothelial ultrastructure (113,750X).	148
22. Vessels of the peripheral choroidal layer (methylene blue, 925X).	150
23. Peripheral choroidal vessel ultrastructure (14,175X).	152
24. Peripheral vessel wall (25,625X).	154
25. Choriocapillaris, Bruch's membrane, and pigment epithelium (13,840X).	156
26. Fenestrated choriocapillaris endothelium.	158
27. Bruch's membrane (41,405X).	160
28. Myeloid bodies within the pigment epithelium (16,560X).	162
29. Photoreceptor outer segment (20,755X).	164
30. Choroidal rete mirabile carbonic anhydrase stain.	166
31. Choroidal rete mirabile carbonic anhydrase stain (295X).	168
32. Peripheral region of the choroidal rete stained for carbonic anhydrase (145X).	170
33. Carbonic anhydrase activity within peripheral collection and distribution vessels (295X). . . .	172

LIST OF FIGURES--Continued	Page
34. Polarization of carbonic anhydrase activity within the choroidal rete vessels (65X).	174
35. General appearance of carbonic anhydrase stained tissues under the electron microscope (25,625X). .	176
36. Carbonic anhydrase activity within the choroidal rete endothelial cells (66,250X).	178
37. Choroid rete endothelial cell carbonic anhydrase activity as compared with erythrocyte carbonic anhydrase activity (102,500X).	180
38. Banding pattern of carbonic anhydrase activity within the choroid rete endothelial cell (102,500X).	182
39. A differential carbonic anhydrase activity in afferent versus efferent retial vessels (102,500X).	184
40. The "pseudobranch-type" or acidophilic cell (9,995X).	186
41. The mitochondrial-smooth endoplasmic reticulum network of the pseudobranch-type cell (25,625X). .	188
42. Basal border of the pseudobranch-type cell (82,000X).	190
43. Pseudobranch-type cell carbonic anhydrase histochemistry (32,030X).	192
44. Carbonic anhydrase stained pseudobranch-type cell basal border (102,500X).	194
45. "Titres flamboyants final": Carbonic anhydrase stained pseudobranch-type cell mitochondrial-endoplasmic reticulum network (66,250X).	196

GENERAL INTRODUCTION

Oxygen tensions at the retial-vitreous interface in teleost fishes are phenomenologically high (Wittenberg and Wittenberg, 1961; Wittenberg and Wittenberg, 1962). In the rainbow trout, Salmo gairdneri, oxygen tensions at this site reach 400 mm Hg which is ten to twenty times arterial levels (Fairbanks, Hoffert and Fromm, 1969). These tensions are established by the operation of a morphologically differentiated network of parallel vessels within the choroid layer of the teleost eye---the choroid rete mirabile. Fonner, Hoffert and Fromm (1973) have established that high oxygen tensions and hence the functional integrity of the retina, are dependent upon carbonic anhydrase. A "short-circuit" model has recently been proposed by Fairbanks, Hoffert and Fromm (1974) in which the counter-current exchanger of oxygen in this system relies upon a localized, highly active focus of carbonic anhydrase activity, presumably in the efferent side of the system. Its presence here, as distinct from the foci of activity present in the retina and red blood cells has yet to be demonstrated.

In most teleosts, the choroid rete mirabile receives oxygenated blood directly from the gills with only a small vestigial gill structure, the pseudobranch, interposed between them. The pseudobranch has exceptionally high levels of carbonic anhydrase activity (Leiner, 1938;

Maetz, 1956; Hoffert, 1966). The capillary network within the pseudobranch is surrounded by very morphologically distinct, "pseudobranch-type" cells (Harb and Copeland, 1969). In as much as the functional significance of the pseudobranch had eluded investigators for years, Copeland (1951) proposed that it may secrete carbonic anhydrase into the blood stream for use in the concentration of oxygen by the swimbladder rete mirabile and Fairbanks et al. (1969) also proposed the same function, this time with the choroid rete oxygen multiplier as an additional site of activity. Laurent and Rouzeau (1972) demonstrated the presence of baroreceptor elements and chemoreceptor elements in the pseudobranch; the chemoreceptors responding to oxygen tensions, pH, and sodium ion concentration of the blood. This neural receptor activity, however, accounts for neither the apparent secretory cellular specializations of the pseudobranch-type cell, nor the high levels of carbonic anhydrase activity reported. Thus, the hypothesis proposed by Fairbanks et al. (1969) remains a viable theory.

Hansson (1967) introduced a light microscopy technique for the histological staining of carbonic anhydrase activity utilizing a cobalt sulfide precipitate. Because cobalt sulfide is electron dense as well as light opaque, the technique has recently been improved and used at the electron microscopic level by Rosen and Musser (1972).

In the current study, through the use of this carbonic anhydrase histochemical technique, at both light and electron microscopic levels, two objectives are sought. First, the possible presence and precise locus of an efferent choroidal carbonic anhydrase activity will be studied in order to provide either supportive or contradictory evidence to the short-circuit model of Fairbanks et al. (1974). Secondly, the localization of carbonic anhydrase activity within the pseudobranch of Salmo gairdneri is attempted, in hopes of correlating its ultrastructural location with morphological evidence for secretory activity, and in so doing lend credence to the hypotheses of Fairbanks et al. (1969) and Copeland (1951).

In order to achieve these objectives, however, it is first necessary to precisely define the vascular patterns and morphological features which distinguish the structures of interest here. The pseudobranch ultrastructural morphology had previously been extensively described (Copeland and Dalton, 1959; Holliday and Parry, 1962; Harb and Copeland, 1969), so that it was merely necessary to reaffirm these findings in Salmo gairdneri. However, the choroid vascular morphology has not been extensively described in teleosts, particularly at an ultrastructural level. Copeland (1974a) and Wittenberg and Wittenberg (1974) have published studies in which gross vascular patterns in several teleost species and preliminary

observations on rete ultrastructure are described. The apparent interspecific variability in gross morphology and remaining paucity of definitive ultrastructural description deemed it necessary to catalogue an atlas of choroidal vascular ultrastructure before proceeding to the histochemical localization of carbonic anhydrase.

In Part I of this study, a description of the normal choroid vasculature in Salmo gairdneri is presented along with a comparative discussion of the functional significance of each vascular segment. Part II is concerned with the localization of carbonic anhydrase in the choroid and pseudobranch of this species.

It is hoped that a much clearer anatomical and functional understanding of the teleost choroidal vascular ultrastructure and an important extension of the evidence for the possible role of carbonic anhydrase in the choroidal oxygen counter-current exchanger will be gained through this study. Further, important problems and precautions in microvascular fixation procedures will be presented which have heretofore gone undefined, but which should be taken into consideration in future ultrastructural research on any vascular bed.

PART I

INTRODUCTION

The circulatory system is designed to supply the body tissues with blood in amounts commensurate with their metabolic requirements. To accomplish this most efficiently, the microvasculature of each tissue and organ must be specialized in 1) its microvascular geometry, 2) the spatial relationship between tissue cells and capillaries, and 3) the structural nature of the capillary endothelium.

Vertebrate retinal tissue has the highest rate of respiration of any tissue in the body comparable only to, and often exceeding, that of cancer tumor tissue and embryonic tissue (Noell, 1959). In keeping with the needs of this metabolic demand, the mammalian ocular tissue is supplied with two microvascular beds---one in the choroid, and one in the retina. Unlike the mammalian retina, however, the teleost retina is avascular. With the exception of the minor vascular contributions made by the lentiform body and the falciform process (Copeland, 1974b) the entire metabolic needs of the teleost retina must be met by the circulation of the choroidal layer.

In meeting these metabolic needs and in keeping with the notion that over-all tissue and organ function is fundamental to and a determinant of vascular architecture, the teleost choroidal vasculature has evolved into a structure---the choroid rete mirabile---capable of the counter-current

exchange of oxygen (Wittenberg and Wittenberg, 1962; Fairbanks, Hoffert and Fromm, 1974). A notable exception is seen in the eels, *Anguilloidei*, which lack the choroid rete (Wittenberg and Haedrich, 1974), but which are also unique among the teleosts in having vascular retinas (Francois and Neetens, 1974). Besides its role in oxygen concentration, the choroid rete has also been implicated in the counter-current exchange of heat (Linthicum and Carey, 1972). The possibility remains that passive diffusion of other substances across the endothelia of the exchange system may also occur. Wittenberg and Wittenberg (1974) suggest that diffusion of water may be important in the process of oxygen concentration. Also, the importance of carbonic anhydrase localized within this vascular bed has been demonstrated (Fairbanks et al., 1974).

Thus, it is essential to define the vascular architectural framework around and upon which these physical and physiological factors must operate. In reviewing the published evidence and in reporting the observations of the current study, emphasis will be placed upon morphological features classically considered to be indicative of: 1) diffusion pathways and transport processes, such as fenestrations, pinocytotic vesicles, and endothelial junctional areas, all of which may represent pathways for water soluble and macromolecular substances; 2) of barriers to such movement, such as basement membranes; and 3) of synthetic

activity, such as rough endoplasmic reticulum, polysomes, mitochondria, and Golgi complexes.

Several authors have published descriptions of the choroidal network in various teleostean species which have touched the surface of the problem. In the present study, an atlas of the light and electron microscopic structures of this vascular bed in Salmo gairdneri will be compiled. Then, the functional implications of these anatomical features will be discussed in light of evidence presented in the literature for other vertebrate systems. Finally, several important points of controversy with respect to fixation procedures have arisen and will be clarified.

LITERATURE REVIEW

An historical review of the elucidation of rete structure and physiology has been presented by Dorn (1961) and Wittenberg and Wittenberg (1974).

General Vascular Patterns

The choroidal rete morphology has been described on a gross structural basis for the cod, Gadus morhua; the bluefish, Pomatomus saltatrix; the bowfin, Amia calva; the swordfish, Xiphias gladius; and the tuna, Lampris regius (Wittenberg and Wittenberg, 1974); the rainbow trout, Salmo gairdneri (Barnett, 1951); and the killifish, Fundulus grandis (Copeland, 1974a).

According to descriptions thus far presented, a pattern of choroidal vascular flow emerges which is quite different from that seen in the human (Hogan, Alvarado and Weddell, 1971). Blood flows into the teleost choroidal vascular bed via the ophthalmic artery. The ophthalmic artery passes through the sclera along the optic nerve and then branches into a thick-walled arterial manifold which parallels the central margins of the horseshoe-shaped choroidal "gland". This arterial manifold lies within the lumen of a venous sinusoid. The arterial manifold bifurcates into parallel afferent vessels of the rete mirabile (Figure 1, p. 105). These vessels again converge into major "distribution" vessels which go peripherally to supply the choriocapillaris.

The choriocapillaris lies directly apposed to Bruch's membrane and the pigment epithelium and is the presumed site of nutrient and metabolite exchange for the retina. Efferent blood returns from the choriocapillaris via major "collection" vessels which again bifurcate into the efferent rete mirabile vessels running parallel to and interspersed among the afferent vessels in a species specific packing pattern. The blood is collected into the previously mentioned venous sinusoid feeding the ophthalmic vein which passes out of the eye along the optic nerve. Figure 2 illustrates this general pattern.

Superimposed upon this pattern is an array of species specific variations. The studies of Copeland (1974a) and Wittenberg and Wittenberg (1974) both demonstrate that the gross morphology of the choroid "gland" itself varies from a horse-shoe shape in most forms to an inverted "Y" seen in the killifish, Fundulus grandis. The killifish also presents a very interesting exchanger conformation (Copeland, 1974a). In F. grandis an intermediate collecting vessel carrying venous blood enters the choroid rete at midstream and bifurcates into an additional set of efferent rete vessels which are also interspersed among and parallel to the rest of the vessels on the central end of the rete. The rainbow trout pattern follows closely that general description presented above (Fairbanks, 1970; Barnett, 1951).

Choroidal and Retial Ultrastructure

In reviewing the choroidal and retial literature on ultrastructure each segment of the vascular bed described above will be considered sequentially. No information on the ultrastructure of the ophthalmic artery and arterial manifold has been located in the literature to date.

Most descriptions of rete mirabile ultrastructure have been performed with the purpose of finding characteristics capable of distinguishing afferent from efferent rete vessels. None of these studies, however, are conclusive enough to allow the definition of either vessel type in Salmo gairdneri.

Swimbladder Rete

One of the only other rete mirabile structures of capillary dimensions occurs in the swimbladder rete. Studies on this system are noteworthy in that the retia of these two organs are very similar in both function and gross structure. The vascular ultrastructure in the swimbladder rete has been studied in the toadfish, Opsanus tau, (Fawcett and Wittenberg, 1959; Wittenberg and Wittenberg, 1974); the perch, Perca fluviatilis; and the pond loach, Misgurnus fossilis (Jasinski and Kilarski, 1971); the eel, Anguilla vulgaris (Dorn, 1961); and in the whitefish, Coregonus lavaretus (Fahlén, 1967).

In the swimbladder rete of Opsanus tau, the afferent and efferent rete vessels are clearly distinguishable from

each other (Fawcett and Wittenberg, 1959; Fawcett, 1961). Afferent vessels possess a thick (2-4 μm) continuous endothelial lining. These cells display the overlapping or interdigitation of their margins that is typical of mammalian capillaries (Rhodin, 1967 & 1968). In Opsanus tau straight afferent endothelial cell boundaries have conspicuous desmosomes of varying sizes. Typically there is one large desmosome situated about midway along the boundary with two or more zonulae occludens above and below the principal desmosome (Fawcett, 1966). The afferent vessel endothelia possess an abundant supply of pinocytotic vesicles.

In contrast, the efferent vessels of the Opsanus tau swimbladder rete display a distinctive variation in wall thickness with thick nuclear areas (1-3 μm) alternating with extremely thin areas (10-70 nm). Within the attenuated portions of the endothelia, there are areas which resemble the diaphragmed fenestrae characteristically seen in the mammalian kidney, intestinal villi, and endocrine glands (Rhodin, 1974). Fawcett and Wittenberg (1959) point out, however, that in the efferent swimbladder rete vessels of Opsanus, actual pores not closed by a membranous diaphragm are rarely, if ever seen. The endothelial cells exhibit very little vesiculation of the cell membranes. Wittenberg and Wittenberg (1974) point out that both the afferent and efferent capillaries of the Opsanus swimbladder rete do not change in appearance throughout their length, either morphologically or in their packing pattern.

Jasinski and Kilarski (1971) reported that afferent and efferent vessels also display separate, distinctive morphologies in the swimbladder rete of the perch, Perca fluviatilis. Afferent rete vessels are apparently very similar to those described in Opsanus tau. They display exceptionally thick endothelia (4 μm) with a great abundance of smooth surfaced vesicles of an average diameter of 103 nm and no fenestrae. In the central prominence of each endothelial cell, an apparently full complement of typical cytoplasmic organelles (e.g., mitochondria, Golgi complexes) is present. The endothelial cell junctions do not overlap and have zonulae occludens and desmosomes. In contrast, the efferent rete vessels have relatively thinner walls showing attenuated areas containing both single pores and local thickenings. Smooth surfaced vesicles are present in large numbers in the cytoplasm. In addition, pericytes are associated with both categories of vessels and a basement membrane surrounds the pericytes and endothelia. Collagen fibers are reported in Perca to be seen occasionally passing through the homogeneous ground substance of the intravascular space.

The swimbladder of the pond loach, Misgurnus fossilis (Jasinski and Kilarski, 1971) is slightly different from those described in the perch and toadfish above. Afferent rete vessels in this species show two types of endothelial cells alternating around the vessel periphery. One is a flattened cell (0.5 μm thick) containing dark cytoplasm with

numerous smooth surfaced vesicles. The others are 1-1.5 μm thick showing light cytoplasm and a smaller number of smooth surfaced vesicles and also large, electron-lucent vesicles of irregular shape. Endothelial junctions in both vessels show not only zonulae occludens and desmosomes, but also marginal flaps which are arm-like extensions of the endothelia into the vessel lumen at the junctional border. The efferent rete vessels are like those previously described in Opsanus and Perca.

Choroidal Rete

Contrary to the description presented for the swimbladder rete ultrastructure the information presented on the ultrastructural details of the choroidal rete has definitely been lacking until only very recently, and the micrographs published may be indicative of the reason why more information has not been published.

Wittenberg and Wittenberg (1974) have published line sketches of electron micrographs provided to them by D.W. Fawcett at Harvard Medical School, of the choroidal rete mirabile in Amia calva, a holostean. This was an unfortunate choice in that Amia is a relatively primitive fish and cannot be considered as representative of the teleostean form. It may be used as an example, only if it is kept in mind that it may at most represent an example of convergent evolution. In contrast to the morphology of the swimbladder retia presented above, Wittenberg and Wittenberg (1974) point out

from their sketches that in the choroidal rete of Amia, the difference in thickness of the walls of afferent and efferent rete vessels is very slight. They state that this must mean that some intracellular process is more developed in the afferent swimbladder rete vessels than in the choroid rete endothelia. The sketch presented depicts the afferent vessels as being characteristically round in cross-section with four or five endothelial cells bordering the lumen. The endothelial cell junctions appear to show the marginal flap configuration. Surrounding the afferent endothelia are pericytes and enclosing this complex is a basement membrane. The efferent vessels are depicted as lacking pericytes and their basement membranes are apparently distinct from those of the afferent vessels. The most striking feature, however, is the fact that the lumen of the efferent vessel is not circular in cross-section, but sinusoidal in appearance. This feature had not previously been reported in the swimbladder rete conformation. Neither category of vessel is shown to possess fenestrae. Unfortunately, because only line sketches are presented, no further observations may be made regarding vesiculation, perivascular structure and other subcellular features.

Copeland (1974a) subsequently published the only actual micrographs of the rete ultrastructure in Fundulus grandis. He first presents the ultrastructure of a rete prepared by immersion in Karnovsky's fixative (Karnovsky, 1965).

The features seen in these sections are obviously unlike any other capillary endothelia reported elsewhere. The endothelia are distinctive in having very large "phagocytotic" vacuoles apparently having been formed by pseudopodia-like extensions of the endothelial wall into the lumen distinct from the marginal flaps at the endothelial cell junctions. There are also numerous smaller pinocytotic vesicles which would perhaps be more typical of what might be expected of capillary endothelia (Bruns and Palade, 1968a; 1968b), except that Copeland points out that these vesicles may be an extensive network of parallel microtubules based upon a longitudinal section through such a suspected area. Finally, the perivascular space seemed to be swollen and basement membranes were not seen surrounding pericyte and endothelial components.

In an attempt to obtain more typical photomicrographs, Copeland (1974a) then developed a perfusion technique which yielded what he deemed to be a more acceptable ultra-structural appearance. Here, as in the choroid rete of Amia, the efferent vessels in Fundulus are seen to be sinusoidal in nature, not discretely circular in cross-section. Pericytes are seen to be associated with the afferent vessels. Vesicles of pinocytotic size are seen included within the thicker areas of both afferent and efferent vessels. There is little difference between the average afferent and efferent endothelial thickness, but areas of the efferent



endothelia become extremely attenuated, but lack either pores or diaphragmed fenestrae. In general, the appearance of this Fundulus choroidal rete preparation appears similar to that seen in the sketch of the choroidal rete of Amia.

The evidence regarding choroidal rete ultrastructure seems to point toward features differing from those seen in the swimbladder rete. Because of the variability displayed, all features must be kept in mind in observing the ultrastructure of the choroidal rete of Salmo gairdneri.

Choriocapillaris

Afferent rete vessels converge into larger distribution vessels which proceed to a vast capillary network, the choriocapillaris, which is the major site of exchange. Large collection vessels drain the choriocapillaris and deliver blood to the efferent rete vessels. No studies have been published on the ultrastructure of either the distribution or collection vessels in teleosts. Braekevelt (1974) has, however, reported on the ultrastructure of the choriocapillaris capillaries and their relationship to Bruch's membrane and the pigment epithelium in the Northern pike, Esox lucius.

In both mammals and teleosts, the choriocapillaris abuts Bruch's membrane, a non-cellular supportive structure. The pigment epithelium lies on the retinal side of Bruch's membrane. In the human (Hogan, Alvarado and Weddell, 1971), and mammals in general, the choriocapillaris endothelial

cells are polarized in structure such that the nucleus and bulk of the endothelial inclusions (i.e., the central prominence) lie toward the scleral side of the capillary. Peripheral extensions of the endothelia then extend around the lumen and form the capillary wall adjacent to Bruch's membrane. In this region, the endothelial wall is extremely attenuated and in mammals, is highly fenestrated. In humans, Bruch's membrane is composed of: 1) the choriocapillary endothelium basement membrane (0.14 μm), 2) an outer collagenous zone containing collagen fibrils and a mucoprotein ground substance (0.7 μm), 3) an elastic layer (0.8 μm), 4) an inner collagenous zone (1.5 μm) of collagen fibers in a finely granular ground substance, and 5) the basement membrane of the pigment epithelium (0.3 μm) (Hogan et al., 1971). The border of the pigment epithelium is characteristically highly involuted in this region, and the pigment epithelium cytoplasm is rich in mitochondria. All of these features are purported to be indicative of a rapid diffusion of large amounts of substrate from the choriocapillaris to the pigment epithelium. Bernstein and Hollenberg (1965) utilizing ferritin injection studies and silver nitrate ingestion in Rhesus monkeys, Macaca mulata, indeed have substantiated this diffusion pathway and pointed out that it may be the preferred pathway over that of the retinal vessels in mammals.

In Esox lucius, Braekevelt (1974) reports that unlike the mammalian features described above, the endothelial wall of the choriocapillaris bordering Bruch's membrane is typically very thin, but relatively non-fenestrated. Diaphragmed fenestrae are occasionally seen, however. The endothelial cell processes often overlap and are bound together by tight junctions. Vesicles are common within the endothelial cytoplasm where no fenestrations are found. The nuclear region of the endothelial cells is rich in cell organelles: Golgi complexes, mitochondria, and rough endoplasmic reticulum. Bruch's membrane is composed of three layers: the basement membrane of the choriocapillaris endothelium, a middle layer of fine fibrils, and the basement membrane of the pigment epithelium. Also in contrast to mammals, the basal border of the pigment epithelial cell is not infolded.

As stated earlier, no information exists on the morphology of the collection vessels draining the choriocapillaris. The efferent rete vessels have been discussed. The final category of vessel, the venous sinusoid, also has not yet been described at an ultrastructural level.

Ultrastructure Summary

All of the above studies suggest certain characteristic properties which should be recalled when viewing the ultrastructure of the choroidal layer of Salmo gairdneri. With regard to the choroid rete, one might speculate based upon the literature reviewed above that the afferent vessels may

show thicker endothelial walls than the efferent vessels, and be composed of either one or two distinct endothelial cell types; or the afferent endothelial wall may show no significant difference in thickness from the efferent rete vessels. The efferent vessel endothelial walls in all cases are invariably reported to be thin and in some cases may or may not show areas with fenestrations. Endothelial junctions in both vessel types show little overlap and have desmosomes associated with zonulae occludens. The junctions may or may not show marginal flaps. Afferent vessels are depicted as being of a smaller diameter than the efferent vessels and in some cases the efferent vessels show a sinusoidal configuration.

Within the choriocapillaris, the features seen in Esox lucius will be the most probable: attenuated, relatively non-fenestrated choriocapillaris endothelia abutting Bruch's membrane which is homogenous in structure, and subtends a smooth pigment epithelium basal border. The remaining choroidal vessel types observed on a light microscopic level have not been studied in teleosts at an ultrastructural level.

MATERIALS AND METHODS

Ocular tissues were collected from 150 to 300 g commercially cultured rainbow trout, Salmo gairdneri (Midwest Fish Farming Enterprises, Inc., Harrison, Michigan). Fish were held in fiberglass tanks at $12 \pm 1.0^{\circ}\text{C}$, with a continuous flow of aerated water which was treated to remove chloride and iron. The animals were exposed to light-dark periods of 16 and 8 hours, respectively. Choroidal tissues for this study were prepared by several techniques.

For light microscopy, tissues were fixed in 10% neutral formalin, dehydrated in tetrahydrofuran, vacuum embedded in paraffin and stained with hematoxylin and eosin. Alternatively, tissues were dehydrated, embedded and stained with Masson's trichrome as above after fixation in Bouin's fixative (Luna, 1968).

Initial electron microscope preparations were fixed in 2% glutaraldehyde in 0.17 M cacodylic acid buffer at 4°C for three to four hours, washed three times in 0.17 M cacodylate buffer with 7% sucrose at twenty minutes per step, and postfixed in 0.17 M cacodylate buffered, 2% osmium tetroxide for three hours at room temperature. The tissues were then dehydrated in either a graded ethanol series (30%, 50%, 70%, 95%, 100%) and embedded in Spurr's low viscosity epoxy resin (Spurr, 1969), or in a graded acetone series and embedded in EPON 812 epoxy resin (Luft,

1961). This fixation procedure is the standard technique utilized in this laboratory for animal tissues and will be referred to as the standard immersion fixation procedure. After sectioning on a Porter-Blum MT-2 Ultramicrotome, the sections were counterstained with lead citrate and uranyl acetate after the method of Reynolds (1963). Sections were then observed on a Philips 300 transmission electron microscope.

After a series of initial observations which indicated that a refinement in tissue preparatory technique was necessary, two experimental tissue treatment regimes were established. The first treatment included heparinization of the fish. One U.S.P. unit is the amount of Panheprin (Abbott Laboratories, N. Chicago, Illinois, 60064) required to maintain fluidity in one ml of plasma. A perfusate of heparinized (2 U.S.P. units/ml) Ringer's solution is routinely used in this laboratory to clear gill arches (Bergman, 1975). On this basis, it was decided that the final circulating concentration of sodium heparin should be between one and two U.S.P. units per milliliter of plasma. In Salmo gairdneri, blood volume is approximately 2.25% of the total body weight, whereas the plasma volume is about 1.50% of the total body weight (Schiffman and Fromm, 1959). Thus, approximately 0.03 U.S.P. units of sodium heparin per gram of total body weight were injected into the caudal vein ten minutes prior to enucleation. The eyes were then fixed in 0.17 M

cacodylate buffered, 2% glutaraldehyde, 2% paraformaldehyde after the technique of Karnovsky (1965). Subsequent steps were identical to the initial treatment. This preparation will hereafter be referred to as the heparinized immersion fixation treatment.

In the second treatment, eyes were enucleated from non-heparinized fish, stored in a moist atmosphere for 20 minutes, and transferred to Karnovsky's fixative as described above.

In order to better visualize the area from which electron micrographs were taken, monitor sections of 1 to 2 μm thickness were frequently taken for each block and stained with methylene blue (Richardson, Jarett and Finke, 1960).

RESULTS

Light Microscopic Choroidal Morphology

Based upon light micrographs presented in Figures 3-12, it is evident that the general arrangement of the choroidal vasculature in Salmo gairdneri follows closely that pattern described previously in the literature review and by Barnett (1951). Blood enters the choroidal vasculature via an ophthalmic artery which branches into an arterial manifold. This then bifurcates into the afferent rete vessels. These vessels then converge upon larger "distribution" vessels on the peripheral side of the rete (Figure 1). These then feed a vast capillary network---the choriocapillaris---supplying all areas of the retinal-choroidal interface at Bruch's membrane. Large "collection" vessels return blood from the choriocapillaris to the rete where they bifurcate into small efferent rete vessels which lie interposed among, and parallel to the afferent rete vessels. These efferent vessels finally drain into a large thin-walled venous sinusoid which encloses the arterial manifold and leads out of the eye via the ophthalmic vein (Figure 2).

There are several points of interest which have not previously been mentioned in the literature. The vessels of the central side of the rete mirabile (i.e., the venous sinusoid and arterial manifold) are distinguishable as being relatively devoid of pigmentation. The arterial

manifold and its bifurcations are distinctly thick-walled, characteristically staining blue-green in the Masson's trichrome preparations indicating an abundant supply of connective tissue (Figures 7-8). On the peripheral side, however, interspersed among the distribution and collection vessels, and indeed, throughout the peripheral choroidal vasculature, pigmentation is characteristically observed (Figures 9-11). The collection vessels are not distinguishable from the distribution vessels at this level.

Within the rete itself, the parallel nature of the vessels is evident in longitudinal section (Figure 4). It is evident from Figure 12 that two types of vessels may be distinguished upon the basis of their size. Although no justification for distinguishing efferent from afferent vessels on the basis of size alone can be made in the current study on Salmo gairdneri, according to the studies of Wittenberg and Wittenberg (1974) and Copeland (1974a) the efferent vessels in all species studied were the larger of the two types. For this reason, it seems reasonable to assume that in Salmo gairdneri, this pattern holds. Thus, on the basis of Figure 12, the efferent vessels appear to be about twice the diameter (9.5 μm) of the afferent vessels (4.5 μm). The packing pattern of the afferent and efferent vessels appears to be one of an orderly array such that four efferent capillaries surround each afferent vessel (Figure 12). This means that the number of afferent vessels

equals that of the efferent vessels. This packing pattern is also seen in the tuna eye, Lampris regius, but in other species such as the swordfish, Xiphias gladius, hexagonal arrays are also encountered (Wittenberg and Wittenberg, 1974). These patterns of close packing are significant for the determination of exchanger efficiency.

Electron Microscopic Fixation Techniques

In order to further characterize the various vessel types in the choroid layer, an electron microscopic examination was undertaken. Prior to pursuing a detailed study of the ultrastructure, however, it was necessary to develop proper fixation techniques.

Initially, nonheparinized tissues were prepared by the standard immersion fixation procedure in which 2% glutaraldehyde was used with postfixation in 2% osmium tetroxide. A sampling of the resulting choroidal rete ultrastructure is depicted in Figures 13, 14, and 15. The most notable features of the rete vessels and endothelia are: 1) very large vacuoles, 2) areas containing numerous micropinocytotic vesicles, 3) areas of extremely attenuated, but non-fenestrated, endothelial walls, 4) swollen adventitia between the vessels, 5) a relatively dense background matrix within the lumen of the vessels, and 6) numerous myeloid configurations and thin-walled vacuoles seen within the lumen of the vessels.

From these results, it was deemed necessary to modify the preparatory technique in hopes of yielding characteristics more typical of endothelial ultrastructure. When the fish were heparinized prior to fixation by immersion in Karnovsky's fixative, much more typical micrographs resulted (Figures 19-21).

To determine whether the heparinization versus the use of Karnovsky's fixative was the cause for the change in appearance, a Karnovsky's fixed, clotted preparation was processed for observation. The latter yielded results identical to those seen in the standard immersion fixation preparation.

Electron Microscopic Choroidal Morphology

Having selected the optimal immersion technique, a detailed survey of the choroidal vascular ultrastructure was pursued. The structure of the ophthalmic artery was not observed in this study.

The arterial manifold wall is very thick and is composed of several cell types (Figure 16-18). There is a rather thick endothelial wall on both surfaces. These cells are richly supplied with rough-surfaced endoplasmic reticulum and polysomes. There are also very many micropinocytotic vesicles which appear to be concentrated on the border facing a layer of closely apposed smooth muscles (Figure 18). Were these vesicles active in the transport of macromolecules across the endothelial wall, one might expect the presence

of an equal number of these structures on the luminal border. It is seen that this is not the case.

The next layer is a thick matrix of collagen fibers. Within this collagenous matrix, one sees fibroblasts which are probably active in the secretion of the collagenous matrix (Rhodin, 1974), a single layer of smooth muscle cells, and occasionally bundles of both myelinated and non-myelinated neurons within Schwann cells (Figures 16-17). Neurons were occasionally seen to be closely associated with the smooth muscle cells. Neither neurons nor muscle cells were ever seen in any other choroidal vessel walls, thus it is possible that the arterial manifold may play a significant role in the regulation of flow through the choroidal vasculature.

Within the rete (Figures 19-21), there is only a single discernable type of endothelial cell in the wall of both the afferent and the efferent vessels. The cell is richly endowed with micropinocytotic vesicles opening on both surfaces. Larger vacuoles are also seen. Dense polysomes are seen throughout the cytoplasm. Endothelial cell junctions are seen to be abutting rather than folded and overlapping and are characterized by possessing a single desmosome close to the endothelial surface and an associated marginal flap. Though the endothelial cells are similar in both afferent and efferent vessels, the afferent vessels have two distinguishing features. First, a single layer of pericytes

is often seen to overlay the afferent endothelia. Second, outside these endothelial and pericyte cells is a very well-defined easily discernable basement membrane. This may serve as a significant barrier to the diffusion of substances between vessel types. Neither pericytes nor basement membrane are seen associated with the efferent vessel. There appear to be no pores or fenestrae in either afferent or efferent vessels.

In summary, there are three characteristic features which may be used to separate the retial vessel types: 1) the size of the vessel, afferent being the smaller of the two, 2) pericytes are seen to be associated with the afferent vessels and not the efferent vessels, and 3) the presence of a distinct, well-defined basement membrane surrounding and outlining the afferent vessel endothelia and any associated pericytes.

Although serial cross-sections through the length of the rete were made, no structural difference was discernable between the two ends. Close to both ends, however, the efferent vessels seemed to conjoin before those of the afferent side. At both ends, then, the efferent vessels appeared to be more sinusoidal in nature while the afferent vessels remained discrete.

At the peripheral end of the rete, the distribution and collection vessels showed no discernable difference in structure (Figures 22-24). These vessels are notable in

having a fairly thin single layer of endothelium. Outside this endothelium and within the overlying collagenous matrix are numerous fibroblasts. Overlying the collagen layer occur many heavily pigmented melanocytes. The granules here are roughly spherical, never rod-shaped. Above the pigment layer is a very loose multilaminar stroma which separates adjacent vessels. No neural elements are ever seen.

These distribution and collection vessels feed and drain respectively the choriocapillaris network which is separated from the pigment epithelium by Bruch's membrane. The structure of this region is identical to that seen in Esox lucius as reported by Braekevelt (1974) (Figures 25-27). The choriocapillaris capillary endothelia show a bipolar nature in that the scleral side is thicker and typically seats the cell nucleus and the bulk of the cytoplasmic constituents, whereas, the Bruch's membrane border is highly attenuated and shows random, but not abundant, diaphragmed fenestrations. Bruch's membrane is uniform, lacking an elastic layer (Figure 27) and is overlain by the basement membrane of the pigment epithelium. The pigment epithelium basal border is smooth as opposed to the highly involuted border seen in mammals.

The ultrastructure of the pigment epithelium cells is interesting in that its cytoplasm has an extremely electron-lucent background substance. Inclusions include numerous mitochondria, rod-shaped pigment granules, and vacuoles

containing phagocytosed photoreceptor outer segments (Anderson and Fisher, 1975) (Figures 28-29). The fact that the pigments present here are rod-shaped versus spherical as seen in the melanocytes within the choroid layer, suggests that they may be of different crystalline structure and thus of different chemical composition.

DISCUSSION

Several points which have heretofore gone unreported regarding the morphology of the choroidal vasculature in teleosts have arisen in the current study. A significant finding for use in subsequent localization studies was the fact that choroidal pigmentation occurred only on the peripheral side of the circulatory bed. At either end of the rete, the vessels unite into larger vessels: the arterial manifold or venous sinusoid on the central side, and large distribution and collection vessels on the peripheral side. These two sides are easily distinguished from one another in that the arterial manifold vessels are very thick-walled, and there is no pigment in or surrounding the vessel walls of the central side, whereas on the peripheral side, heavily pigmented melanocytes are interspersed among the collection and distribution vessels. Knowing this, it will be possible to distinguish central from peripheral vessels within the vascular bed during electron microscopic examination. Aside from this point, the choroidal vasculature of Salmo gairdneri appears to follow the pattern displayed by other species.

Vascular Artifacts

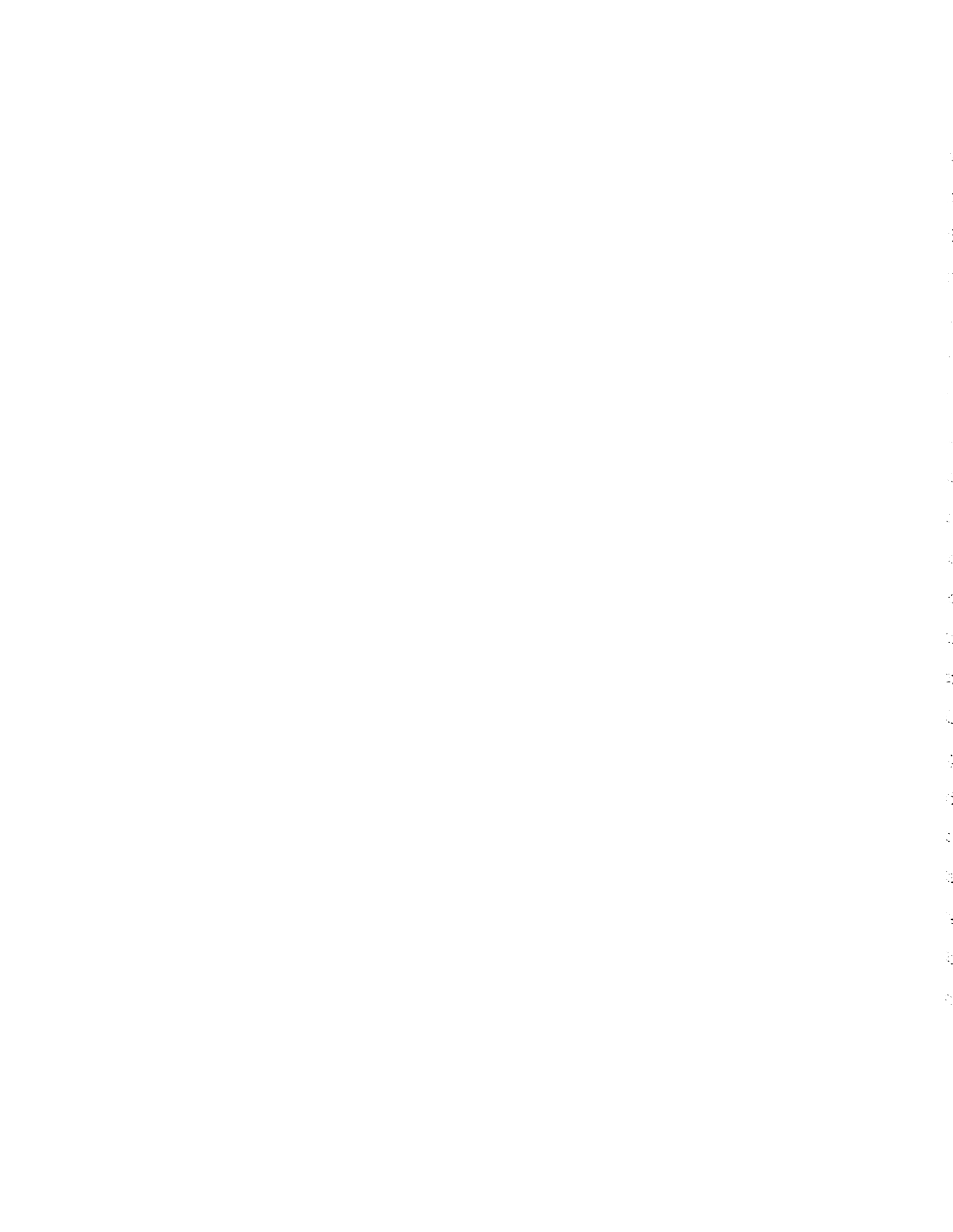
At the onset of the electron microscopic examination of the choroidal tissues, no problems had been anticipated with respect to fixation and tissue preparation. Eyes were enucleated from fish and were processed by the standard

immersion fixation procedures used for other tissues in this laboratory (i.e., fixation in 2% glutaraldehyde, with postfixation in 2% osmium tetroxide). The results of these initial preparations have been described. After obtaining similar results, Copeland (1974a) reported that perfusion of the fixative is necessary to obtain relatively artifact-free electron microscopic preparations in the choroid rete mirabile of the killifish, Fundulus heteroclistus. In arriving at this conclusion, he had likewise initially attempted fixing the tissues by immersion in Karnovsky's fixative (2% glutaraldehyde, 2% paraformaldehyde, with postfixation in 2% osmium tetroxide). Karnovsky's fixative is characterized by penetrating much more rapidly due to the presence of the paraformaldehyde. Copeland's results and the results of the current investigation were comparable with these immersion techniques.

In that the Copeland report had been published after the onset of the present investigation, the literature was reviewed in an attempt to find an explanation for the unusual appearance of these tissues in order to determine whether they were indeed artifactual. It was discovered that Brown, Stalker and Hall (1969) had investigated the ultrastructural changes in renal glomerular capillaries in which blood had undergone defibrination experimentally induced by thromboplastin and liquoid. Defibrination may be defined as the intravascular precipitation of fibrinogen

and/or its conversion to fibrin monomer or polymer, either 1) by artificial agents acting directly or through the thrombin mechanism, or 2) by naturally occurring thromboplastins. Thromboplastin initiates the conversion of prothrombin to thrombin with consequent fibrin deposition, and is the natural activator of this reaction. Liquoid is an artificial fibrin precipitating agent.

In their studies, Brown et al. (1969) showed that both agents resulted in the same ultrastructural changes. Within the lumen, granular material which they describe as "fuzzy" in appearance is seen in small amounts at three minutes after application, and it becomes progressively more distinct and abundant. This granular background material is seen in the lumen of the choroidal vessel of Figure 14. After 100 minutes, the amount of granular material is considerable and more electron dense. In the early stages, endothelial "blebs" are formed in a process they refer to as endothelial stripping. The fenestrated endothelial layer typical of renal glomerular capillaries is lifted from the basement membrane. The bleb space may be clear or may contain granular material. Thus, in the electron micrographs, the endothelium is elevated well above the subadjacent basement membrane and separated from it by a clear zone or by granular material (i.e., the bleb space). At several points local swelling of endothelial cytoplasm was noted. The small blebs can apparently form larger vacuoles which may



detach completely from the endothelial layer and lie free in the capillary lumen. Vacuoles similar to those published by Brown et al. (1969) are seen in the electron micrograph of the choroidal vessels in Figure 15. Brown et al. continued to explain that the endothelial cell nucleus itself becomes prominent and bulges into the lumen. It remains, however, surrounded by a thin cytoplasmic rim. Vacuolation occurs in both the fenestrated layer of endothelial cytoplasm and the perinuclear cytoplasm. This perinuclear vacuolation is more common between the nucleus and the basement membrane. Vacuolation proceeds from both sides of the nuclear attachment zone, and there is detachment and extrusion of the nucleus together with a small cytoplasmic rim. Granular material assists in this process. By the 100 minute stage, all the endothelial changes are greater in degree. In some capillaries, however, endothelial nuclei are notably absent, and the capillaries appear bare. In the early stages there is an irregular slight indistinctness of the basement membrane especially where granular material is stripping the overlying fenestrated endothelial cytoplasm. Later, the basement membrane is irregularly thick and coarse in appearance.

Brown et al. (1969) conclude that:

"We believe that granular material penetrates as far as the basement membrane, is temporarily held up and then spreads laterally to a subnuclear position. Vacuolation of the endothelial cytoplasm adds to the insecure position of the nucleus.

This vacuolation may in part represent a method of disposal of the granular material; it may also be the result of filtration activity. A link with production of plasminogen activator by the endothelial cell must also be borne in mind but it is not yet possible to test this view. The accumulation of granular material and the vacuolation could each cause nuclear extrusion, but presumably they could be synergistic."

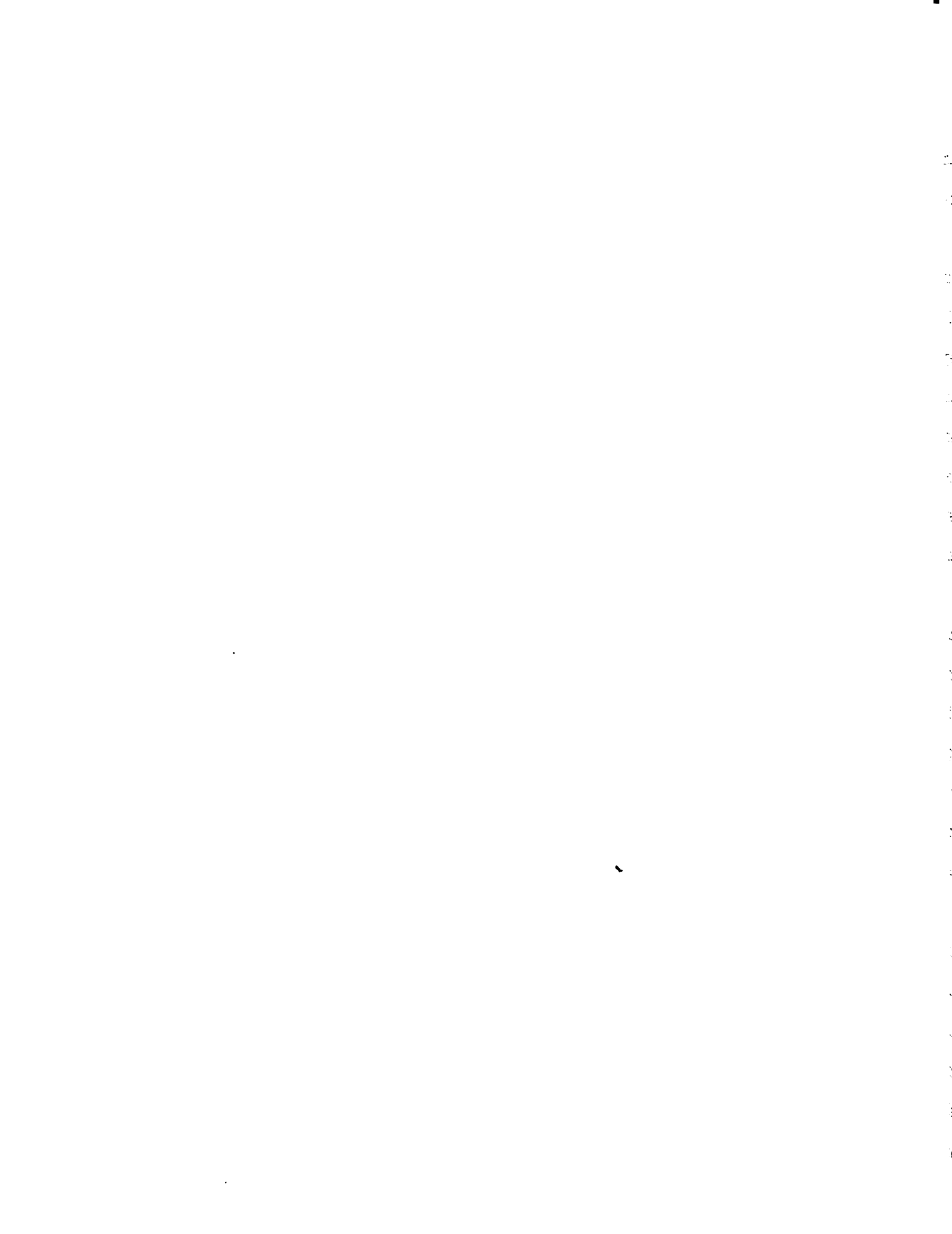
It is noted that many of the changes reported by Brown et al. (1969) were also seen both in the material presented in the current study and in Copeland's (1974a). Vacuolization of the endothelia, local swelling, granular background substance, endothelial stripping, and degeneration of the basement membrane were all prominent. Nuclear extrusion was not observed in our material and was not reported by Copeland, but this is explainable by the fact that these preparations would not probably have reached the 100 minute stage in the process of clot formation. It was noted that Copeland (1974a) had used heparin in his perfusion technique, but had not in his immersion technique. No precautions had likewise been taken against clotting prior to fixation in the standard immersion fixation preparations of the current study. Thus, based on the reports of Brown et al. (1969), and due to the fact that teleost blood had been observed to display extremely rapid clotting times, averaging about 30 seconds in Salmo gairdneri (Smith, Lewis and Kaplan, 1952; Wolf, 1959), it was believed that the blood of tissues of Figures 13, 14, and 15 had clotted prior to the time of fixation. In light of the difficulties of

the perfusion technique where pressures must be carefully monitored and any unusual hydrostatic imbalances may profoundly affect the appearance of a capillary network, a suitable immersion technique is held to be preferable, provided that fixation is rapid and results are repeatable. For these reasons, a study was undertaken to try to establish an acceptable, optimum immersion fixation technique and to confirm that clotting induced artifacts had occurred in our preparations and in Copeland's (1974a) as described by Brown et al. (1969). The results of prior heparinization and of prior clotting have been shown. It was concluded that clotting had indeed occurred and that heparinization prior to fixation was necessary in order to obtain a suitable immersion fixation preparation and the subsequent study was undertaken under these conditions.

The precaution against clotting is apparently extremely important in the study of any vascularized tissues in that ultrastructural appearance is drastically altered. This point should perhaps be emphasized to a greater degree in future electron microscopic examinations.

Choroidal Ultrastructure and Function

The only literature thus far presented regarding the teleost choroidal vascular ultrastructure has been of questionable value due to what is deemed to be artifactual tissue preparatory techniques. Thus, the findings of the current study warrant a rather detailed discussion. Functional



implications as well as strict anatomical description will be considered.

The arterial manifold wall is seen to be a thick structure consisting of two endothelial layers enclosing a dense collagenous matrix in which fibroblasts, smooth muscle, and myelinated and non-myelinated neurons may be found (Figures 16, 17 & 18). Although the arterial manifold lies within the lumen of the venous sinusoid, it is unlikely that any exchange of substances between the contents of these two vessels occurs based upon the barrier presented by the arterial manifold wall.

It seems significant that the only area in which any innervation is observed within the choroidal layer is within the arterial manifold wall. Although no physiological basis for drawing conclusions regarding regulatory control is presented in this study, the occurrence of neural tissues within the wall of this vessel raises the suspicion that regulation of blood flow through the rete in response to any of a variety of factors may be possible via these tissues.

There is evidence for such neural influence in the choroidal vasculature in mammals. In the human choroidal layer and uveal tract in general, myelinated and non-myelinated nerves supply filaments to the blood vessels and the stroma (Wolter, 1960; Hogan, Alvarado and Weddell, 1971; Castro-Correia, 1967). In mammals, there are apparently two types of fibers: intervascular and perivascular.

Perivascular branches course along the vessels sending branches into the wall, where they end as small filaments without end-plates. These perivascular elements are also found closely connected to melanocytes. In the peripheral regions of the choroid of S. gairdneri, where numerous melanocytes are found, perivascular neural elements were seen to innervate neither the vessels nor any of the melanocytes, and indeed, no nerves were ever present anywhere in this region. This raises questions concerning the function and/or mechanism of dispersion of pigment within the melanocytes found within the choroidal layer of S. gairdneri.

With regard to the intravascular nerves, Castro-Correia (1967) speculated that nerve cells of a ganglionic type found within mammalian choroidal vessels might have some relation to the regulation of the ocular temperature as well as the intraocular pressure. The role of the teleost choroidal rete as a thermal exchanger seems to be in debate at this time (Barraco, 1975; Linthicum and Carey, 1972). In light of the fact that the arterial manifold in S. gairdneri is muscular and innervated it is interesting to speculate upon the possible role which this vessel may play in the regulation of flow, and hence, in the regulation of oxygen concentration, and thermal gradients. The importance of such a control mechanism to the operation of the counter-current exchanger definitely warrants further investigation.

Although several papers have been published concerning the ultrastructure of the swimbladder rete, there has been a general paucity of work done on the ultrastructure of the choroidal rete mirabile. According to the evidence presented in the current study, it may be concluded that in S. gairdneri, afferent and efferent vessels are definitely morphologically differentiated from one another. The afferent vessels are the smaller diameter vessels, being approximately 4.5 μm in diameter. There is no discernable difference between the endothelial wall thicknesses of the afferent versus efferent vessels. The afferent vessels are surrounded by a clearly distinct basement membrane. The packing pattern displayed in S. gairdneri is a cubic, checker board array with four efferent vessels surrounding a single afferent vessel (Figure 12). The packing pattern of the vessels is not the same in all teleosts, as for instance the swordfish, Xiphias gladius, displays an hexagonal array (Wittenberg and Wittenberg, 1974).

The efferent vessels are clearly discrete as typical cylindrical vessels as opposed to sinusoidal in nature as reported in Amia calva (Wittenberg and Wittenberg, 1974) and in Fundulus grandis (Copeland, 1974a). There may be several reasons for the discrepancy. To begin with, there may very well be species-specific differences in the structure. A second possibility is that the micrographs published by these investigators may have been of tissue located very

close to the distal or proximal ends of the rete at a point where the efferent vessels were still of a larger vessel dimension. Indeed, such sinusoidal areas of the efferent vessels may be seen in a tangential section when the ends of the rete are approached. Finally, Copeland's preparation was perfused at a pressure of 0.75 psi (Copeland, 1974a) and based upon his published micrographs, and upon the fact that the vessel walls separating adjacent endothelial cells are very attenuated, and presumably delicate, any non-physiological trans-luminal pressure caused by the perfusion technique may have broken these walls. In fact, it appears that instead of the sinusoidal case which he chose to illustrate, the more common case is one of a single arterial vessel surrounded by five or six venous vessels. Close inspection of Copeland's micrographs reveals that the endothelial lining of the venous sinusoid vessel reveals areas which may easily have been endothelial bridges which have been torn away. Line diagrams of micrographs of the rete of Amia also illustrate the presence of an efferent sinusoidal arrangement (Wittenberg and Wittenberg, 1974). Unfortunately, the technique of tissue preparation used was not described. The importance of the tissue preparatory technique in studies of the ultrastructural morphology of this network has already been pointed out. If indeed, the micrographs thus far published are erroneous, it will not have been the first time that the elucidation of rete

physiology has suffered at the hands of fixation artifacts. According to Dorn (1961) who also worked on the swimbladder rete ultrastructure, Jaeger, in 1905, reached the conclusion that gas was accumulated in the lumen of the swimbladder by the physical rupture of blood cells by a toxin released by the gas gland epithelium at the site of the rete. This surprising conclusion it seems was arrived at by light microscopic observation of poorly fixed tissues.

It is my contention that Copeland's perfusion technique may lead to as much artifactual results as did his initial clotted tissues and that yet another appearance may be obtained by using a heparinized immersion technique which is deemed to be closer to the true morphology. Assuming that the results seen in the heparinized preparations adequately represent the closest approximation to the true condition, comparisons to other vascular beds may be made and certain functional implications drawn.

Bennett, Luft and Hampton (1959) have developed a classification scheme for mammalian capillary types based upon three morphological features---basement membrane, pericytes, and endothelial fenestrations. In keeping with the established terminology seen in the microvascular literature of classifying capillary vasculature according to Bennett's classification scheme, the vessels of the choroid rete mirabile may be roughly categorized as follows. The afferent component of the choroidal rete in Salmo gairdneri would

be classified as belonging to vessel types represented by muscle capillaries (type A1a) having a complete basement membrane, lacking fenestrations, and being partially surrounded by pericytes. Efferent components of the rete contain few, if any, fenestrae and should be grouped together with capillaries of the mammalian kidney and endocrine glands (type A2a). The categorization of these rete vessels into Bennett's classification scheme cannot be considered to specifically describe the morphology or function of the vessels present, but it is interesting from a comparative standpoint.

With regard to the ultrastructure of the swimbladder rete mirabile, Fawcett and Wittenberg (1959) suggest the hypothesis that "the differences observed in fine structure of the capillary walls may possibly be correlated with different physiological mechanisms of transcapillary exchange in the two categories of vessels comprising the counter-current system." Jasinski and Kilarski (1971) also suggest that the general organization of the rete mirabile and differences in the structure of the afferent and efferent capillaries probably reflect some functional role different for both types of capillaries. Capillaries are extremely permeable to oxygen and carbon dioxide (Pappenheimer, Renkin and Borrero, 1951), thus allowing counter current exchange of these two gases. Marked differences between the fine structure of the afferent and efferent capillaries have been

noted. However, these differences would not be expected to affect the transcapillary diffusion of gases. Thus, there must be some other functional significance to the structural difference if this hypothesis is true.

Jasinski and Kilarski (1971) noted that despite the large number of smooth surface vesicles found in individual sections of the swimbladder rete endothelial cells, very few are seen to empty at either of the cell surfaces, i.e., basal or lumenal. They suggest that these vesicles may represent smooth endoplasmic reticulum in cross-section. Copeland (1974a) noted the possible presence of a similar microtubular system, as opposed to the more commonly expected pinocytotic vesicles, in his immersion-fixed choroidal rete endothelial preparations. The tubular structures shown by Copeland (1974a) were present in clotted tissues and may not be indicative of typical rete endothelial ultrastructure. Bruns and Palade (1968a) have reconstructed models from serial sections of endothelia from mammalian skeletal vasculature. In so doing they have found that a common feature of capillary endothelia is the presence of many true pinocytotic vesicles as opposed to a tubular network of smooth endoplasmic reticulum. These vesicles do open frequently to the surfaces of the cell. The findings of the current study suggest that there are numerous vesicles within the choroidal rete endothelial cell cytoplasm. That these are not likely tubules in cross-section is evidenced by the

fact that one rarely sees a tubular structure in longitudinal section (Figure 20). The vesicles present do not, however open frequently at the cell surface as noted by Jasinski and Kilarski (1971) indicating that pinocytotic activity is not a very active process thus negating this as a viable mode of transcapillary exchange.

Movement of water across the afferent-efferent interface has been postulated by Wittenberg and Wittenberg (1974) as being possibly significant in the oxygen concentrating mechanism. The possibility of movement of other substances has also not been ruled out. Like other capillaries, they are probably readily permeable to lipid soluble substances such as carbon dioxide, whereas water and sodium, for example, would enter and leave the endothelial wall less easily. The permeability of the basement membrane is not known. According to Rhodin (1974), the basement membrane consists of a thin basal lamina rich in mucopolysaccharides, amino acids and a reticular network composed of delicate collagenous fibrils. He does state that the basal lamina establishes a microenvironment for the adjacent cells and acts as a diffusion barrier to rapid ion exchange. It is interesting to note that the basement membrane may be present around the afferent vessels to act as a barrier to diffusion of certain substances between afferent and efferent vessels, whereas it is not seen surrounding efferent vessels which often lie adjacent to one another. At these locations no

gradient for diffusion exists, thus eliminating the necessity for a diffusion barrier. In contrast to this notion is the fact that there is a dual basement membrane between the pigment epithelium and the choriocapillaris, the presumed site of major metabolite and nutrient exchange for the retina. The question of whether the basement membrane acts as a significant diffusional barrier awaits further investigation. The endothelial cell junctions in the chorioidal rete, although not overlapping, characteristically are seen to possess desmosomes and zonulae occludens whose structure presumably represents a significant barrier to the passage of substances by a pericellular route (Fawcett and Wittenberg, 1962; Wade and Karnovsky, 1974; Spitznas and Reale, 1975). Finally, if the pinocytotic vesicles within the endothelia were indeed active in the movement of substances from one vessel to another, it would seem likely that they would be seen to open more frequently onto both the luminal and basal surfaces of the endothelial cells. Thus, it seems that the movement, and hence, the counter-current concentration of substances not readily permeable both to the endothelial cell membrane itself and to the basement membrane is unlikely in this system. This supposition is again based upon presumptive morphological evidence and requires further experimental verification.

At either end of the rete, the vessels converge into larger vessels; the arterial manifold or venous sinusoid

at the central end, and large distribution and collection vessels at the peripheral end. These two sides are easily distinguished from one another in that the arterial manifold vessels are very thick-walled, and there is no pigment in or surrounding the vessel walls in this end, whereas on the peripheral end, heavily pigmented melanocytes are interspersed among the collection and distribution vessels.

The collection and distribution vessels pass out to the choriocapillaris through a loose connective tissue stroma. These vessels are seen to be embedded in a collagenous matrix which is secreted by numerous fibroblasts. Melanocytes are also seen throughout this layer. It has already been stated that no innervation of either the vessels of this region or of the melanocytes has been observed in Salmo gairdneri which is contrary to the case in man, rat, hamster, and guinea pig (Castro-Correia, 1967). In addition, the human also displays mast cells, macrophages, plasma cells, and lymphocytes (Hogan, Alvarado and Weddell, 1971), none of which have been observed in S. gairdneri in this region. It has been pointed out (Hogan et al., 1971) that the functional significance of the melanocytes within the choroidal layer is not yet clear. The function of light screening should have been accomplished by the pigment epithelium by this point. The tapetum lucidum in this fish is located at the back of the choroid in the region of the suprachoroid layer, next to the sclera. If this reflective layer is

functional in light gathering in the dark, as has been proposed (Arnott et al., 1974), this would mean that light would indeed have to pass through the pigment epithelial layer and the choroid layer as well, suggesting the possibility that the light-absorbing function of the melanocytes within the choroid may remain at certain times.

The structure of the choriocapillaris, Bruch's membrane, and pigment epithelium are identical to those described by Braekevelt (1974) in Esox lucius, but differs drastically from that seen in the human (Hogan et al., 1971). The major differences are three-fold: 1) the choriocapillaris is much more highly fenestrated in man than in teleosts, 2) Bruch's membrane displays a slightly different arrangement, and 3) the basal border of the pigment epithelium is very highly involuted in man, whereas in teleosts, all signs of involution are lacking.

Functionally, the choriocapillaris has been implicated in mammals as being the primary site of nutrient exchange rather than oxygen and gas exchange, the latter function being provided by the retinal vasculature (Braekevelt, 1974). In teleosts, there is no retinal vasculature, hence the choriocapillaris must meet all circulatory needs. As already pointed out, in keeping with the notion that the vascular architecture must be designed to meet and indeed determine tissue functional demands, the teleost choroidal rete has evolved into a counter-current gas exchanger. It is likely,

however, that the exchange of other metabolic substances and products does not rely on the concentrating effects of a counter-current multiplier, but upon the architecture of the choriocapillaris, Bruch's membrane, and pigment epithelium.

In agreement with the report of Braekevelt (1974) with respect to the choriocapillaris architecture in Esox lucius, numerous fenestrations do occur in the endothelial border lying adjacent to Bruch's membrane in Salmo gairdneri, which would presumably allow or facilitate passage of macromolecular nutrients and metabolites into and out of the retina. If the choriocapillaris is the major site of nutrient delivery in the vertebrate eye, as indeed it must be in the case of teleosts, the occurrence of fenestrations is significant. Fenestrations have classically been characterized as the site of macromolecular passage (Karnovsky, 1967). The only alternative would be pinocytotic activity which is typical of some capillary beds (eg. mammalian skeletal capillaries (Bruns and Palade, 1968a & 1968b)), but is notably lacking in the vicinity of Bruch's membrane in S. gairdneri (Figure 26). Another possible route would be extracellular passage at the site of the endothelial cell junctions. These borders, like those seen in the choroidal rete mirabile capillaries, characteristically display desmosomes bordered by zonulae occludens which, by the nature of their structure, present significant barriers to the passage of substances. The

diaphragmed fenestrae, then, are the only remaining site possible for the passage of macromolecular nutrients. Braekevelt (1974) points out, however, that in Esox lucius the degree of choriocapillaris fenestration is significantly less than that seen in mammals. This was also seen in S. gairdneri. The role of the falciform process in nutrient supply in teleosts also remains unclear (Walls, 1963). Thus, the question of where macromolecular exchange occurs in this region awaits further study, perhaps by the techniques of ferritin or horse radish peroxidase injection (Clementi and Palade, 1969).

The pigment epithelium has been reported to be active in the disposal of shed rod and cone outer segments (Anderson and Fisher, 1975) along with its light absorbing characteristics. The cytoplasmic inclusions seen in Figures 28 & 29 tend to imply that these functions are also characteristic of the pigmented epithelium of S. gairdneri.

The significance of the lack of involutions in the pigment epithelium is not known. This feature of the ultrastructure seen in the mammalian system is observed in several secretory tissues such as the adrenals (Hillman, Seliger and Burk, 1975) and teleost pseudobranch (Copeland and Dalton, 1959), the latter of which has been implicated as a source of carbonic anhydrase production (Copeland, 1951; Fairbanks, Hoffert and Fromm, 1969).

CONCLUSIONS

The ultrastructure of the rete mirabile of Salmo gairdneri differs considerably from the morphology presented for Fundulus grandis, the only other choroidal rete to have been studied and published at an electron microscopic level (Copeland, 1974a). Rather than a species specific difference, it has been pointed out that the apparent difference is probably due to the fixation technique employed in the preparation of each tissue. In teleosts, it has been concluded that when working with vascular tissues, extra precautions must be taken in the collection procedure to avoid clotting of the blood which has been shown to cause drastic changes in the ultrastructural morphology of capillaries. Also, an immersion fixation technique is deemed preferable to a perfusion technique due to the delicate nature of the endothelial walls, particularly in those areas of the choroidal rete in which the wall is composed merely of two adjacent endothelial cells lacking supportive basement membranes or pericytes.

Discussion of the functional significance of each structure studied within the choroid layer has been based only upon the morphological findings and not upon direct experimental evidence. The features seen, however, must still be taken into account when explaining any empirical evidence regarding this tissue. Indeed, the structures seen

suggest directions which may be taken in future investigations which have heretofore gone uninvestigated. Perhaps the most significant example is that of the role which neuro-muscular elements within the arterial manifold may play in the regulation of flow through the choroidal vascular bed and of its influence upon the operation of the counter-current exchanger. Also, no morphological barriers were seen to exist for the counter-current exchange of gas within the rete. It was concluded, however, from the morphological evidence presented herein that it is very unlikely that the counter-current exchange of any other molecular substance requiring specialized diffusional or transport pathways occurs. This, however, remains to be verified by empirical measurements. Finally, morphological features which typically characterize active areas of exchange are relatively scarce in the one area of the choroid which is the only possible site of exchange for the retina, that is, the choriocapillaris, Bruch's membrane, pigment epithelium complex. The resolution of this apparent contradiction also awaits further experimental evidence.

Having presented the basic ultrastructure in Salmo gairdneri upon which any functional model must operate, it remains to demonstrate the possibility of a local focus of carbonic anhydrase in the counter-current exchanger and its likely source of origin as suggested by the short-circuit model (Fairbanks, Hoffert and Fromm, 1974).



PART II

INTRODUCTION

In tracing the path along which blood must flow from the heart to the eye, it is seen that in Salmo gairdneri blood passes from the heart sequentially through the conus arteriosus, ventral aorta, afferent branchial artery, afferent filamental vessels, and out into the microcirculation of the secondary lamellae. Here oxygen and carbon dioxide are exchanged, and a certain degree of ionic regulation occurs. From the secondary lamellae, blood then flows through the efferent filamental vessels, the efferent branchial vessels and then unite to form the dorsal aorta where oxygenated blood may either flow anteriorly to the head through the internal carotid arteries, or posteriorly to the bulk of the systemic circulatory beds.

In the first branchial arch (anterior-most arch), unlike in the other arches, oxygenated blood may also flow ventrally in the efferent branchial vessel to the point of junction between the branchial arch, the operculum, and the lower jaw. Without branching, this vessel, which is now termed the afferent pseudobranch artery, leads directly to the inner surface of the operculum where it proceeds dorsally and laterally roughly paralleling the opercular cover margin until arriving at the pseudobranch. The pseudobranch is morphologically and phylogenetically a vestigial gill lying on the inner surface of the operculum, and in the

rainbow trout is isolated from the buccal chamber by an overlying layer of dermal tissue. In the pseudobranch, blood flows into vessels homologous to afferent filamental vessels, through a system of capillaries similar to that of the secondary lamellae and leaves via efferent filamental vessels to the efferent pseudobranch artery. Qualitative changes in the blood passing through the pseudobranch remain to be definitively determined, and the possible role of the pseudobranch is discussed below.

Blood passes directly from the pseudobranch to the choroid layer of the eye. Thus, the efferent pseudobranch artery is synonymous with the ophthalmic artery. Interposed between the pseudobranch and the choroid is a communicating artery which allows an anastomosing pathway between the right and left ophthalmic arteries, presumably as a protective mechanism should one afferent blood supply become damaged or otherwise occluded.

The pattern of blood flow through the choroidal vasculature has been discussed (Part I). It now remains to be seen what happens to the blood in passing through the pseudobranch and choroidal rete mirabile counter-current exchange system, and more specifically, where along this path are the foci of carbonic anhydrase activity, which are essential in the counter-current concentration of oxygen.

Fairbanks, Hoffert and Fromm (1974) have proposed a theoretical mechanism for the counter-current multiplication

of oxygen by the choroidal rete mirabile. They postulated that strategically placed foci of carbonic anhydrase activity must be present within the choroidal vasculature in order to prevent the diffusion of carbon dioxide from the efferent to the afferent retial vessels. They reasoned that if carbon dioxide were allowed to diffuse into the afferent vessels, a premature release of oxygen from the hemoglobin would occur creating a gradient for oxygen to flow into the efferent vessels and entirely bypass the circulation carrying it to the retinal border. The retial carbonic anhydrase activity was proposed to be present at some location in the efferent vessels to trap this carbon dioxide before a short circuiting could occur. They further speculated that it must be present on lumenal membrane receptor sites on the efferent rete endothelia since carbonic anhydrase inhibitor of low diffusibility, CL-11,366, not only rapidly stopped oxygen concentration by the system, but also accumulated in the rete in a time course paralleling the inhibitory effects, and not in the erythrocytes or retina. Finally, it was speculated that if the carbonic anhydrase were on membrane receptors, it may have originated from an exogenous source. All blood passing to the choroidal rete must first pass through the pseudobranch, and it has long been known that pseudobranch tissue has a high concentration of carbonic anhydrase. Copeland (1951) and Fairbanks, Hoffert and Fromm (1969) proposed that the pseudobranch may secrete

carbonic anhydrase for use in the swimbladder and choroid retia. Finally, with the advent of electron microscopy, it was discovered that the pseudobranch had a very characteristic cell type of unknown function which appeared suspiciously to be of secretory nature, that is, having a mitochondrial network associated with a massive tubular system which emptied onto the capillary endothelium (Harb and Copeland, 1969).

Since the work of Fairbanks, Hoffert and Fromm (1974), an improved technique for staining carbonic anhydrase had been developed and applied to electron microscopy largely by Seymour Rosen and colleagues at Harvard Medical School. The technique is based on the degradation of bicarbonate into carbon dioxide and hydroxyl ion by carbonic anhydrase. The tissue is floated on an incubation medium allowing loss of carbon dioxide to the atmosphere and causing a localized alkalization in the tissue at the site of carbonic anhydrase activity. The alkalization causes a local deposition of a cobalt salt which is later converted to cobalt sulfide, a black precipitate in light microscopy and an electron dense precipitate in the electron microscope.

In Part II, the localization of sites of carbonic anhydrase activity in the choroidal vasculature and the pseudobranch was attempted using both light and electron microscopic techniques. It was hoped that an important addition could be made to the body of evidence regarding the short-

circuit model of counter-current multiplication of oxygen.

LITERATURE REVIEW

The Historical Elucidation of Retial Function

Upon anatomical investigation of the choroid rete mirabile, it became obvious that the choroidal rete morphology is very much like that of the swimbladder rete mirabile-gas gland complex. The structural similarities of these two organs are striking. Both contain a rete mirabile associated with a specialized epithelial layer; the gas gland epithelium in the swimbladder, and the pigment epithelium in the choroid.

In 1806, Biot had shown that oxygen tensions within the swimbladder were so high that a pressure gradient of over 100 atmospheres exists between the dissolved blood gases and the bladder gases so secretion had to occur. Much later, in 1911, Woodland showed that this secretion was accomplished by the complex of the gas gland and rete mirabile (Haldane, 1927). Upon discovery of the choroidal rete, it was then natural to question whether the rete of the choroid performed a similar function in the eye.

It was with this reasoning that Wittenberg and Wittenberg (1962) first undertook the task of measuring the oxygen tensions in the eye of various teleost species. According to their findings, oxygen tensions at the vitreal surface of the retina were found to attain levels far above arterial oxygen tensions, often ranging from 400 torr to

1000 torr in those species with well-developed choroidal rete mirabiles. With the development of better recording devices, Fairbanks, Hoffert and Fromm (1969) then demonstrated the same phenomenon to occur in the rainbow trout, Salmo gairdneri.

With a similar structure and function having been demonstrated, the elucidation of the mechanism behind this capability remained. The swimbladder mechanism has long been discussed and much empirical evidence has accumulated upon which a working hypothesis has been constructed. Steen (1970) has reviewed the distribution, structure, and the historical development of thought regarding the mechanism of function proposed for the swimbladder oxygen multiplier. It has thus far been presumed that the mechanism behind the function of both the choroidal and swimbladder retia is identical. An explanation of these proposals and some of the assumptions upon which they are based are presented below.

The configuration of the rete is one which may act both as a counter-current exchanger and a counter-current multiplier. A counter-current exchanger is a system in which all exchange processes are strictly passive, substances merely diffusing down their respective gradients. In a counter-current multiplication mechanism, other active processes which involve more complex chemical reactions are involved. Here, the processes which make the rete an active multiplier are due to the characteristics of both hemoglobin and ionic

solutions which affect their gas transporting capabilities.

The Rete Mirabile As An Exchanger

The importance of the rete as a counter-current exchanger stems from the fact that it presents a barrier to the leakage of gas down the extremely large gas gradients present. As blood passes through the swimbladder or eye, it is exposed to very high oxygen tensions, for example, 450 torr in the eye of S. gairdneri (Fairbanks, Hoffert and Fromm, 1969). The blood leaving this region will possess comparable partial pressures of oxygen. Upon entering the efferent vessels of the rete mirabile, blood comes into close contact with blood in the afferent rete vessels of much lower partial pressure. The gas will then flow down its pressure gradient such that the partial pressures in both streams will approach each other. Depending upon the efficiency of this counter-current exchange system, the oxygen tension of the blood leaving the efferent rete vessels will be very close to, but slightly higher than that of the blood entering the afferent rete vessels. The efficiency of the rete as a gas exchanger is determined by the area, the thickness, and the gas permeability of the membrane shared by the afferent and efferent blood, as well as by the rate of flow which determines the length of time the two streams of blood are in contact.

Marshall (1972) has extensively surveyed the occurrence and form of the swimbladder rete in marine teleosts. He

points out that in the deep water forms, in order to maintain neutral density, the swimbladder, as a buoyancy device, must secrete gasses into the bladder lumen at much higher pressures. As stated above, the efficiency of the rete mirabile as an exchanger is dependent among other things upon the length of its capillaries. Marshall (1972) did indeed find a direct correlation between depth of occurrence and rete length: 0.75-2.0 mm in upper mesopelagic species (ca. 200-600 m); 3.0-7.0 mm in lower mesopelagic species (ca. 600-1200 m); and 15-25 mm in the deepest living benthopelagic species (1500 m and below); 8-12 mm in species between 800-2000 m. In two interesting apparent exceptions to this trend, the retia were shorter than expected, but the fish had evolved such that the vessels were smaller diameter so that the exchange surface area was greater and the erythrocytes had become enucleate so that they could pass through the smaller bore vessels. Wittenberg and Haedrich (1974) recently surveyed the occurrence of the choroid rete and found no correlation between rete capillary length and depth of habitat. In fish with larger eyes, the number, not the length, of vessels increased. The vessel length was quite uniform.

In summary, the importance of the rete mirabile in its capacity as a counter-current exchanger lies in the fact that it prevents blood leaving the circulation of the swimbladder or eye from depleting the high oxygen tensions

present. Workers all agree that the rete provides a barrier for depletion of high oxygen tensions, but this, of itself, does not explain how the high tensions are generated.

The Rete Mirabile as a Multiplier

Because blood does not act as a simple solution in transporting gases, other processes must be taken into account. The concentration and multiplication of oxygen arises from the fact that there is a reduction in gas solubility in the vicinity of the area of buildup. The phenomena which create this reduction in whole blood carrying capacity are as follows:

1) Bohr effect: as the pH decreases and carbon dioxide increases, it takes higher partial pressures of oxygen to saturate the blood, thus the affinity of hemoglobin for oxygen is reduced,

2) Root effect: as the partial pressure of carbon dioxide rises, the oxygen carrying capacity of the hemoglobin is reduced, and

3) Salting-out effect: in any solution an increase in ionic concentration results in a decreased solubility for gases.

In both choroidal and swimbladder retial systems, the epithelial layers and related tissues are characterized by having intense glycolytic activity such that lactic acid is produced at a great rate even under aerobic conditions (D'Aoust, 1970; Hoffert, Eldred and Fromm, 1974). This

lactic acid acts to acidify and to increase the ionic strength of the blood passing through these tissues. This activates all three of the above mechanisms and insures that oxygen and other gases, such as nitrogen, which may be in solution, are released and trapped in the exchanger mechanism. The importance of the lactic acid in the operation of the counter-current multiplier of the swimbladder has been demonstrated. D'Aoust (1970), using oxamic acid, a competitive inhibitor of lactic dehydrogenase, demonstrated the complete inhibition of the secretory capability of this tissue. He further demonstrated that the lactic acid is derived from circulating blood glucose rather than from endogenous glycogen stores in the secretory epithelium.

The Role of Carbonic Anhydrase

The counter-current multiplication mechanism has also been shown to be dependent upon the enzyme, carbonic anhydrase. Acetazolamide inhibition completely and rapidly destroys the elevated oxygen tensions in the eye (Fairbanks, Hoffert and Fromm, 1969) and also in so doing disrupts the functional integrity of the retina as seen by a decline in the ERG b-wave (Fonner, Hoffert and Fromm, 1973). There are three sources of carbonic anhydrase in the vicinity of the counter-current multiplier mechanism: the retina, the erythrocytes, and the rete endothelia. Fairbanks, Hoffert and Fromm (1974) have recently proposed a "short-circuit" model which offers an explanation for the effect of carbonic anhy-

drase inhibitors, and the roles which are played by each site of carbonic anhydrase activity. Retinal carbonic anhydrase catalyzes the dissociation of carbonic acid which results from the neutralization of lactic acid by bicarbonate, thus producing carbon dioxide and water. The carbon dioxide enters the efferent blood and a portion enters the erythrocytes where erythrocyte carbonic anhydrase hydrates it to form bicarbonate, the latter of which leaves the red blood cell to aid in neutralizing more lactic acid in the retina. Hydrogen ion is also formed and this causes the Bohr and Root shifts to occur, thus releasing oxygen from the hemoglobin. The remaining carbon dioxide which was not sequestered by the erythrocytes enters the plasma to increase the carbon dioxide tension. The natural tendency would be for this carbon dioxide to diffuse down its gradient into the afferent stream causing a premature release of oxygen which then would diffuse down its gradient into the efferent rete vessel and pass out of the eye without ever reaching the choriocapillaris. In order to prevent this short-circuiting of the counter-current multiplication mechanism, Fairbanks et al. (1974) deduced that there must also be a rete mirabile carbonic anhydrase somewhere in the efferent endothelial wall which would act to hydrate the carbon dioxide before it can do this. In so doing bicarbonate ion would be produced which would flow into the afferent rete in exchange for chloride ion. In this manner, not only is the

buildup of carbon dioxide prevented, but recycling of bicarbonate ion for lactic acid neutralization is accomplished.

Acetazolamide would inhibit all of these forms of carbonic anhydrase so that the specific site of activity which was crucial for the operation of the counter-current multiplication mechanism remained in question. Fairbanks, Hoffert and Fromm (1974) then found that CL-11,366, a carbonic anhydrase inhibitor of low diffusivity, inhibited oxygen concentration as rapidly and to the same degree as acetazolamide. They also were able to demonstrate that only in the rete was there evidence of a retention and progressive accumulation of the inhibitor in a time course paralleling the inhibition of the counter-current multiplication mechanism. Because CL-11,366 is an inhibitor of low diffusivity, they concluded that either the rete endothelia walls could be more permeable to it than the retina or erythrocytes; or the rete carbonic anhydrase could be bound to the luminal wall of the capillary so that it is exposed to the non-diffusible inhibitor.

It has long been a matter of debate as to the possibility of the pseudobranch being active in the secretion of carbonic anhydrase for use in the counter-current multiplication systems of the swimbladder and choroidal retina. Wittenberg and Haedrich (1974) suggested that the pseudobranch acts in consort with the choroid rete to create a

high oxygen tension without a simultaneous buildup of carbon dioxide. The pseudobranch is known to contain a large concentration of carbonic anhydrase (Hoffert and Fromm, 1966; Maetz, 1956). Copeland (1951) and Fänge (1953) demonstrated a depression of secretion of gas into the swimbladder after cauterization or extirpation of the pseudobranch and Copeland thus suggested that the pseudobranch might be serving to secrete carbonic anhydrase for use in the swimbladder. Later, Fairbanks, Hoffert and Fromm (1969) suggested a similar function for the choroid rete multiplier. Maetz (1956), however, could find no difference in the carbonic anhydrase concentration in the afferent versus the efferent pseudobranch artery and he therefore concluded that the pseudobranch did not secrete carbonic anhydrase. Also, Fairbanks et al. (1974) followed the accumulation of the inhibitor CL-11,366 in the various tissues in conjunction with the time course of oxygen decline at the retinal-vitreous interface. No CL-11,366 was found in the pseudobranch ten minutes after injection, although the oxygen concentrating mechanism was still repressed at this time. That the pseudobranch does have a very intense carbonic anhydrase activity is not questioned, however, and its usefulness at this site has proved to be a persistent conundrum despite repeated efforts to find the reason for its presence. Wittenberg and Haedrich (1974) suggested that pseudobranchial carbonic anhydrase acts to remove carbon dioxide from the blood.

entering the rete and thus acts in consort with the choroid rete to create a high oxygen tension without a simultaneous buildup of carbon dioxide.

The pseudobranch possesses a very characteristic cell type whose origin was for many years a matter of considerable debate. It was believed by some to be a form of chloride cell (Newstead, 1971), but it has since been fairly well-established as an independent cell type. With light microscopy, these cells appear to be characteristically acidophilic (Hoffert and Fromm, 1965). At the electron microscopic level, it is seen to have a large number of mitochondria in association with a dense network of smooth endoplasmic reticulum.

Numerous speculations regarding the function of the acidophilic pseudobranch-type cells have been made. Since they resemble chloride cells of the gills, much work has been done in futile attempts to prove an osmoregulatory function for the pseudobranch-type cells (Newstead, 1964; Holliday and Parry, 1962; Kessei and Beams, 1962). Perhaps the most convincing evidence thus far presented has come from the work of Laurent and Rouzeau (1972). In studying the innervation of the pseudobranch, they have shown that neural receptors from the glossopharyngeal nerve are sensitive to changes in blood pH, P_{CO_2} , P_{O_2} , osmotic concentration, sodium ion concentration and to pressure. For this reason, they have suggested an apparent homologous role to

the mammalian carotid body and carotid sinus complexes. They have also noted the presence of carbonic anhydrase in the pseudobranch-type cell and have demonstrated on a light microscopic level of resolution its localization within the pole of the cell which is rich in smooth endoplasmic reticulum tubular system. They suggest that this morphology is indicative of a specialized receptor ending associated with the receptor functions which they demonstrated. Until more definitive evidence is presented, however, this conclusion may not be entirely correct. In view of the anatomical relationship between the pseudobranch and the eye, and the function of carbonic anhydrase in the retial oxygen multiplication mechanism, there is still a possibility that the pseudobranch plays a vital role in the operation of this mechanism in teleosts.

Carbonic Anhydrase Histochemistry

A relatively recent technique has been developed which was used by Laurent, Dunel and Baretts (1969) for the histochemical localization of carbonic anhydrase. The technique had been criticized, but the criticisms have been countered (Rosen and Musser, 1972; Lönnerholm, 1974) and the technique is now fairly well-established. Details of the method have been reviewed and revised by Cassidy and Lightfoot (1974) and Rosen (1974). Essentially, the reaction which is utilized in the staining procedure is the dehydration of bicarbonate ion into carbon dioxide and hydroxyl ion (Cassidy

and Lightfoot, 1974). The carbon dioxide is lost to the air and the tissue is alkalinized in the vicinity of the reaction. A cobalt salt is the basic metal salt which is precipitated at the site of tissue alkalinization. The cobalt salt (either as a carbonate, phosphate, or hydroxylate) is then converted to cobalt sulfide which is visible as a black precipitate under the light microscope and which, according to Rosen (1974), is visible as an electron dense precipitate in the electron microscope. Cassidy and Lightfoot, however, were not able to visualize cobalt sulfide in the electron microscope, so they modified the procedure to convert it to lead sulfide which is presumably more electron dense. Because the Cassidy and Lightfoot modification was not known until after the present investigation, the technique of Rosen and Musser (1972) was followed in the current study.

MATERIALS AND METHODS

Utilizing the techniques of Rosen and Musser (1972) and Hansson (1967) with consideration for the precautions which were determined to be necessary against clotting, the following procedure was used for the histochemical localization of carbonic anhydrase activity within the choroid and pseudobranch.

Rainbow trout, Salmo gairdneri, were taken from holding tanks kept at $12 \pm 1.0^{\circ}\text{C}$ and anaesthetized with MS 222 (tricane methane sulfonate). The fish were then heparinized (0.03 U.S.P. units/g total body weight) through the caudal vein and released into fresh water for ten minutes to allow circulation of the heparin. They were then single pithed. Pseudobranchs were removed and the eyes were enucleated and placed immediately into a glass petri dish containing cold (ca. 4°C) 0.17 M cacodylate buffered, 3% glutaraldehyde containing 7% sucrose and 2 U.S.P. units per ml Panheprin. The sclera was removed from over the choroid, and the cornea, iris, and lens were removed from the eyes while immersed in the fixative. The pseudobranchs were cut into strips of about 1 x 2 x 5 mm. These tissues were then placed in fresh fixative and allowed to stand for three hours at 4°C with hourly changes of fixative. At the end of this period, the tissues were washed three times in cold (4°C) buffer (0.17 M cacodylate buffered 0.9% saline with 7% sucrose) at ten

minutes per step. They were then frozen onto cryostat chucks with Ames O.C.T. Compound (Ames Company, Elkhart, Indiana, 46514). Frozen tissues were then sectioned at 8-10 μm and picked up on Millipore filters (25 μm thick, 0.45 μm pore size). These sections were then floated on the surface of an incubation medium ($1.75 \times 10^{-3}\text{M}$ CoSO_4 , $5.3 \times 10^{-2}\text{M}$ H_2SO_4 , $4.7 \times 10^{-3}\text{M}$ KH_2PO_4 , $1.57 \times 10^{-1}\text{M}$ NaHCO_3). As a control, adjacent sections were floated simultaneously on an identical incubation medium containing 10^{-5}M sodium acetazolamide. Tissues were not allowed to dip below the surface of the incubation medium which would prevent the staining reaction. The concentration of NaHCO_3 is ten times the concentration of that published by Rosen (1970), but the same as that published originally by Hansson (1967), a point which caused much difficulty at the onset of the experiment. The incubation time was ten minutes. This was followed by flotation of the sections sequentially for: two minutes in a wash solution ($6.7 \times 10^{-4}\text{M}$ KH_2PO_4 , 0.17 M cacodylic acid, 7% sucrose); three minutes in a blackening solution (0.6% $(\text{NH}_4)_2\text{S}$); and twice at two minutes per step in a 0.9% saline solution.

Wet tissues were then placed on a microscope slide and observed under a light microscope to check for proper staining and occasionally for photography. Tissues were then either permanently mounted on glass slides or embedded for ultra-thin sectioning for electron microscopy.

For light microscopy, sections were dehydrated in a 70°C oven for several hours and then mounted on a glass slide with Permount. The Millipore filter usually remained attached to the section throughout the procedure so that it was dehydrated and mounted along with the tissue. Both cleared upon mounting in Permount.

For electron microscopy, tissues were dehydrated in a graded ethanol series (30%, 50%, 70%, 95%, and 100%) at 15 minutes per step and in fresh 100% ethanol overnight. Whenever possible, the Millipore filters were removed during the dehydration process because they seemed to dissolve and interfere with the complete polymerization of the Spurr's embedding medium with which the tissues were impregnated and molded. Sections were then taken on a Porter-Blum Ultramicrotome MT-2. Some of the experimental sections were observed unstained in order to detect the CoS precipitate. Other experimental sections and the acetazolamide inhibited sections were counterstained with lead citrate and uranyl acetate according to the method of Reynolds (1963).

Also, pseudobranch tissues were fixed in heparinized Karnovsky's fixative and postfixed in 2% osmium tetroxide, dehydrated, and embedded in Spurr's embedding medium as above.

RESULTS

Light Microscopic Carbonic Anhydrase Histochemistry

Initial attempts at visualization of the foci of carbonic anhydrase activity within the choroid rete mirabile utilizing light microscopy were made. The results of these initial investigations are shown in Figures 30-33.

It took a great deal of effort to obtain the proper staining conditions under which it could be stated with certainty that the stain seen was actually the result of carbonic anhydrase activity, and that it could be inhibited at low concentrations of acetazolamide. The technique is difficult in that the tissues must be floated on the surface of the incubation medium so that carbon dioxide may be lost to the atmosphere allowing a very localized alkalinization to occur. If any portions of the tissue had dipped below the surface of the incubation medium, the rate of CO₂ diffusion away from the site of activity would become rate limiting and the alkalinization and subsequent salt deposition would not occur. This was often found to be a major problem, even when using a piece of Millipore filter as a raft upon which the tissues were floated and subsequently transferred from dish to dish.

Realizing that the rete mirabile itself has its own focus of carbonic anhydrase activity from the evidence of Fairbanks, Hoffert and Fromm (1974), only those areas which

stained positively were interpreted as having been treated properly. Any unstained areas were deemed to be portions which had sunk below the media surface. Figures 30-33 were interpreted initially with this in mind.

In these micrographs it is seen that certain regions of the rete contain very intense loci of carbonic anhydrase activity. Recall that in the short-circuit model for oxygen concentration proposed by Fairbanks et al. (1974), it was hypothesized that the retial carbonic anhydrase was localized to the efferent vessel endothelia, and indeed evidence was presented which suggested that it may have been bound to the luminal membrane of the endothelium versus an intracellular site. Neither of these hypotheses was resolvable by the evidence provided by the micrographs at this level of magnification. The carbonic anhydrase activity attributable to endothelial vessel walls was seen to extend beyond the choroidal rete itself into the distribution and/or collection vessels (Figure 33). This micrograph suggested that the vessel was entirely lined by carbonic anhydrase activity and that the activity was not in this instance restricted only to the endothelial membrane lining the vessel lumen.

Choroidal Electron Microscopic Carbonic Anhydrase Histochemistry

An electron microscopic study was initiated in order to further visualize the exact foci of carbonic anhydrase activity. In preparing the tissues for embedding after

staining, thick sections were taken and observed under the light microscope in order to select the best stained areas. When this was done, it was noted that there was a definite localization of carbonic anhydrase activity toward the peripheral side of the rete vessels (Figure 34), but it was not possible to determine whether the activity was localized to the afferent or efferent vessel. Upon re-examination of the previous slides of the choroidal rete, it became evident that this was a persistent pattern so that what was once believed to have been improperly stained tissue was frequently actually inactive retial tissue located toward the central side of the rete mirabile.

The results of the electron microscopic examination of the choroidal rete tissues are presented in Figures 35-39. The appearance of the tissue was disappointing. The stain was not discrete as large, distinct grains of electron-dense precipitate marking beyond doubt the precise focus of activity. Rather, it was a very fine precipitate whose localization had often to be told by finer distinctions between different intensities of gray. Thus, only the most electron dense regions were interpreted to be areas of positive stain. Cassidy and Lightfoot (1974) also reported difficulty with this aspect of the technique.

Basically, two patterns of staining were seen within the retial endothelial cells. In Figures 37 and 38, dark bands of stain are seen to run through the cytoplasm. These

areas do not appear to be associated with any particular subcellular organelles, but more like localized regions of concentration within the cellular cytoplasmic sap. The endoplasmic reticular network is often depicted in cell biology as a large lacunar network of interconnected concentric shells which almost compartmentalize the cytoplasm. Thus, this observation may not be as surprising as first seemed. There was no evidence in this pattern which suggested in any way, that the activity may have been localized to the luminal membrane or to be in areas of direct communication with the vessel lumen.

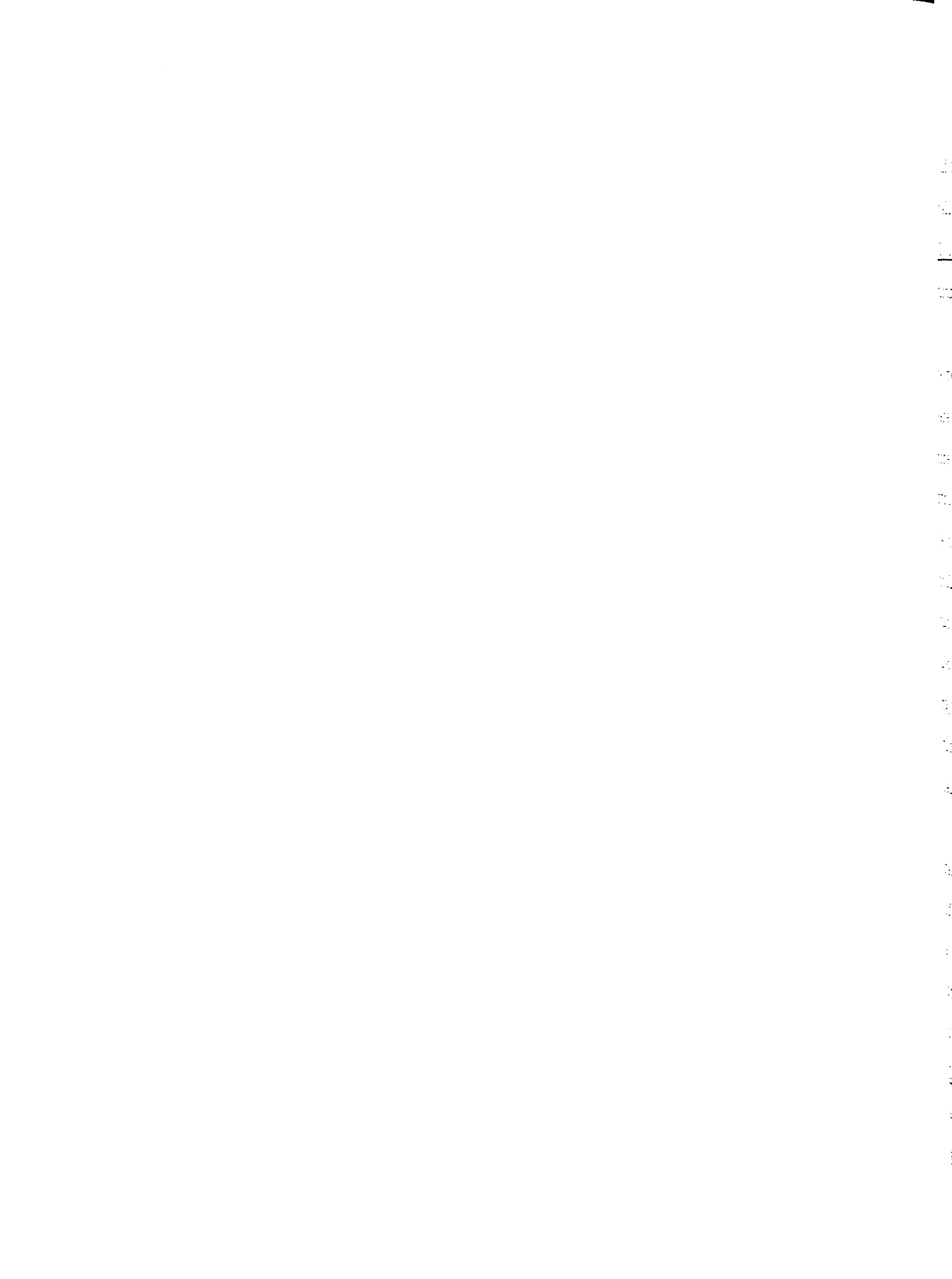
A second pattern of activity was displayed in Figure 39. Here, the activity seemed to be homogeneously distributed throughout the cytoplasm rather than in concentrated regions. More importantly, however, the activity seems to be located specifically in the endothelial cell of one vessel and not in the endothelia of two adjacent vessels. This is the only evidence seen which might suggest that the carbonic anhydrase activity might be located specifically in one vessel type and not in another. Due to the nature of the preparation it is impossible to determine whether the active cell borders on afferent or efferent vessels. Because, efferent vessels are often seen to abut one another, whereas afferent vessels rarely do (Figure 12), it might be probable that the two adjacent inactive endothelia belong to efferent vessels and the active one is of an afferent vessel. This

may not be concluded with certainty, however.

No electron microscopic observations were made on the apparent carbonic anhydrase activity in the peripheral distribution and collection vessels.

Electron Microscopic Pseudobranch Morphology

The pseudobranch was next observed in order to detect a correlation between the ultrastructural localization of the carbonic anhydrase activity and any ultrastructural features which may have been indicative of secretory activity. The pseudobranch contains a very characteristic cell type known as the acidophilic cell or pseudobranch-type cell (Figures 40-42). This is characterized as having a system of densely packed parallel mitochondria localized at the midway point between the apex of the cell and the basal border of the cell which lies adjacent to the capillary endothelium (Figure 40). Associated with these mitochondria is an extensive network of agranular or smooth endoplasmic reticulum which appear to originate in the vicinity of the mitochondria (Figure 41) and empty into the interstitial space at the basal border of the cell (Figure 42). The basal border of the pseudobranch-type cell is marked also by the presence of a distinct basement membrane. The endothelial cells associated with the pseudobranchial capillary network appears to closely resemble the pillar cells present within the secondary lamellae of the gill. They are columnar in shape sending flanges out at either end which extend



halfway around the capillary lumen (Figure 40). This endothelial wall has been reported to be fenestrated in Perca fluviatilis (Laurent and Rouzeau, 1972), but no fenestrations were observed in Salmo gairdneri.

A point of interest is the fact that there appeared to be two distinct forms of pseudobranch-type cells. Both were identical morphologically, but one counter-stained much more densely, almost to the point of obscuring its ultrastructure. A similar observation was briefly mentioned by Newstead (1964) in the chloride cells of the tide pool sculpin, Oligocottus maculosus. In that the chloride cell has its own very distinctive morphology (Harb and Copeland, 1969), the possibility that the more electron dense form may have been a chloride cell has been rejected. The functional significance of these two forms of pseudobranch-type cell in Salmo gairdneri remains to be elucidated.

One final observation which was made, was the occurrence in the pseudobranch-type cell of a very dense packing of tubules such that in cross-section they appeared to form a microrete. Unfortunately, this was observed once and not photographed. Abel (1973) has reported that he found a similar arrangement of tubules in the chloride cell of Salmo gairdneri. No explanation of its role was offered, and none may currently be advanced in the present investigation.

Pseudobranch Carbonic Anhydrase
Histochemistry

With the light microscope, the carbonic anhydrase stain appeared to be dense and ubiquitous throughout the pseudobranchial tissue. This is consistent with the fact that the pseudobranch has a very high carbonic anhydrase activity (Hoffert, 1966), but inconsistent with the findings of Laurent, Dunel and Baretts (1969) who, using a similar technique, found the stain within the pseudobranch-type cell to be localized to the tubular system in the basal border of the cell at a light microscopic level.

The electron microscopic investigation of carbonic anhydrase activity in the pseudobranch, like that in the choroidal rete tissue, proved to be disappointing. The results are shown in Figures 43, 44 & 45. Again, the nuclei were seen to "artificially" stain heavily in this preparation. In comparison to the control acetazolamide inhibited tissues, a ubiquitous background cytoplasmic stain was seen and the mitochondrial matrix seemed denser as well (Figure 45). Very close inspection of Figure 43 reveals, however, that there is a very distinct black grainy precipitate concentrated around the nuclear envelope of the pseudobranch cell and it is detectable in widely dispersed locations throughout the cell. There is a distinct possibility that this may be the carbonic anhydrase precipitate and that the difference in density of the background of Figure 45 may be due to variations in tissue thickness. A second possi-

bility is that the cell seen is a dense form of the pseudobranch cell versus a light form. If this is the case, then the actual amount of this grainy precipitate present in the cell of Figure 43 nowhere approaches the amount which must have been present at the time of light microscopic examination. This would indicate that an extraction of the precipitate may have occurred somewhere in the dehydration and/or embedding process. It had been observed upon trimming of the polymerized blocks for subsequent ultramicrotomy, that the tissues had seemed less densely stained than before embedding, but this was merely a subjective observation and not considered serious at that time. A further refinement of the technique is deemed desirable at this point. Decisive conclusions regarding the localization of carbonic anhydrase activity within the pseudobranch should await resolution of this problem.

DISCUSSION

Interpretation of Carbonic Anhydrase Histochemistry

The information contained within this section is based entirely upon the reliability of the histochemical method utilized for the demonstration of carbonic anhydrase activity. Difficulties were encountered in the interpretation of the electron micrographs. Consequently, it would be appropriate to justify the basis for the interpretations presented and to reiterate the degree of reliability which may be placed upon each of these interpretations.

Perhaps the most valuable information comes from the study of the choroidal rete mirabile under the light microscope. Here it was seen that the carbonic anhydrase intensifies in activity down the length of the rete toward the periphery. Utmost confidence should be placed in the validity of this conclusion due to the consistency of these observations over all sections viewed, and to the abolition of the pattern upon treatment with acetazolamide. That carbonic anhydrase activity was seen to be associated with vessels beyond the rete is also a certainty.

Once the technique was refined, no problems were encountered with light microscopic carbonic anhydrase histology. Because identical procedures were used in staining the tissues embedded for electron microscopy, no problems

were anticipated in the subsequent electron microscopic investigation. Several authors had used this technique in electron microscopy with apparent success in a variety of tissues, including the rabbit retina (Bhattacharjee, 1971), frog and turtle lungs (Fain and Rosen, 1973), turtle and toad urinary bladder (Rosen, 1972a), and toad, turtle, pigeon, rat, rabbit, dog, and monkey renal tissues (Rosen, 1972b). Most of this work had been done by Seymour Rosen and colleagues at Harvard Medical School and he has recently published a chapter in an electron microscope histochemistry text (Rosen, 1974). Without exception the reaction product visualized in the electron micrographs published in these works has been a very fine precipitate. No micrographs of acetazolamide inhibited tissues, however, have ever accompanied these figures. Rather "control" sections used were tissues which had been fixed in osmium tetroxide and glutaraldehyde and subsequently counter-stained with lead citrate and uranyl acetate in much the same manner utilized in the Part I of this current study. In the most dramatic of the micrographs, a very high magnification of the carbonic anhydrase stained tissue appears as if it could be a negative of the normally prepared tissues (Musser and Rosen, 1973). It is normal histochemical procedure to observe the localization of reaction product in comparison with an identically treated tissue in which only the enzyme of interest has been inhibited. With the carbonic anhydrase stain, this is

particularly important due to the occurrence of significant amounts of reaction product deposited as a result of the uncatalyzed reaction. In addition, the appearance of tissues is very different when osmium tetroxide fixation is omitted. Among other things, lipids will be extracted and membranes will be absent. Hayat (1970) presents an extensive description of the differences to be expected.

The problems encountered in interpretation of the electron micrographs of the current investigation should now be familiar. Cassidy and Lightfoot (1974) have noted that they, too, have had difficulty in the visualization of the cobalt sulfide reaction product in their tissue preparations and found it necessary to modify their techniques such that the cobalt salt is converted by one additional step into lead sulfide ($\text{CoS} + \text{Pb}(\text{NO}_3)_2 \rightarrow \text{PbS}$) which appears to be a much more electron dense precipitate. The electron micrographs published by these authors seem to be much more convincing and their technique should be seriously considered in any future histochemical studies.

In the current study, the differences between carbonic anhydrase stained tissues and acetazolamide inhibited tissues may be interpreted in two ways. First, the difference was often dependent upon a subjective, qualitative estimate of degrees of grayness (Figure 45). Secondly, the possibility that the grainy regions in Figure 43 could be the true reaction product has also been pointed out. Conclusions based

upon the electron microscopic investigations must, therefore, be interpreted with these reservations in mind.

Choroidal Carbonic Anhydrase

It was decided that only the most electron-dense regions in the electron micrographs presented herein could be interpreted as valid signs of carbonic anhydrase activity. The two observations which appeared to be the most conclusive are based upon Figures 37, 38 & 39. The banding patterns of very electron-dense stain seen in areas of the rete endothelial cytoplasm were not seen in acetazolamide treated tissues (Figure 36). As stated previously, they do not appear to be associated with any specific subcellular organelles and their significance is not known at this time. Figure 39 provides more definite contrast within a single micrograph and may perhaps be interpreted with more confidence. Here, evidence is seen for a difference in activities between vessels.

In summary, the evidence which has been accumulated is: 1) there is a definite polarization of carbonic anhydrase activity along the length of the rete, the higher concentrations occurring toward the peripheral side, 2) the activity may include sites in larger vessels located distal to the rete itself, and 3) there is some evidence for the existence of a difference in activity between the two classes of retial vessel. It cannot yet be stated with certainty that the regional localization of carbonic anhydrase activity is also

accompanied by a structural differentiation in the endothelial cells. In Part I of this study, no ultrastructural differences were seen along the length of the retial vessels. Wittenberg and Wittenberg (1974) noticed a distinct difference between the ends of the rete on a gross structural level, but not at an ultrastructural level. Any model for the operation of the oxygen concentrating mechanism must now be able to account for these findings in addition to the existing evidence.

Functional Implications

Fairbanks, Hoffert and Fromm (1974) have most conclusively demonstrated the dependence of the oxygen multiplication mechanism upon a source of carbonic anhydrase found within the choroidal rete vasculature itself. That this activity does exist is demonstrated in the current study. According to the short-circuit theory presented by Fairbanks et al. (1974) the carbonic anhydrase was postulated to have been localized in the efferent rete endothelia. In this position the enzyme system could operate to sequester carbon dioxide and convert the carbon dioxide to bicarbonate before the gas has a chance to diffuse down its concentration gradient and cause a premature release of oxygen by the Bohr and Root shifts in the afferent rete capillaries. The finding that the carbonic anhydrase is localized to the peripheral end of the rete is certainly consistent with this notion. The highest concentration of carbonic anhydrase activity is in

the location where the highest carbon dioxide concentrations are encountered in the returning blood. The assumption now is that the quantities of carbonic anhydrase at this end are adequate to handle all excess carbon dioxide which would cause a short-circuiting of the multiplier before reaching the central end of the rete. A restriction of the activity to only the efferent vessel endothelia would seem to be unnecessary. As long as the carbonic anhydrase were interjected somewhere along the diffusion path of the carbon dioxide it would be capable of operating in the proper manner.

The current study has presented evidence that carbonic anhydrase may indeed be restricted to only one vessel type (Figure 39). Even though it is impossible to state to which category of vessel the apparent activity is restricted on the basis of ultrastructural features, the likelihood of the active vessel being an afferent vessel is fairly good. As already stated, because the efferent vessels are often seen to abut one another, whereas afferent vessels rarely do, it is probable that the two adjacent inactive endothelia belong to efferent vessels and the active one is of an afferent vessel. Thus, based upon evidence presented above, a high degree of carbonic anhydrase activity is suggested to be localized in the peripheral end of the afferent rete vessel endothelia.

Note that the carbonic anhydrase activity also exists in the endothelia of the peripheral vessels. If the activity were found to be restricted to only one vessel type (i.e., distribution vs. collection vessel), then the distribution vessel would likely be the one containing carbonic anhydrase activity. In this case it would merely represent an extension of endothelial cellular specialization for carbonic anhydrase production from the afferent retial vessels. At this time, however, this postulate must remain speculative.

Due to the rapidity of inhibition of the oxygen multiplication mechanism by the non-diffusible carbonic anhydrase inhibitor, CL-11,366, Fairbanks et al. (1974) speculated that the carbonic anhydrase activity may have been restricted to membrane receptor sites or some sort of lacunae in the endothelial cell which was in direct contact with the vessel lumen. This was not seen to be the case in the present study. The activity in all cases seemed to be localized in the cytoplasm. In accounting for the rapidity with which CL-11,366 worked, and for the fact that its accumulation only in the rete paralleled the time course of inhibition, possibly pinocytotic activity of these endothelia may account for this observation. No such pathway for uptake would exist in either the erythrocytes or the retinal cells whose carbonic anhydrase may also be involved.

The pseudobranchial ultrastructure in Salmo gairdneri was seen to fit the description for other species. Fenestrae

present in the capillary endothelium adjacent to the basal border of the pseudobranch-type cell have been seen in Perca fluviatilis (Laurent and Rouzeau, 1972), but were not seen in S. gairdneri. Were the pseudobranch active in the secretion of carbonic anhydrase or any other large molecular species, one would suspect the presence of endothelial fenestrae as a passageway into the vessel lumen. In addition, a cell type specialized for carbonic anhydrase synthesis would be expected to contain ultrastructural features more characteristic of protein synthesis (eg. rough endoplasmic reticulum, free ribosomes, and mitochondria). Smooth endoplasmic reticulum in association with mitochondria as found in the pseudobranch are seen in other tissues and have been implicated in steroid synthesis and glycogen and lipid metabolism (Rhodin, 1974). In a light microscopic study, Laurent, Dunel and Baretts (1969) demonstrated polarization of carbonic anhydrase activity to the basal pole of the pseudobranch-type cell which is characterized by a dense tubular network. Although carbonic anhydrase within this cell was not conclusively localized in the current study at the resolution attainable by electron microscopy, it may be stated with confidence that no stain was seen within the tubules of this region. Thus, it is unlikely that carbonic anhydrase might be produced in the vicinity of the mitochondria and passed through the tubules to the capillary

lumen, to be carried to the swimbladder and choroidal retia as has been implied previously.

SUMMARY AND CONCLUSIONS

Problems do exist with the histochemical technique for carbonic anhydrase localization at the electron microscopic level. The results have been interpreted with these reservations in mind. Recommendations that future attempts be made utilizing the techniques recently proposed by Cassidy and Lightfoot (1974) have been discussed.

Based upon the findings presented it has been found that carbonic anhydrase activity within the choroidal rete mirabile is localized to the peripheral half of the rete and may extend out into the peripheral distribution and collection vessels. Suggestions have been made that this activity is further restricted to the afferent rete endothelium. These sites of activity have also been shown to be consistent with the short-circuit model for oxygen multiplication. This mechanism requires that retial carbonic anhydrase be made available at the proper location in order to intercept diffusing carbon dioxide and thus prevent the premature release of oxygen in the afferent blood.

The normal ultrastructure of the pseudobranch-type cell was studied and found to be structurally similar to those investigated elsewhere. A light and dense form were identified and the presence of a microretial arrangement of smooth endoplasmic reticulum was noted. The significance of these structures is not known. Due to the nature of the results

of the histochemical study no conclusions may be drawn regarding the possibility that pseudobranchial secretion of carbonic anhydrase may occur for subsequent usage in the choroidal counter-current oxygen multiplier.

COMBINED SUMMARY AND CONCLUSIONS

Before the onset of any detailed carbonic anhydrase localization studies, it became necessary to become thoroughly familiar with the vascular pattern and normal ultrastructural features of the vessels within the choroidal layer of Salmo gairdneri. Both light and electron microscopic investigations were pursued.

The major findings and conclusions are dividable into three main categories: technique information, morphological information, and carbonic anhydrase histochemical information. The latter of these categories is then useful in clarifying the current understanding of the mechanism behind the operation of the counter-current oxygen multiplier.

Techniques Findings

Methods of tissue preparation may drastically affect the appearance of delicate endothelial tissue in the choroid rete mirabile under the electron microscope. Perfusion fixation of this tissue was particularly dangerous in that delicate efferent endothelial walls may easily be damaged. Hence, an optimal immersion technique was sought. Teleost blood clots very rapidly, therefore, special precautions need to be taken to prevent clot formation which is seen to drastically affect the appearance of the vascular tissues in particular. The final optimal technique involved in vivo

heparinization of the ocular tissues prior to enucleation and fixation in Karnovsky's fixative.

Technical problems also arose related to the visualization of the carbonic anhydrase stain reaction product, cobalt sulfide, under the electron microscope. The precipitate appeared very fine and difficult to visualize. This problem was delineated and all interpretations were made with this reservation in mind. It was noted that other investigators had apparently found the same difficulty and a newer technique utilizing lead sulfide as the electron dense precipitate is recommended for further studies.

Morphological Findings

The general outlay of the choroidal vasculature has been carefully examined and found to be similar to patterns reported elsewhere (Barnett, 1951; Wittenberg and Wittenberg, 1974; Copeland, 1974a). The arterial manifold wall is seen to be a thick structure with a single layer of endothelia facing the lumen of the arterial manifold and venous sinusoid, and sandwiching a thick collagenous layer through which run fibroblasts, smooth muscle cells, and myelinated and non-myelinated neurons. The possible importance of the arterial manifold as an effector organ for the regulation of rete counter-current multiplier operation is discussed. The rete mirabile ultrastructure reported here is slightly different from the structures reported elsewhere for both the swimbladder and the choroid retina. The vessel packing

pattern is cubic, with an equal number of afferent and efferent vessels. The endothelia lining both afferent and efferent vessels appear essentially identical in structure. Nonetheless, afferent vessels are differentiable on the basis of their size (4.5 μm vs. 9.5 μm) and by the fact that only afferent vessels are seen associated with pericytes and basement membranes. Peripheral distribution and collection vessels pass through a loose, laminar stroma containing numerous melanocytes. No features were seen to distinguish collection from distribution vessels. The choriocapillaris and associated Bruch's membrane and pigment epithelium were seen to be identical to those of Esox lucius (Braekevelt, 1974). The choriocapillaris is relatively nonfenestrated compared to the choriocapillaris of humans. Bruch's membrane has fewer structural features than that in the human and the pigment epithelium lacks a convoluted basal border typical of the human pigment epithelium.

The ultrastructural features of the pseudobranch-type cells were identical to those reported elsewhere. The most characteristic features are numerous densely packed mitochondria associated with an extensive network of smooth endoplasmic reticulum. In addition, it was noted that two morphologically identical forms of the cell were seen differing in their affinity for normal stains.

Carbonic Anhydrase Histochemistry

Light microscopic observations revealed that within the choroidal vasculature carbonic anhydrase activity is found to increase in intensity toward the peripheral side of the rete vessels. It was also seen to be located in the walls of some larger vessels peripheral to the rete.

Electron microscopic observations were interpreted with great caution. It appeared, however, that carbonic anhydrase activity in the rete endothelia was within the general cytoplasm either in bands or spread evenly throughout the cytoplasm. No evidence was seen for a luminal membrane-bound focus of carbonic anhydrase activity. Evidence was cited for the localization of carbonic anhydrase to one type of retial vessel and not another, and that the active vessel was probably afferent.

It is suggested that retial carbonic anhydrase activity is restricted to the peripheral side of the afferent rete endothelium and extends out into the endothelia of the distribution vessels. It is argued that location is sufficient to prevent the short-circuiting of the counter-current multiplier.

RECOMMENDATIONS

As in any study, more questions remain unanswered than answered. A few of these questions which are seen to be of immediate significance are listed below.

Morphological studies on the choroidal vasculature remain incomplete. The structure of the venous sinusoid remains to be elucidated.

Laurent and colleagues at the Laboratoire de Neurophysiologie Generale du College de France, have done the most extensive work on the pseudobranch and their studies have lent the most credible evidence thus far offered as regards pseudobranchial function. Their work had included light microscopic studies of innervation, in which neural tracts have been traced from their central origins to their terminations in the pseudobranch (Laurent and Dunel, 1966); histochemical studies of carbonic anhydrase activity (Laurent, Dunel and Baretts, 1969); and perfusion studies in conjunction with microelectrode recordings of afferent neural impulses which has revealed much information on receptor function (Laurent and Rouzeau, 1972). The current study has shown the presence of neural elements within the choroidal arterial manifold wall and the suggestion has been made that there may exist a regulatory role for this structure in the operation of the oxygen multiplier mechanism. A series of studies very similar to those mentioned above

would yield invaluable evidence to support or contradict this hypothesis. If such a mechanism were discovered, it would be interesting to compare its responses with the autoregulatory responses seen in the ocular vasculature of higher forms. There would be reason to believe that this mechanism might also be an integral part of other retial systems, such as that in the swimbladder rete, and possibly, the thermoregulatory retia in the carotid arterial pathway to the brain of some desert antelopes, or in the retia of the flippers of the whale.

Within the choroidal rete mirabile a localization of carbonic anhydrase activity along the length of the rete has been demonstrated. Although no evidence was seen regarding a parallel structural differentiation in the current study, the results are not conclusive, and a more detailed examination of this possibility would definitely be instructive.

The structures of the choriocapillaris, Bruch's membrane, and pigment epithelium in Salmo gairdneri have been noted to be markedly different from those seen in the human eye. It has been suggested that in the higher vertebrates, the choroidal vasculature is the major site of nutrient exchange while the retinal circulation is largely the site of gas exchange (Braekevelt, 1974). Because there is no retinal circulation in teleosts all exchange processes must occur at the choriocapillaris. It would naturally follow that the teleost morphology would display structures which are



associated with an augmented exchanger role, such as numerous pores or fenestrae. The opposite is seen, however. The degree of fenestration is vastly reduced in the two teleosts now studied. It would seem that classical electron microscopic tracer studies are called for here, perhaps starting with such tools as horseradish peroxidase (Karnovsky, 1967).

The carbonic anhydrase histochemical technique obviously needs improvement. The procedures utilized by Cassidy and Lightfoot (1974) have been recommended as the next viable alternative. When this procedure is perfected for use in electron microscopy, the findings which were seen in this study should be reconfirmed and extended. It would be of value to determine the extent of the activity present in the peripheral vessels of the choroid. Also, with an important functional significance described for this enzyme in the choroidal rete, it would seem likely that a similar function might exist certainly in the swimbladder rete and perhaps in other counter-current systems. This possibility should be investigated. The subcellular localization of carbonic anhydrase activity in the pseudo-branch-type cells would also be of value. If morphological evidence existed for the secretion of carbonic anhydrase by the pseudobranch, one would then logically search for a specific isoenzyme of carbonic anhydrase produced by the pseudobranch and to trace its possible role in the choroidal and swimbladder counter-current multipliers.

Finally, as a comparative study, phylogenetic and developmental variations on the general scheme drawn from the evidence from the above studies might be researched.

LITERATURE CITED

LITERATURE CITED

- Abel, P. D. 1973. An Unknown Structure in the Chloride Cells of the Gill Epithelium of the Rainbow Trout (Salmo gairdneri). Z. Zellforsch., 146:293-295.
- Anderson, D. H. and S. K. Fisher. 1975. Disc Shedding in Rodlike and Conelike Photoreceptors of Tree Squirrels. Science, 187: 953-955.
- Arnott, H.J., A. C. G. Best, S. Ito and J. A. C. Nicol. 1974. Studies on the Eyes of Catfishes with Special Reference to the Tapetum Lucidum. Proc. R. Soc. Lond. B., 186:13-36.
- Barnett, C. H. 1951. The Structure and Function of the Choroidal Gland of Teleostean Fish. J. Anat., 85:113-119.
- Barraco, D. A. 1975. Thermal Consideration of the Choroidal Gland Rete Mirabile in the Rainbow Trout (Salmo gairdneri). M.S. Thesis, Michigan State University, East Lansing, Michigan.
- Bennett, H. S., V. H. Luft and J. C. Hampton. 1959. Morphological Classifications of Vertebrate Blood Capillaries. Amer. J. Physiol., 196:381-390.
- Bergman, H. L. 1973. Regulation of Blood Flow Through the Isolated-Perfused Gills of Rainbow Trout: Effects of Vasoactive Agents on Functional Surface Area. Ph.D. Thesis, Michigan State University, East Lansing, Michigan.
- Bernstein, M. H. and M. J. Hollenberg. 1965. Fine Structure of the Choriocapillaris and Retinal Capillaries. Invest. Ophthal., 4:1016-1025.
- Bhattacharjee, P. 1971. Distribution of Carbonic Anhydrase in the Rabbit Eye as Demonstrated Histochemically. Exp. Eye Res., 12:356-359.
- Braekevelt, C. R. 1974. Fine Structure of the Retinal Pigment Epithelium, Bruch's Membrane, and Choriocapillaris in the Northern Pike (Esox lucius). J. Fish. Res. Bd. Canada, 31:1601-1605.

- Brown, L. J., A. L. Stalker and J. Hall. 1969. Experimental Defibrination. II. Histological Studies by Light and Electron Microscopy. *Microvas. Res.*, 1: 295-307.
- Bruns, R. R. and G. E. Palade. 1968a. Studies on Blood Capillaries: I. General Organization of Blood Capillaries in Muscle. *J. Cell Biol.*, 37:244-276.
- Bruns, R. R. and G. E. Palade. 1968b. Studies of Blood capillaries: II. Transport of Ferritin Molecules Across the Wall of Muscle Capillaries. *J. Cell Biol.*, 37:277-299.
- Cassidy, M. M. and F. G. Lightfoot. 1974. "Carbonic Anhydrase," in Electron Microscopy of Enzymes: Principles and Methods. Edited by M. A. Hayat. Vol. 3, pp. 77-106. VanNostrand Reinhold Co., New York.
- Castro-Correia, J. 1967. Studies on the Innervation of the Uveal Tract. *Ophthalmologica*, 154:497-520.
- Clementi, F. and G. E. Palade. 1969. Intestinal Capillaries: I. Permeability to Peroxidase and Ferritin. *J. Cell Biol.*, 41:33-58.
- Copeland, D. E. 1951. Function of Glandular Pseudobranch in Teleosts. *Amer. J. Physiol.*, 167:775.
- Copeland, D. E. 1974a. The Anatomy and Fine Structure of the Eye of Teleost. I. The Choroid Body in Fundulus grandis. *Exp. Eye Res.*, 18: 547-561.
- Copeland, D. E. 1974b. The Anatomy and Fine Structure of the Eye of Teleost. II. The Vascular Connections of the Lentiform Body in Fundulus grandis. *Exp. Eye Res.*, 19:583-589.
- Copeland, D. E. and A. J. Dalton. 1959. An Association Between Mitochondria and the Endoplasmic Reticulum in Cells of the Pseudobranch Gland of a Teleost. *Biophys. Biochem. Cytol.*, 5:393-395.
- D'Aoust, B. G. 1970. The Role of Lactic Acid in Gas Secretion in the Teleost Swim Bladder. *Comp. Biochem. Physiol.*, 32:637-668.
- Dorn, E. 1961. Uber den Feinbau der Schwimmblase Von Anguilla vulgaris L: Licht- und Elektronenmikroskopische Untersuchungen. *Z. Zellforsch.*, 55:849-912.

- Fahlén, G. 1967. Morphological Aspects on the Hydrostatic Function of the Gas Bladder of Clupea harengus L. Acta Univ. Lund., 28:1-37.
- Fain, W. and S. Rosen. 1973. Carbonic Anhydrase Activity in Amphibian and Reptilian Lung: A Histochemical and Biochemical Analysis. Histochem. J., 5:519-528.
- Fairbanks, M. B. 1970. The Importance of the Enzyme Carbonic Anhydrase in Ocular Oxygen Concentration in the Rainbow Trout, Salmo gairdneri. Ph.D. Thesis, Michigan State University, East Lansing, Michigan.
- Fairbanks, M. B., J. R. Hoffert and P. O. Fromm. 1969. The Dependence of the Oxygen-Concentrating Mechanism of the Teleost Eye (Salmo gairdneri) on the Enzyme Carbonic Anhydrase. J. Gen. Physiol., 54:202-211.
- Fairbanks, M. B., J. R. Hoffert and P. O. Fromm. 1974. Short Circuiting of the Ocular Oxygen Concentrating Mechanism in the Teleost Salmo gairdneri Using Carbonic Anhydrase Inhibitors. J. Gen. Physiol., 64:263-273.
- Fänge, R. 1953. Mechanisms of Gas Transport in the Euphysoclist Swim Bladder. Acta Physiol. Scand., 30:1-133.
- Fawcett, D. W. 1961. Intercellular Bridges. Exp. Cell Res., Suppl., 8:174-187.
- Fawcett, D. W. 1966. An Atlas of Fine Structure: The Cell. Its Organelles and Inclusions. W. B. Saunders Co., Philadelphia, 448 p.
- Fawcett, D. W. and J. Wittenberg. 1959. The Fine Structure of Capillaries in the Rete Mirabile of the Swim Bladder of Opsanus tau. Anat. Rec., 133:274.
- Fawcett, D. W. and J. Wittenberg. 1962. Structural Specializations of Endothelial Cell Junctions. Anat. Rec., 142:231.
- Fonner, D. B., J. R. Hoffert and P. O. Fromm. 1973. The Importance of the Counter Current Oxygen Multiplier Mechanism in Maintaining Retinal Function in the Teleost. Comp. Biochem. Physiol., 46A:559-567.

- Francois, J. and A. Neetens. 1974. "Comparative Anatomy of the Vascular Supply of the Eye in Vertebrates," in The Eye: Comparative Physiology. Edited by H. Davson and L. T. Graham, Jr. Vol. 5, pp. 1-66. Academic Press, Inc., New York.
- Haldane, J. S. 1927. Respiration. Yale Univ. Press, New Haven. 427 p.
- Hansson, H. P. J. 1967. Histochemical Demonstration of Carbonic Anhydrase Activity. Histochemie, 11:112-128.
- Harb, J. M. and D. E. Copeland. 1969. Fine Structure of the Pseudobranch of the Flounder Paralichthys lethostigma: A Description of Chloride-Type Cell and Pseudobranch-Type Cell. Z. Zellforsch., 101:167-174.
- Hayat, M. A. 1970. Principles and Techniques of Electron Microscopy: Biological Applications. Vol. I. VanNostrand Reinhold Co., New York. 412p.
- Hillman, J. R., W. G. Seliger and P. E. Burk. 1975. "Cytochemical Studies of Protein Uptake by Adrenal Cortical Cells of the Golden Hamster," in Electron Microscopic Concepts of Secretion: Ultrastructure of Endocrine and Reproductive Organs. Edited by M. Hess. pp. 419-433. John Wiley and Sons, New York.
- Hoffert, J. R. 1966. Observations on Ocular Fluid Dynamics and Carbonic Anhydrase in Tissues of Lake Trout (Salvelinus namaycush). Comp. Biochem. Physiol., 17:107-114.
- Hoffert, J. R., G. E. Eldred and P. O. Fromm. 1974. Comparison of Direct and Indirect Calorimetry as a Method for Determining Total Energy Produced by the Isolated Retina of Rainbow Trout (Salmo gairdneri). Exp. Eye Res., 19:359-365.
- Hoffert, J. R., M. B. Fairbanks and P. O. Fromm. 1971. Ocular Oxygen Concentrations Accompanying Severe Chronic Ophthalmic Pathology in the Lake Trout (Salvelinus namaycush). Comp. Biochem. Physiol., 39:137-145.
- Hoffert, J. R. and P. O. Fromm. 1965. Biomicroscopic, Gross, and Microscopic Observation of Corneal Lesions in the Lake Trout, Salvelinus namaycush. J. Fish. Res. Bd. Canada, 22:761-766.

- Hoffert, J. R. and P. O. Fromm. 1966. Effect of Carbonic Anhydrase Inhibition on Aqueous Humor and Blood Bicarbonate Ion in the Teleost (Salvelinus namaycush). *Comp. Biochem. Physiol.*, 18:333-340.
- Hogan, M. J., J. A. Alvarado and J. E. Weddell. 1971. Histology of the Human Eye: An Atlas and Textbook. W. B. Saunders Co., Philadelphia. 687p.
- Holliday, F. G. T. and G. Parry. 1962. Electron Microscopic Studies of the Acidophil Cells in the Gills and Pseudobranchs of Fish. *Nature*, 193:192.
- Jasinski, A. and W. Kilarski. 1971. Capillaries in the Rete Mirabile and in the Gas Gland of the Swim Bladder in Fishes, Perca fluviatilis L. and Misgurnus fossilis L.: An Electron Microscopic Study. *Acta Anatomica*, 78:210-223.
- Karnovsky, M. J. 1965. A Formaldehyde-Glutaraldehyde Fixative of High Osmolality for Use in Electron Microscopy. *J. Cell Biol.*, 27:137A-138A.
- Karnovsky, M. J. 1967. The Ultrastructural Basis of Capillary Permeability Studied with Peroxidase as a Tracer. *J. Cell Biol.*, 35:213-236.
- Kessei, R. C. and H. W. Beams. 1962. Electron Microscope Studies on the Gill Filaments of Fundulus heteroclitus from Sea Water and Fresh Water with Special Reference to the Ultrastructural Organization of the "Chloride Cell". *J. Ultrastructure Res.* 6:77-87.
- Laurent, P. and S. Dunel. 1966. Recherches sur l'innervation de la pseudobranchie des teleosteens. *Arch. d'Anatomie Microscopique*, 55:633-656.
- Laurent, P., S. Dunel and A. Baretts. 1969. Localisation histochemique de l'anhydrase carbonique au niveau des chemorecepteurs arteriels des mammiferes, des batraciens et des poissons. *Histochemie*, 17:99-107.
- Laurent, P. and J. D. Rouzeau. 1972. Afferent Neural Activity from Pseudobranch of Teleosts. Effects of P_{O_2} , pH, Osmotic Pressure, and Na^+ Ions. *Resp. Physiol.*, 14:307-331.
- Leiner, M. 1938. Die Augen Keimendruse (Pseudobranchie) der Knochen Fische. Experimentelle Untersuchungen über ihre Physiologische Bedeutung. *Z. Vgl. Physiol.*, 26:416-466.

- Linthicum, D. S. and F. G. Carey. 1972. Regulation of Brain and Eye Temperatures by the Bluefin Tuna. *Comp. Biochem. Physiol.*, 43A:425-433.
- Lönnerholm, G. 1974. Carbonic Anhydrase Histochemistry, A Critical Study of Hansson's Cobalt-Phosphate Method. *Acta Physiol. Scand. Suppl.*, 418:1-43.
- Luft, J. H. 1961. Improvements in Epoxy Resin Embedding Methods. *J. Biophys. Biochem. Cytol.*, 9:409-414.
- Luna, L. G. 1968. Manual of Histologic Staining Methods of the Armed Forces Institute of Pathology. 3rd ed. McGraw-Hill Book Co., New York. 258p.
- Maetz, J. 1956. Le role biologique de l'anhydrase carbonique chez quelques teleosteens. *Bull. Biol. France and Belgique, Suppl.* 40:1-129.
- Marshall, N. B. 1972. Swimbladder Organization and Depth Ranges of Deep-Sea Teleosts. *Symp. Soc. Exp. Biol.*, 26:261-272.
- Musser, G. L. and S. Rosen. 1973. Localization of Carbonic Anhydrase Activity in the Vertebrate Retina. *Exp. Eye Res.*, 15:105-119.
- Newstead, J. D. 1964. Morphological Changes in "Chloride Cells" in the Gills of the Sculpin Oligocottus maculosus after Transfer from Sea Water to Fresh Water. *J. Cell Biol.*, 23:66A.
- Newstead, J. D. 1971. Observations on the Relationship between the 'Chloride-Type' and 'Pseudobranch-Type' Cells in the Gills of a Fish, Oligocottus maculosus. *Z. Zellforsch.*, 116:1-6.
- Noell, W. K. 1959. The Visual Cell: Electric and Metabolic Manifestations of Its Life Processes. *Amer. J. Ophthalm.*, 48:348-370.
- Pappenheimer, J. R., E. M. Renkin and L. M. Borrero. 1951. Filtration, Diffusion and Molecular Sieving Through Peripheral Capillary Membranes : A Contribution to the Pore Theory of Capillary Permeability. *Amer. J. Physiol.*, 167:13-46.
- Reynolds, E. S. 1963. The Use of Lead Citrate at High pH as an Electron-Opaque Stain in Electron Microscopy. *J. Cell Biol.*, 17:208-211.

- Rhodin, J. A. G. 1967. The Ultrastructure of Mammalian Arterioles and Precapillary Sphincters. *J. Ultrastructure Res.*, 18:181-223.
- Rhodin, J. A. G. 1968. Ultrastructure of Mammalian Venous Capillaries, Venules, and Small Collecting Veins. *J. Ultrastructure Res.*, 25:452-500.
- Rhodin, J. A. G. 1974. Histology: A Text and Atlas. Oxford Univ. Press, New York. 803p.
- Richardson, K. C., L. Jarett and E. H. Finke. 1960. Embedding in Epoxy Resins for Ultrathin Sectioning in Electron Microscopy. *Stain Tech.*, 35:313-323.
- Rosen, S. 1970. Localization of Carbonic Anhydrase Activity in Transporting Urinary Epithelia. *J. Histochem. Cytochem.*, 18:668-670.
- Rosen, S. 1972a. Localization of Carbonic Anhydrase Activity in Turtle and Toad Urinary Bladder Mucosa. *J. Histochem. Cytochem.*, 20:696-702.
- Rosen, S. 1972b. Localization of Carbonic Anhydrase Activity in the Vertebrate Nephron. *Histochem. J.*, 4:35-48.
- Rosen, S. 1974. "Carbonic Anhydrase - An Alternative Method," in Electron Microscopy of Enzymes: Principles and Methods. Edited by M. A. Hayat. Vol. 3, pp. 109-131. VanNostrand Reinhold Co., New York.
- Rosen, S. and G. L. Musser. 1972. Observations on the Specificity of Newer Histochemical Methods for the Demonstration of Carbonic Anhydrase Activity. *J. Histochem. Cytochem.*, 20: 951-954.
- Schiffman, R. H. and P. O. Fromm. 1959. Measurement of some Physiological Parameters in Rainbow Trout (Salmo gairdneri). *Can. J. Zool.*, 37:25-32.
- Smith, C. G., W. M. Lewis and H. M. Kaplan. 1952. A Comparative Morphologic and Physiologic Study of Fish Blood. *Prog. Fish Cult.*, 14:169-172.
- Spitznas, M. and E. Reale. 1975. Fracture Faces of Fenestrations and Junctions of Endothelial Cells in Human Choroidal Vessels. *Invest. Ophthalm.*, 14:98-107.
- Spurr, A. R. 1969. A Low-Viscosity Epoxy Resin Embedding Medium for Electron Microscopy. *J. Ultrastructure Res.*, 26:31-43.

- Steen, J. B. 1970. "The Swim Bladder as a Hydrostatic Organ," in Fish Physiology. Edited by W. S. Hoar and D. J. Randall. Vol. 4, pp. 413-443. Academic Press, New York.
- Wade, J. B. and M. J. Karnovsky. 1974. The Structure of the Zonula Occludens: A Single Fibril Model Based on Freeze-Fracture. *J. Cell Biol.*, 60:168-180.
- Walls, G. L. 1963. The Vertebrate Eye and Its Adaptive Radiation. Hafner Pub. Co., New York, 785p.
- Wittenberg, J. B. and R. L. Haedrich. 1974. The Choroid Rete Mirabile of the Fish Eye: II. Distribution and Relation to the Pseudobranch and to the Swimbladder Rete Mirabile. *Biol. Bull.*, 146:137-156.
- Wittenberg, J. B. and B. A. Wittenberg. 1961. Active Transport of Oxygen into the Eye of Fish. *Biol. Bull.*, 121:379.
- Wittenberg, J. B. and B. A. Wittenberg. 1962. Active Secretion of Oxygen into the Eye of Fish. *Nature*, 194:106-107.
- Wittenberg, J. B. and B. A. Wittenberg. 1974. The Choroid Rete Mirabile of the Fish Eye. I. Oxygen Secretion and Structure: Comparison with the Swimbladder Rete Mirabile. *Biol. Bull.*, 145:116-136.
- Wolf, K. 1959. Plasmoptysis and Relation of Erythrocytes in Coagulation of Blood of Freshwater Bony Fishes. *Blood*, 14:1339-1344.
- Wolter, J. R. 1960. Nerves of the Normal Human Choroid. *Arch. Ophthal.*, 64:120-124.

APPENDIX

APPENDIX: FIGURES CITED IN TEXT

FIGURE 1.--Microfil casts of the afferent vessels of the choroidal vasculature.

The photomicrographs depicted here have been taken from Fairbanks (1970). Microfil, a low viscosity silicone-based injection compound was injected into the afferent vessels of the choroidal vasculature, and the surrounding tissues were dehydrated in alcohol, and cleared in methyl salicylate.

- A. From the back of the eye after removal of the sclera, the choroidal rete mirabile is seen to be a horseshoe-shaped mass of parallel vessels overlying the optic nerve. The optic nerve is not shown here, but its position is at the center of the circle outlined by the margins of the choroidal rete. The horseshoe normally opens ventrally. The large vessel in the inner margin of the horseshoe is the arterial manifold. Normally, this is entirely enclosed by the venous sinusoid which has not been filled in this preparation. (5X)
- B. The arterial manifold bifurcates on the central side into the parallel retial vessels which then are seen to anastomose into large distribution vessels on the peripheral side. The large globular structures are artifacts resulting from rupturing of the blood vessels. (25X)

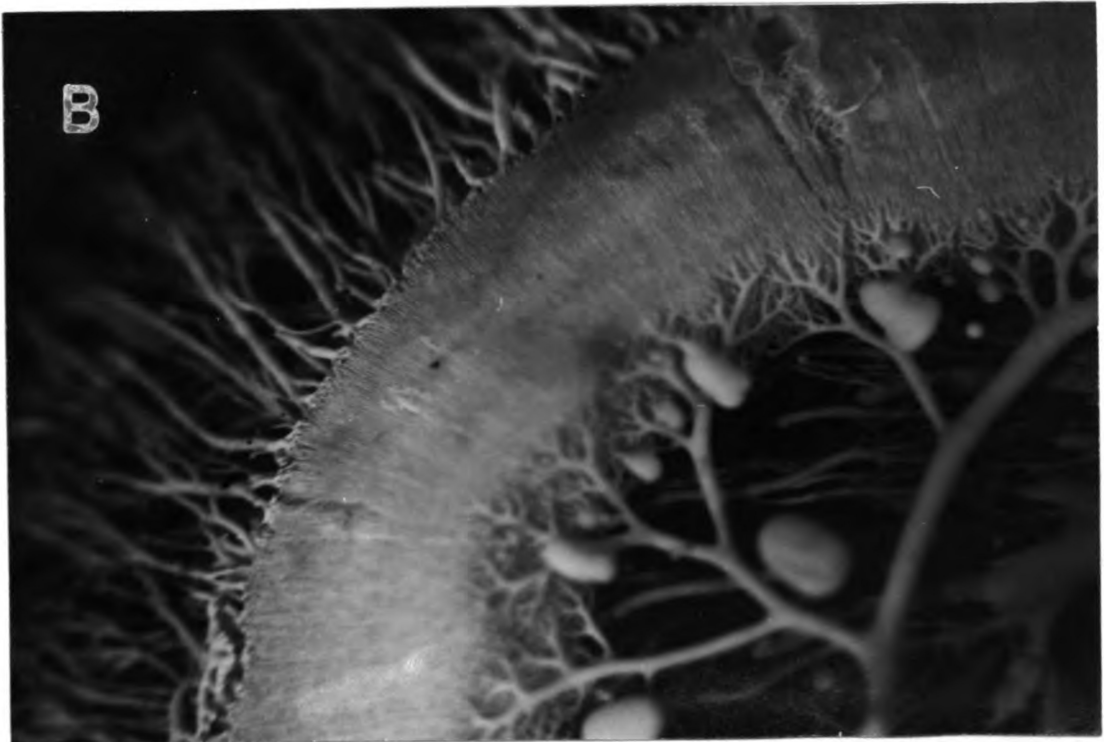
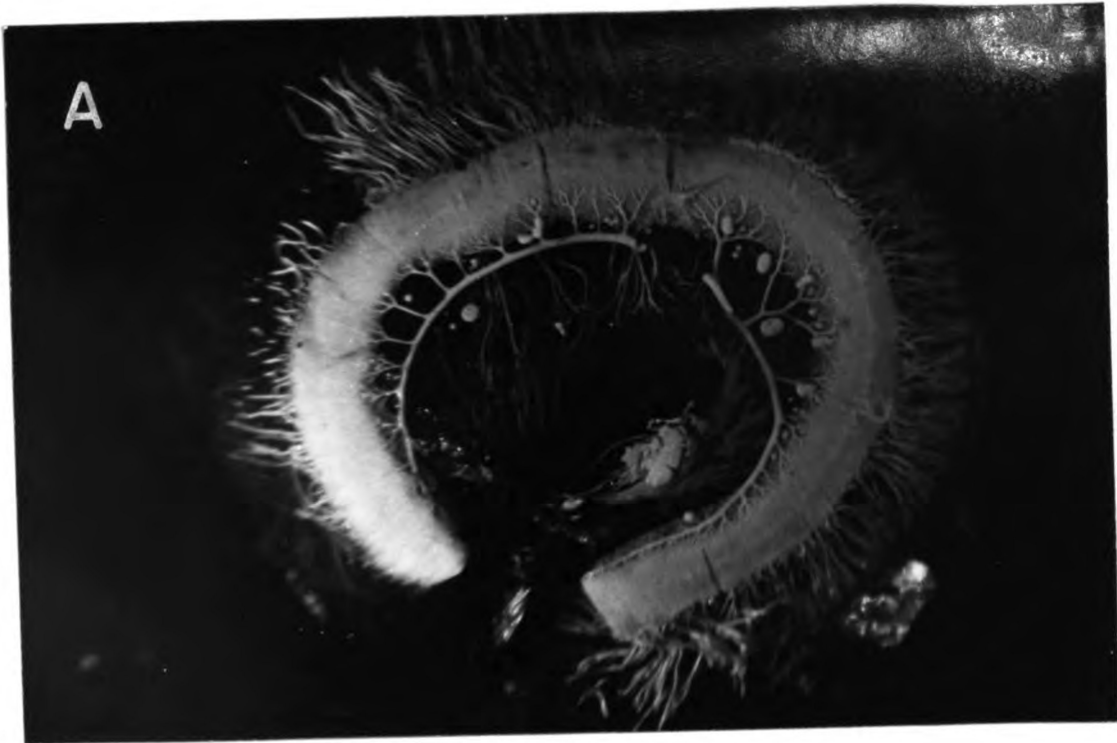


FIGURE 1

FIGURE 2.---Generalized diagram of the choroidal vascular pattern within the eye of Salmo gairdneri.

Blood enters the choroidal vasculature via an ophthalmic artery (OA) which branches into an arterial manifold (AM) which then bifurcates down into the afferent rete vessels. These vessels then converge upon larger distribution vessels (DV) on the peripheral side of the rete. These then feed a vast capillary network, the choriocapillaris (CC), supplying all areas of the retinal-choroidal interface at Bruch's membrane (BM). Large collection vessels (CV) then return blood from the choriocapillaris to the rete where they bifurcate down to small afferent vessels which lie interposed among and parallel to the afferent rete vessels. These efferent vessels finally drain into a large thin-walled venous sinusoid (VS) which encloses the arterial manifold (AM) and leads out of the eye via the ophthalmic vein (OV).

The diagram does not represent the actual scale of the vessels, but is intended to merely represent the vascular pattern for reference in further micrographs and discussion.

AM-----Arterial manifold	OA-----Ophthalmic artery
BM-----Bruch's membrane	ON-----Optic nerve
CC-----Choriocapillaris	OV-----Ophthalmic vein
CV-----Collection vessel	PE-----Pigment epithelium
DV-----Distribution vessel	RL-----Receptor cell layer
MEL-----Melanocyte	VS-----Venous sinusoid
NL-----Nerve cell layer	

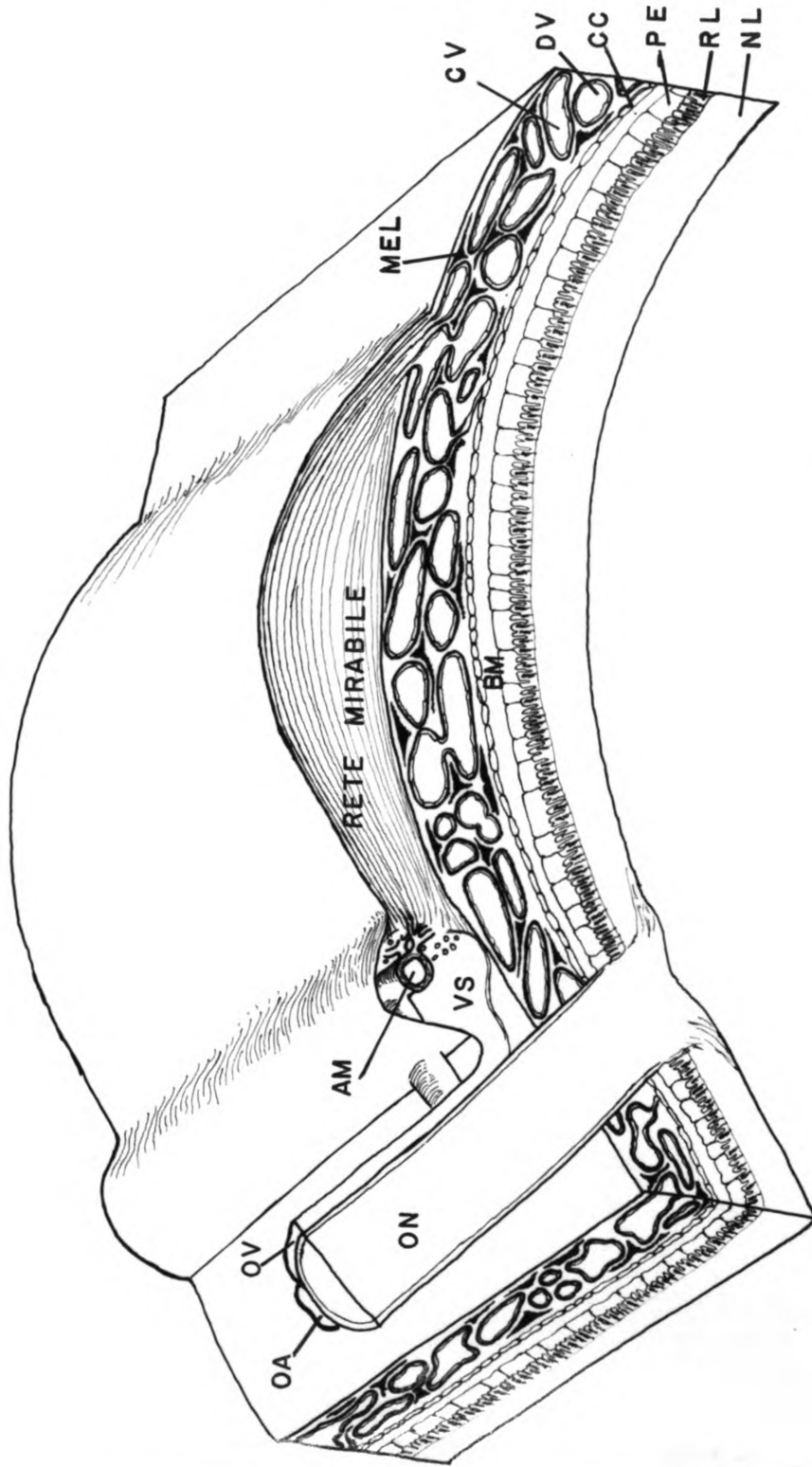
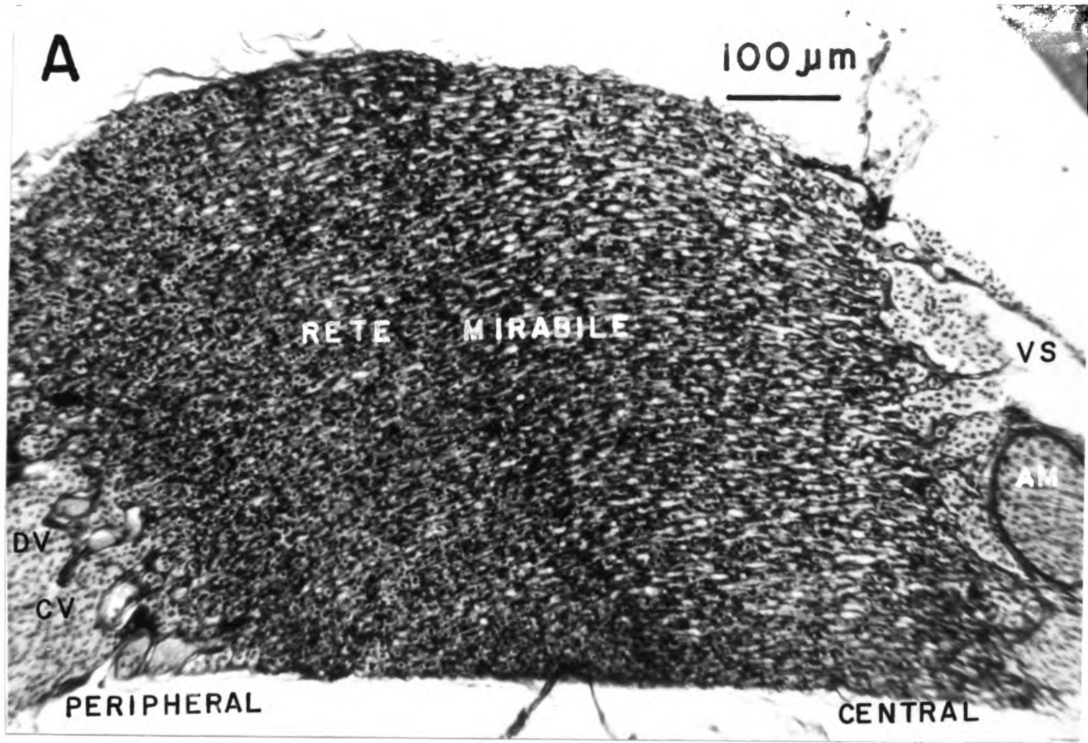


FIGURE 2

FIGURE 3.--Choroid rete mirabile (hematoxylin and eosin, 145X).

- A. Note the arterial manifold (AM) lying within the venous sinusoid (VS) at the central side of the rete mirabile, the parallel rete vessels, and their convergence into large collection and distribution (CV and DV) vessels at the peripheral end of the rete.
- B. The area enclosed within the heavy line represents the region from which the above micrograph was taken.

AM----Arterial manifold
CV----Collection vessel
DV----Distribution vessel
VS----Venous sinusoid



B

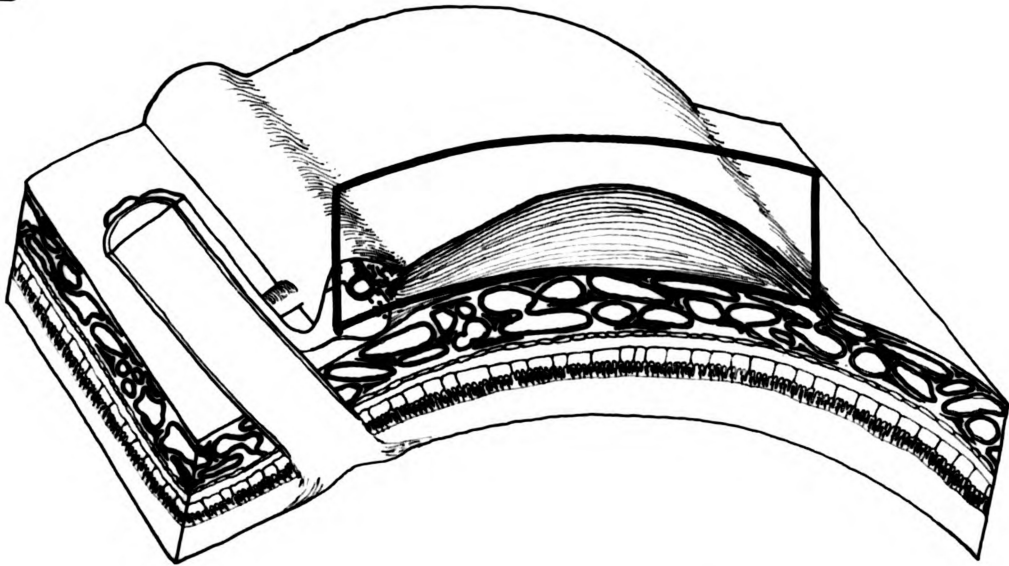


FIGURE 3

FIGURE 4.--Parallel rete vessels (Masson's trichrome, 1,480X).

- A. In longitudinal section, the afferent and efferent rete vessels are seen to lie parallel to and interspersed among each other. In this section, there is no apparent difference between the afferent and efferent rete vessels. Note that these vessels are of capillary dimensions allowing the passage of the nucleated red cells (RBC) in single file only.
- B. The area enclosed within the heavy lines represents the region from which the above micrograph was taken.

RBC----Erythrocyte

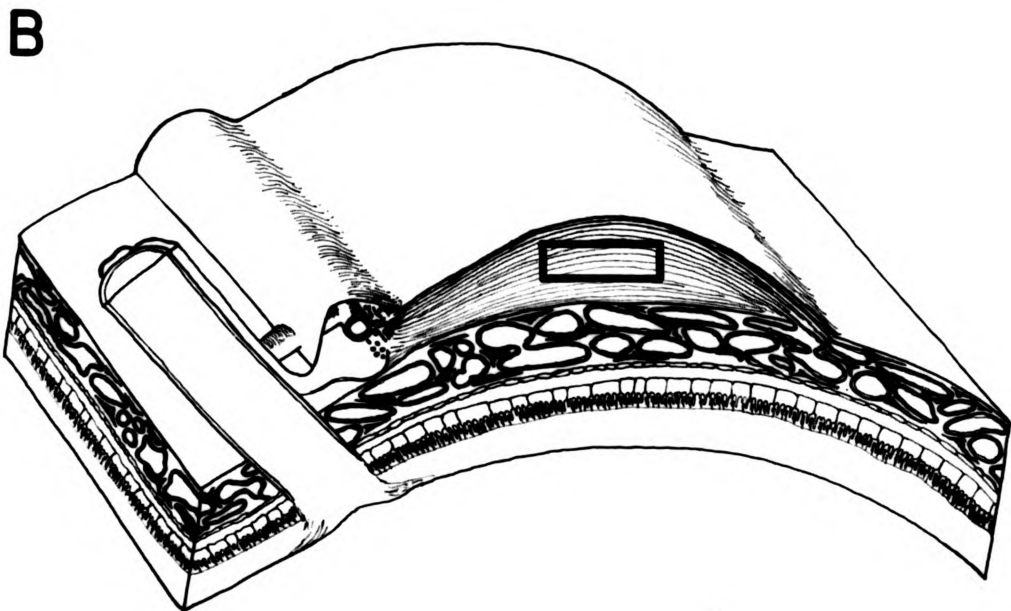
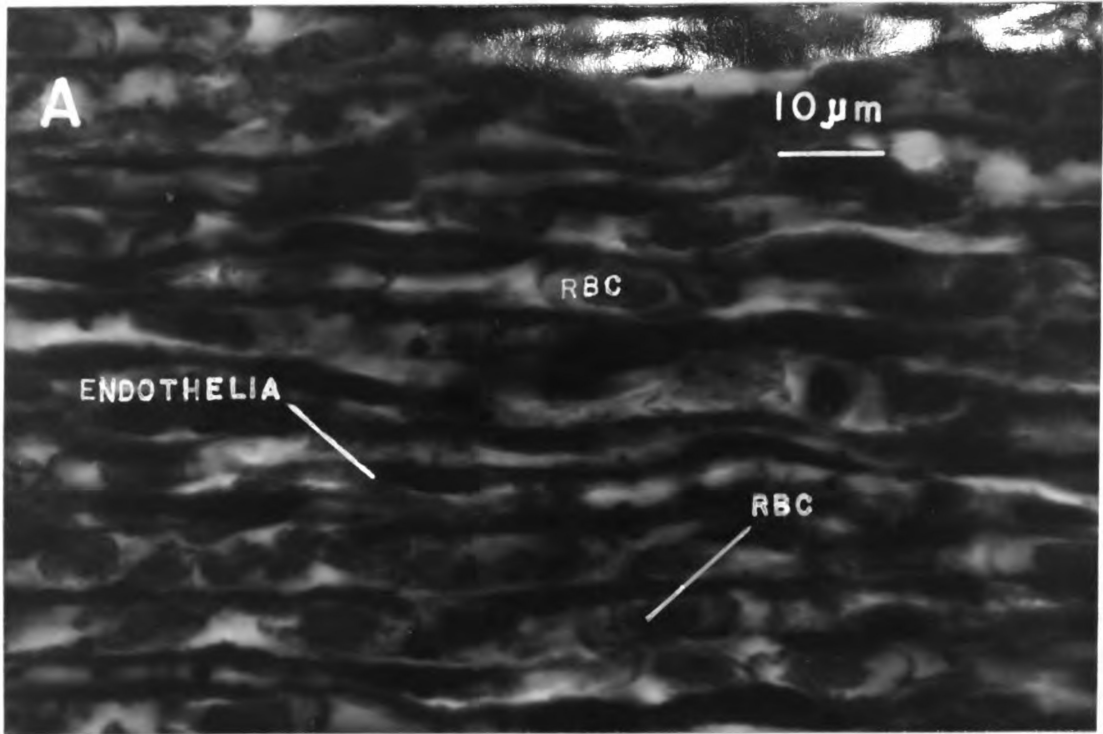


FIGURE 4

FIGURE 5.--Central side of the rete mirabile (hematoxylin and eosin, 145X).

- A. This micrograph serves to illustrate the discrete arterial manifold (AM) and the less discrete venous sinusoid (VS).
- B. The area enclosed within the heavy line represents the region from which the above micrograph was taken.

AM----Arterial manifold

VS----Venous sinusoid

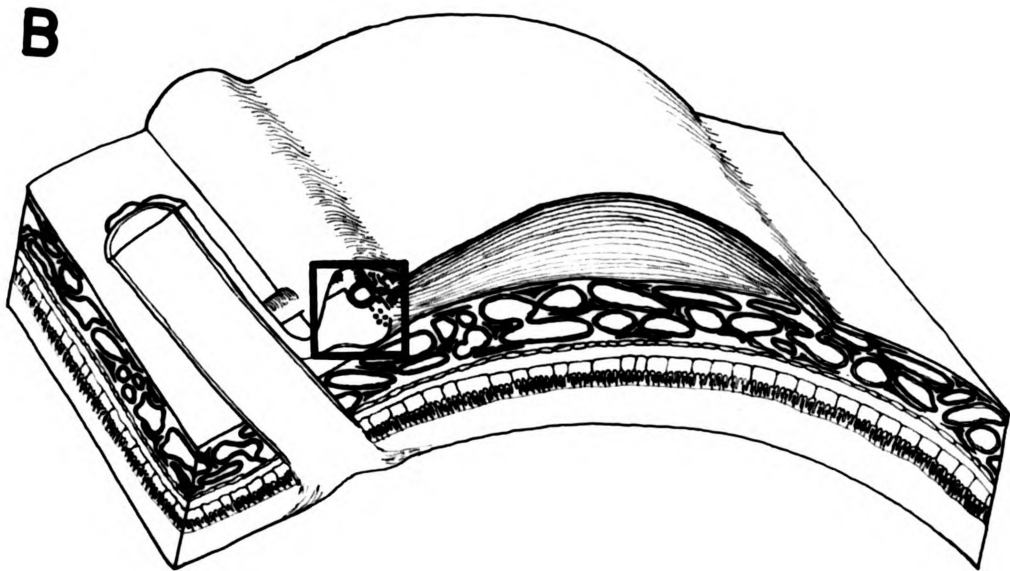
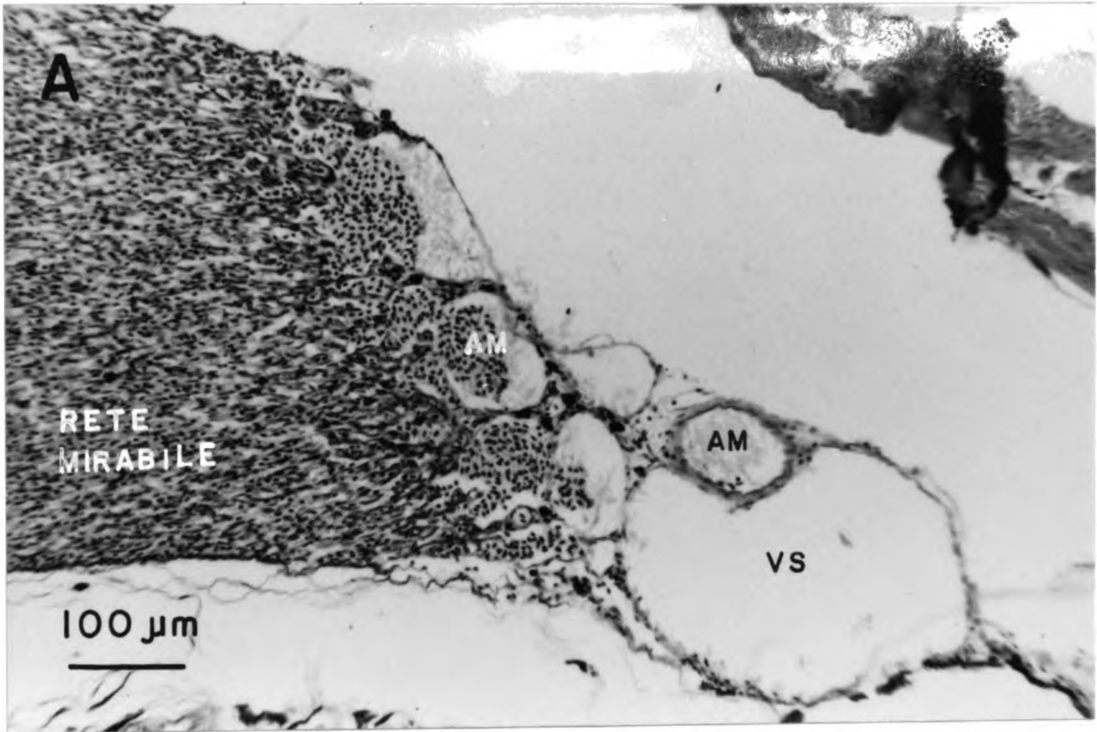


FIGURE 5

FIGURE 6.--Central side of the rete mirabile (hematoxylin and eosin, 440X).

This micrograph is from the same section seen in Figure 5. Here it is evident that the arterial manifold wall (AMW) is much thicker than is that of the venous sinusoidal wall (VSW).

AMW-----Arterial manifold wall
VSW-----Venous sinusoidal wall

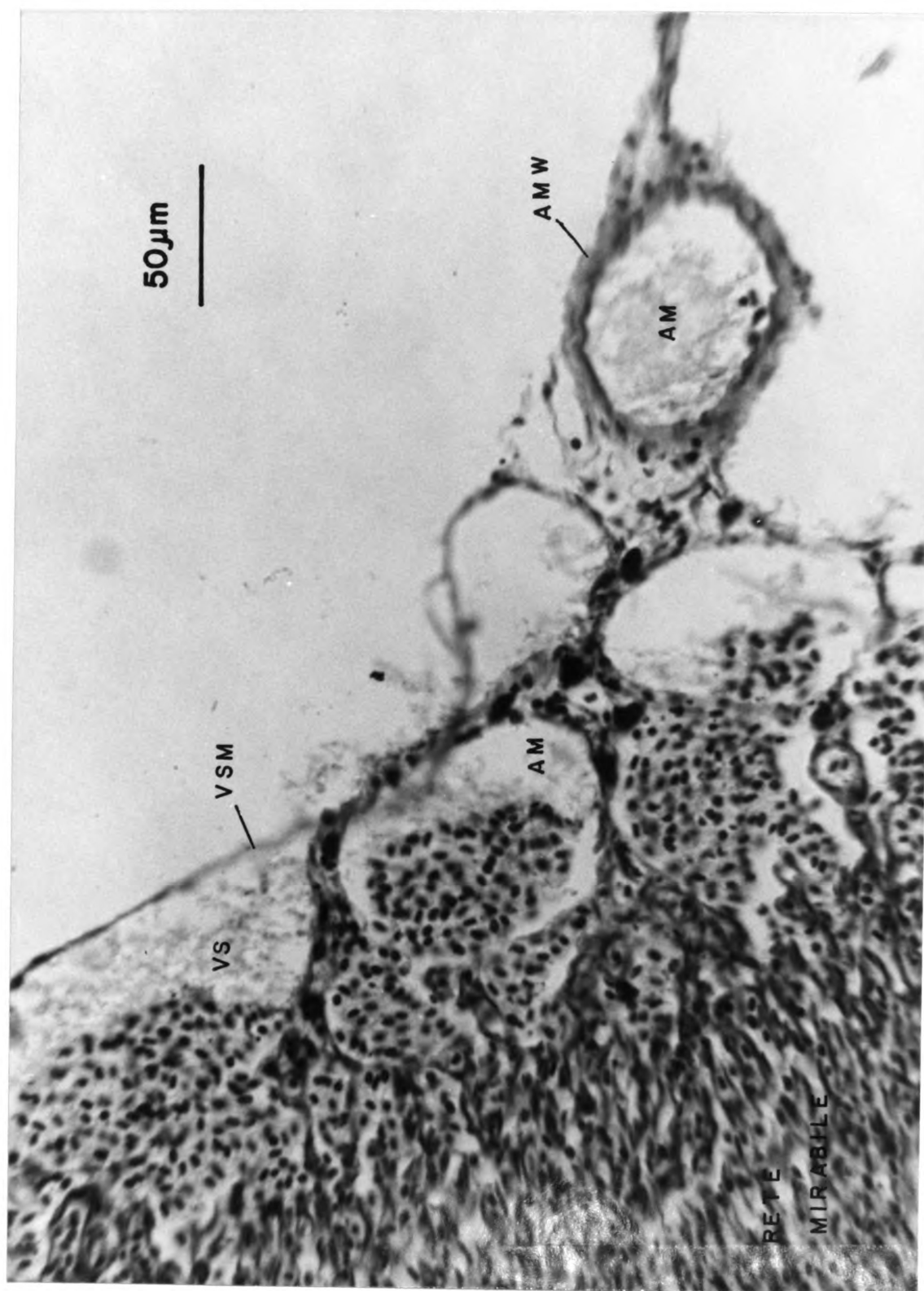


FIGURE 6

FIGURE 7.--Central side of the rete mirabile (Masson's trichrome, 295X).

- A. Masson's trichrome stains specifically for connective tissue. The arterial manifold (AM) is seen to possess a much thicker wall, rich in collagenous connective tissue, than that of the venous sinusoid (VS).
- B. The area enclosed within the heavy line represents the region from which the above micrograph was taken.

AM----Arterial manifold
VS----Venous sinusoid

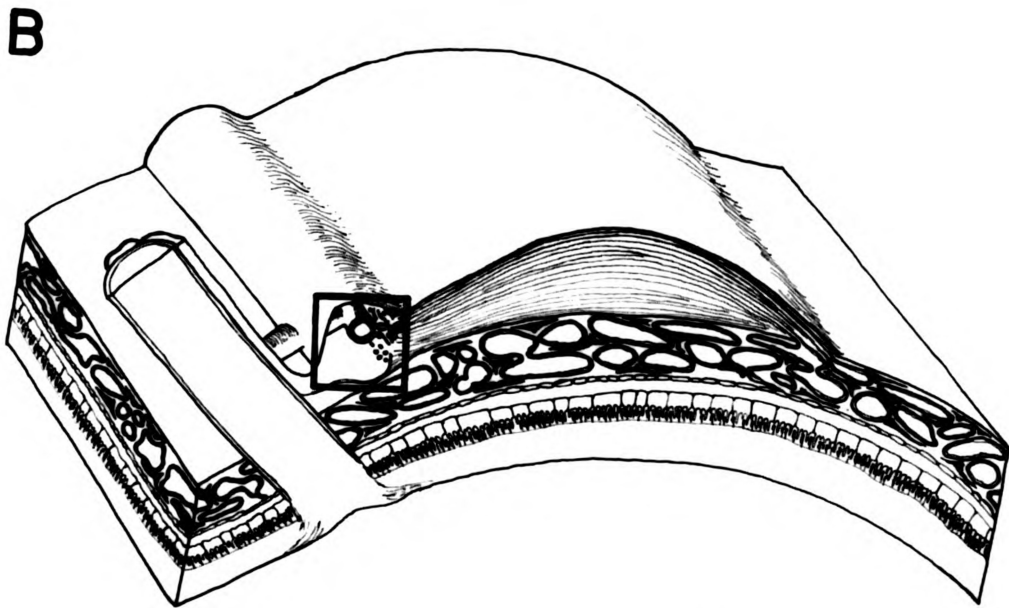
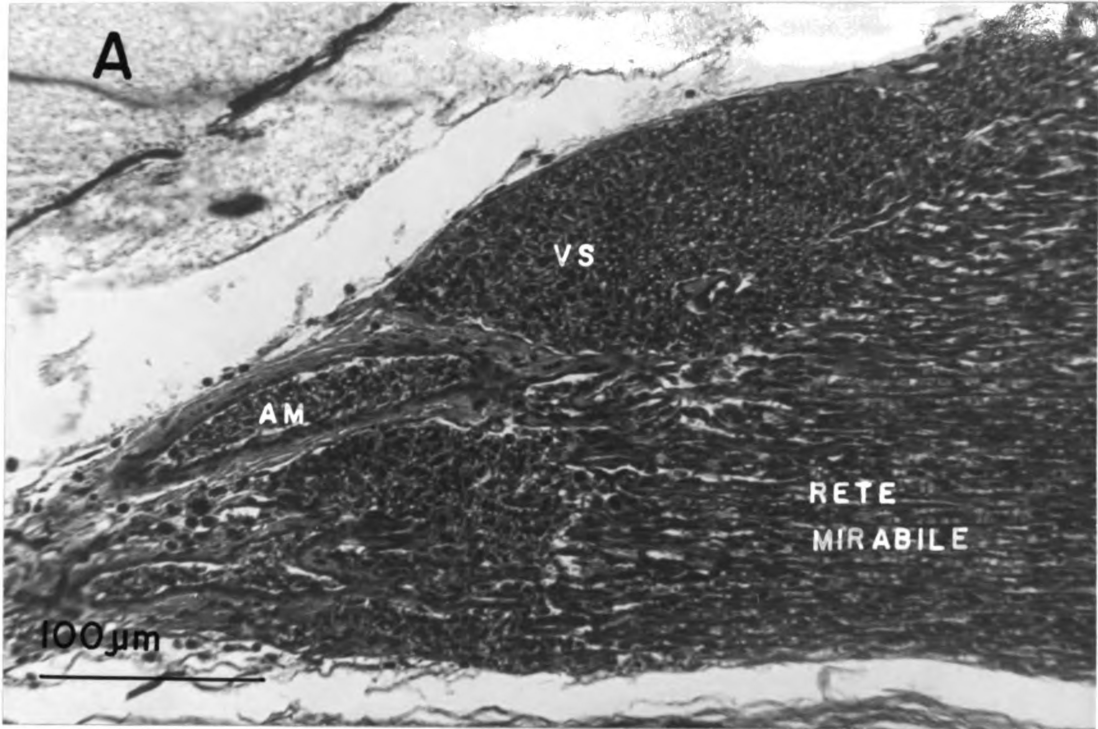


FIGURE 7

FIGURE 8.--Central side of the rete mirabile (Masson's trichrome, 145X).

- A. This micrograph shows a tangential section through the central side of the rete and serves to illustrate the manner in which the arterial manifold (AM) bifurcates to feed the afferent rete vessels.
- B. Generalized diagram illustrating the region from which the above micrograph was taken. The plane shown is the likely plane of sectioning.

AM----Arterial manifold
VS----Venous sinusoid

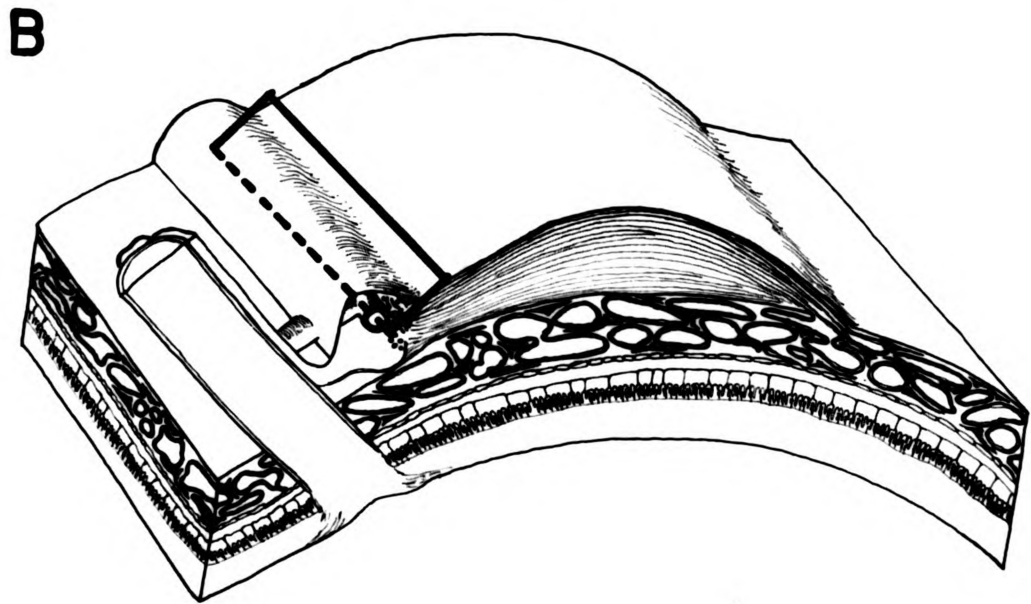
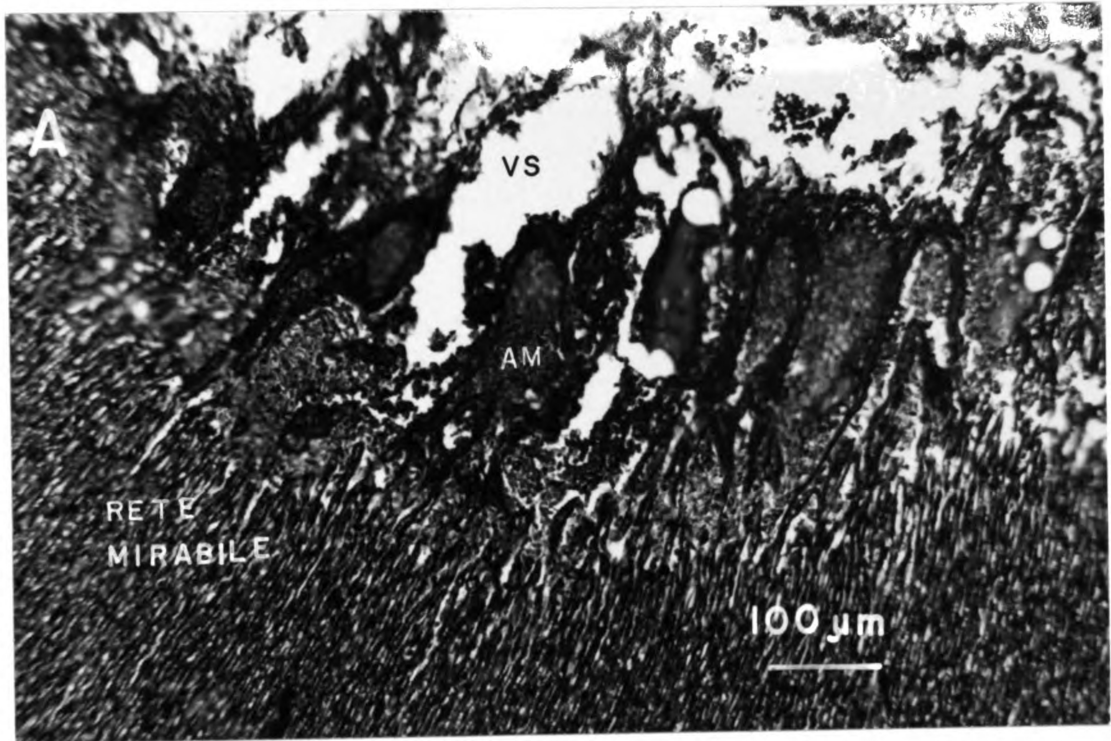


FIGURE 8

FIGURE 9.--Peripheral side of the rete mirabile (hematoxylin and eosin, 145X).

- A. The afferent rete vessels converge upon large distribution vessels (DV) which carry the blood peripherally to the choriocapillaris (not shown here) which supplies all portions of the retina. The blood then is collected from the choriocapillaris in large collecting vessels (CV) which feed the efferent rete vessels. Note that there is no apparent difference between distribution and collection vessels at this level and, thus, the labelling was made arbitrarily for the sake of illustration. There is a rather large number of melanocytes (MEL) associated with the vessels of the central region (Figures 5-8).
- B. The area enclosed within the heavy line represents the region from which the above micrograph was taken.

CV-----Collection vessel
DV-----Distribution vessel
MEL----Melanocyte

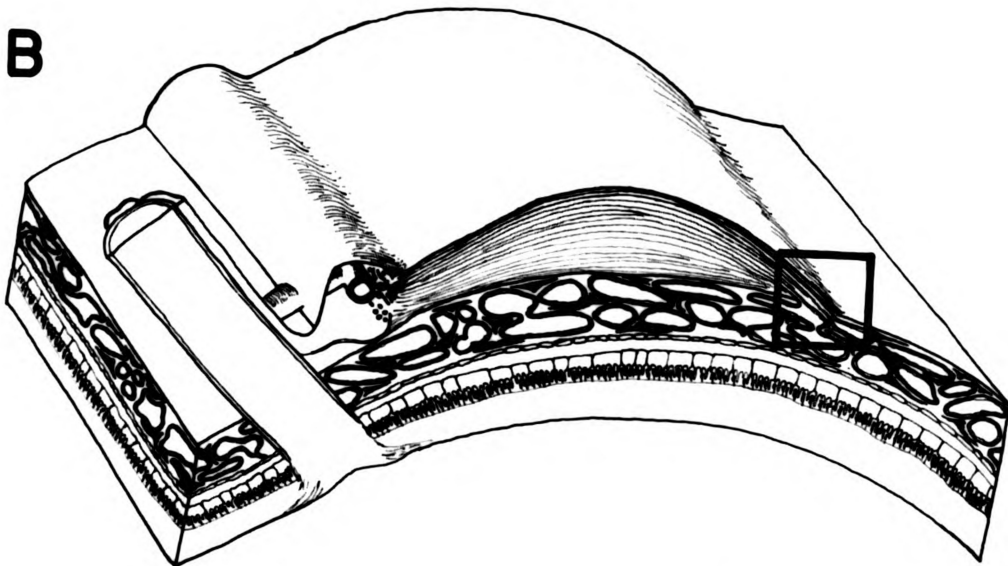
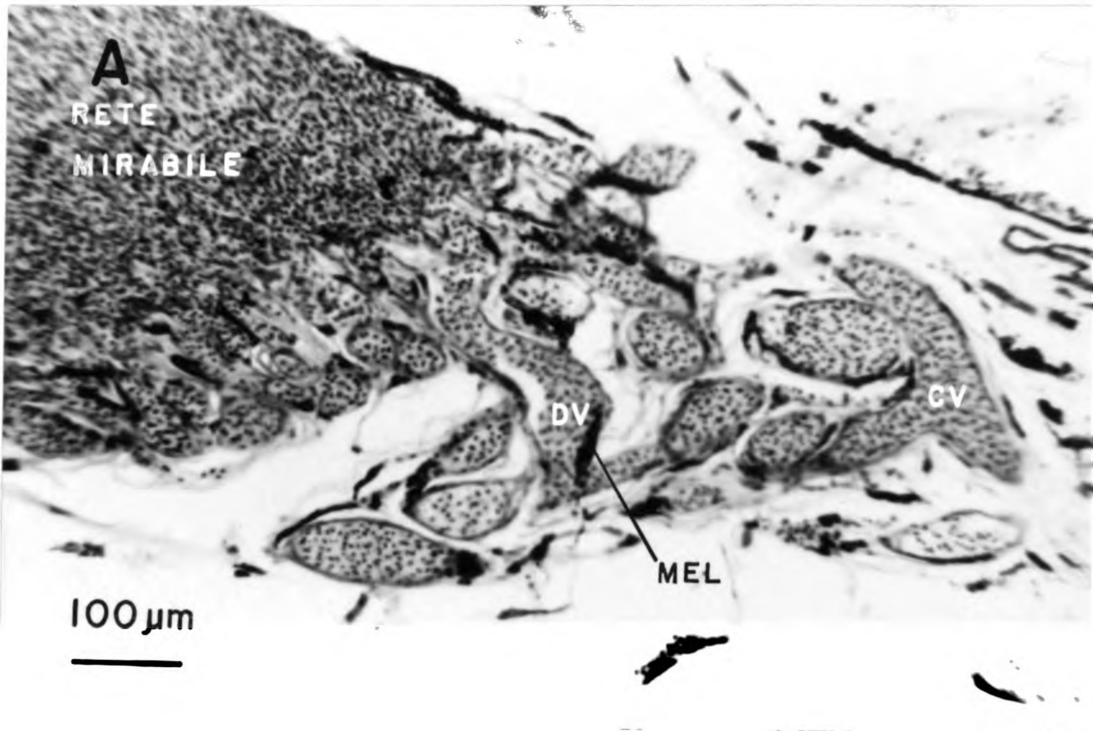


FIGURE 9

FIGURE 10.--Vessels of the peripheral region (hematoxylin and eosin, 145X).

- A. Distribution and collection vessels form an extensive vascular network in the choroid layer. The choriocapillaris (CC) abuts the retina at the site of Bruch's membrane (BM) which is not resolvable at this magnification. Underlying Bruch's membrane is the pigment epithelium and adjacent retinal layers.
- B. General diagram illustrating the region from which the above micrograph was taken (area enclosed by the heavy lines).

BM-----Site of Bruch's membrane
 CC-----Choriocapillaris
 CV-----Collection vessel
 DV-----Distribution vessel
 GCL----Ganglion cell layer
 INL----Inner nuclear layer
 IPL----Inner plexiform layer
 NFL----Nerve fiber layer
 OLM----Outer limiting membrane
 ONL----Outer nuclear layer
 OPL----Outer plexiform layer
 PE-----Pigment epithelium
 RCL----Rod and cone layer

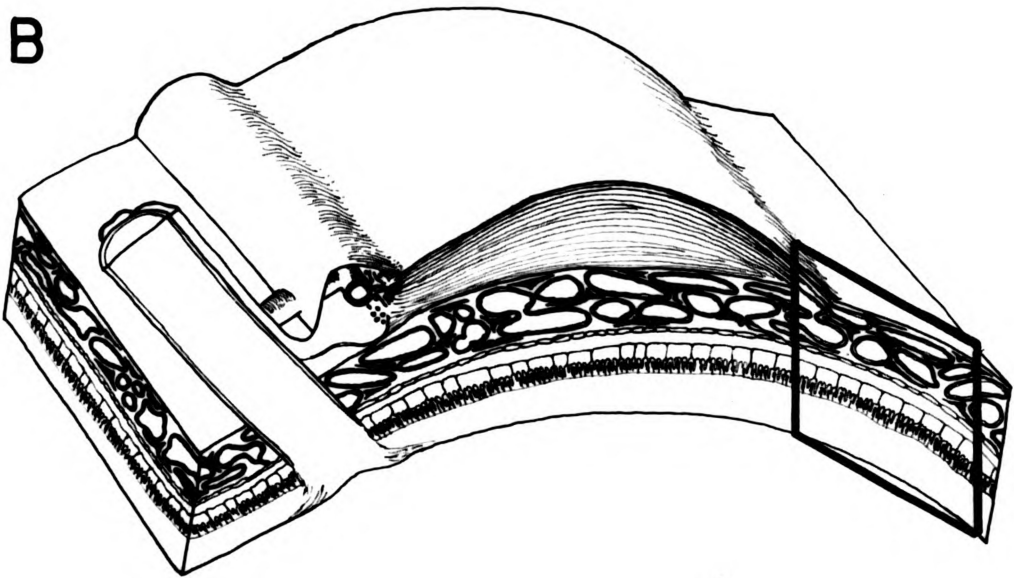
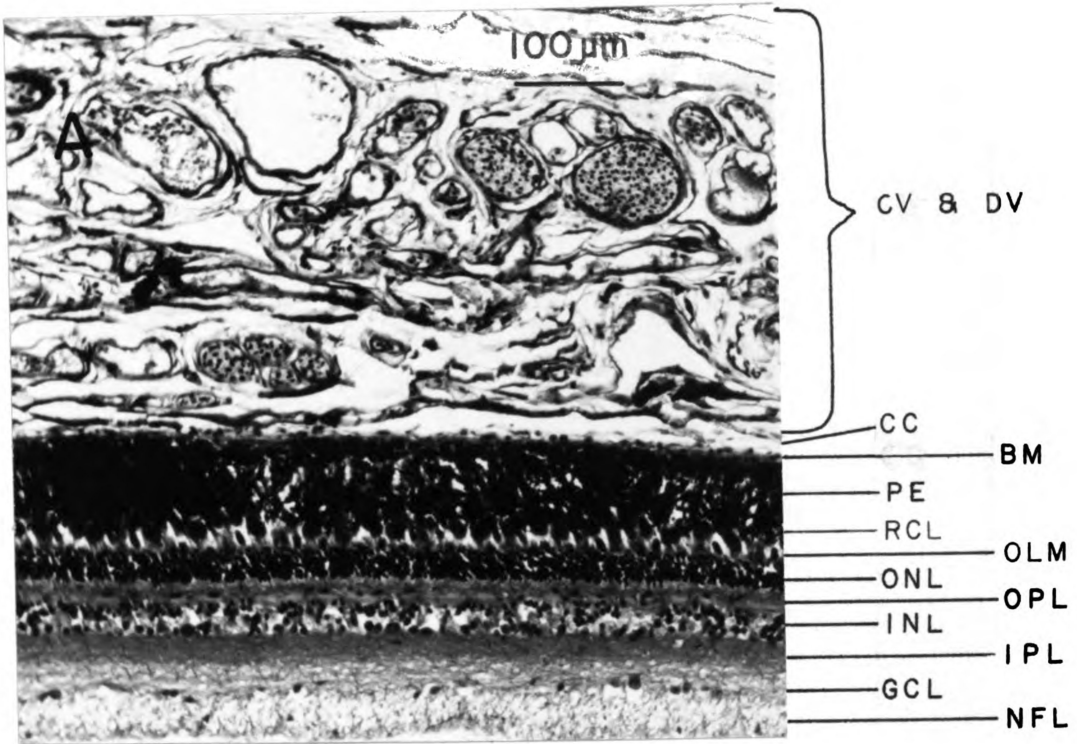


FIGURE 10

FIGURE 11.--Peripheral collection and distribution vessels (hematoxylin and eosin, 440X).

The collection and distribution vessels are not distinguishable from one another at this level of magnification. Melanocytes (MEL) are abundant. Note, here that the surrounding stroma is very loose and laminar in appearance.

MEL---Melanocyte



FIGURE 11

FIGURE 12.--Choroidal rete mirabile cross-section (methylene blue, 925X).

In cross-section, two very distinct vessel types are distinguishable, one being approximately $4.5\ \mu\text{m}$ in diameter and the other being about $9.5\ \mu\text{m}$ in diameter. On the basis of previous publications (see text), it is assumed that the smaller vessels are afferent retial vessels (ARV) and that the larger vessels are efferent retial vessels (ERV). Upon closer observation, it appears that each afferent rete vessel is surrounded by four efferent vessels and vice versa, such that there is a one-to-one relationship between the vessel types. This cubic packing pattern outlined in white is opposed to the hexagonal packing pattern sometimes seen in other species.

ARV----Afferent retial vessel
ERV----Efferent retial vessel

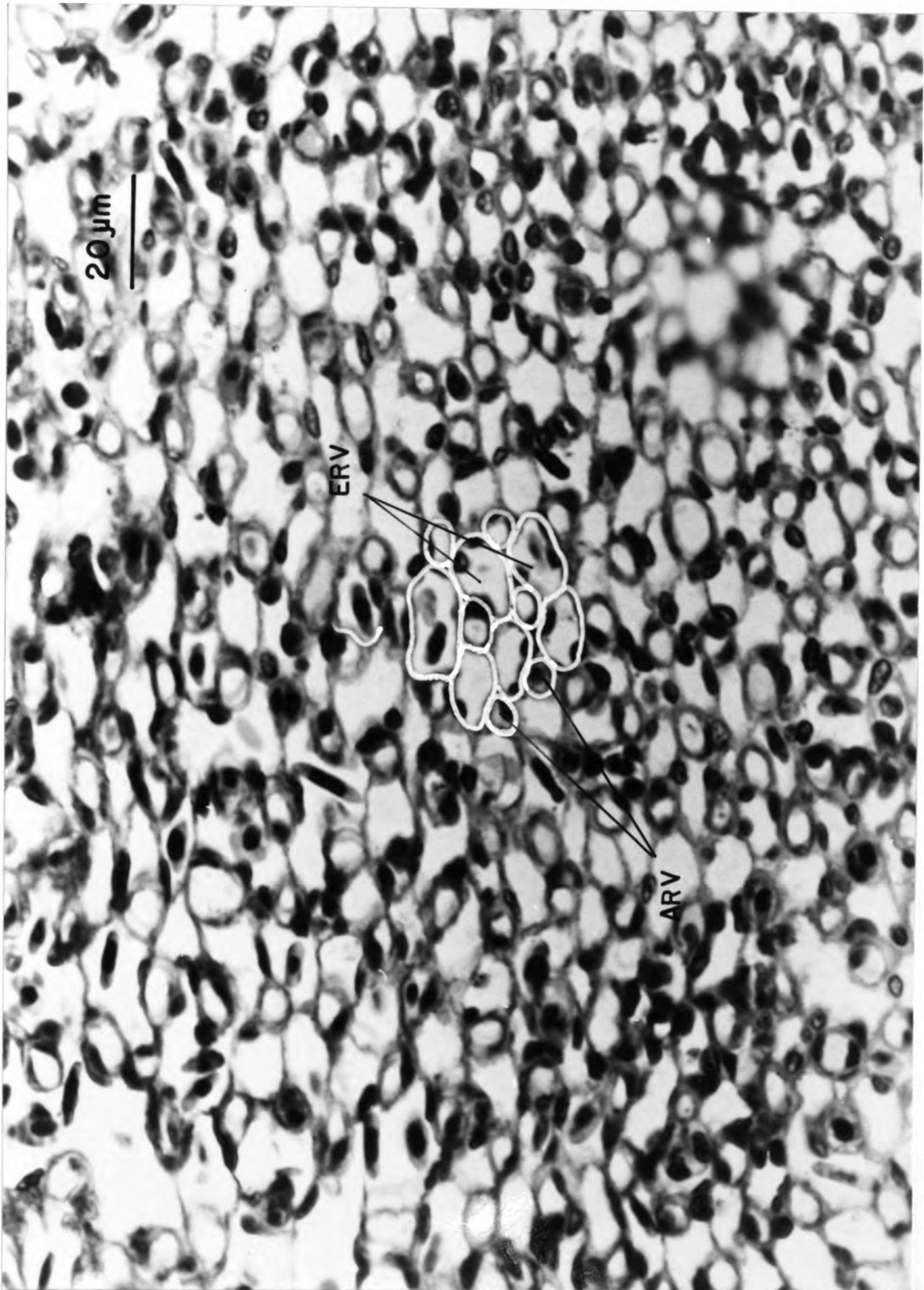


FIGURE 12

FIGURE 13.--Standard immersion fixed rete in cross-section (18,975X).

The rete vessel endothelia seen here are considered to be abnormal. Note the very large phagocytic vacuoles (PV), the numerous arm-like appendages reaching into the vessel lumen, micropinocytotic vesicles (arrows), extremely attenuated endothelia lacking fenestrae or pores, swollen adventitia, and a lack of a distinct basement membrane.

- | | | | |
|----------|----------------------|-------------|---------------------------|
| ARV---- | Afferent rete vessel | N----- | Nucleus |
| BM----- | Basement membrane | P----- | Pericyte |
| E----- | Endothelial cell | PV----- | Phagocytic vacuole |
| ERV----- | Efferent rete vessel | RBC----- | Erythrocyte |
| L----- | Lumen | Arrows----- | Micropinocytotic vesicles |

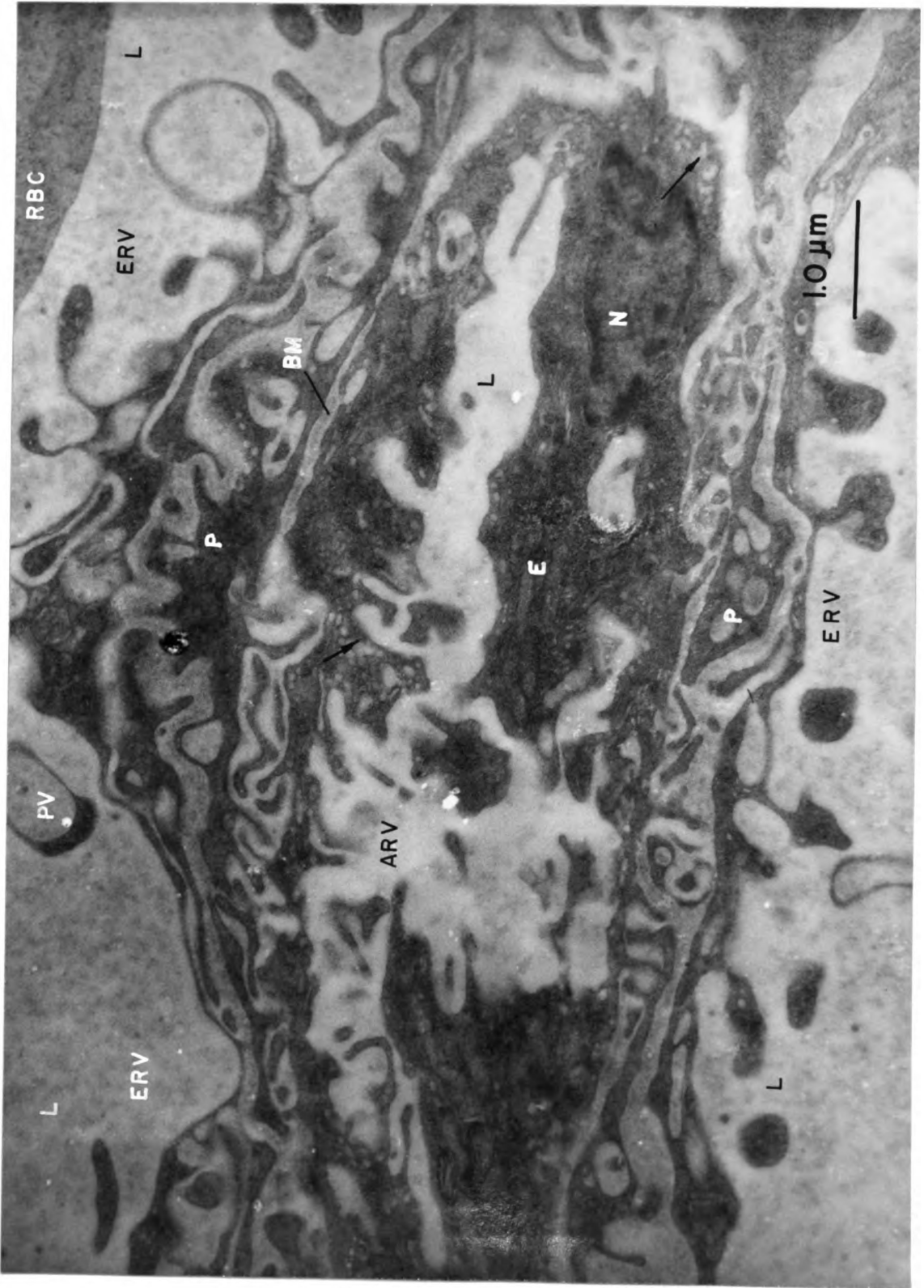


FIGURE 13

FIGURE 14.--Standard immersion-fixed rete: Area with myeloid configurations in the lumen.

- A. Abnormal appearance of rete. Note the densely granular background matrix in the lumen and the multilaminar myeloid configuration (MC) within the vessel lumen. (16,560X).
- B. Higher magnification of a similar myeloid-type configuration within the lumen of a rete vessel. The configuration seen here appears to suggest some ongoing extrusion activity. (41,405X).

L-----Lumen
MC-----Myeloid configuration
PV-----Phagocytic vacuole
RBC-----Erythrocyte
WBC-----Leucocyte

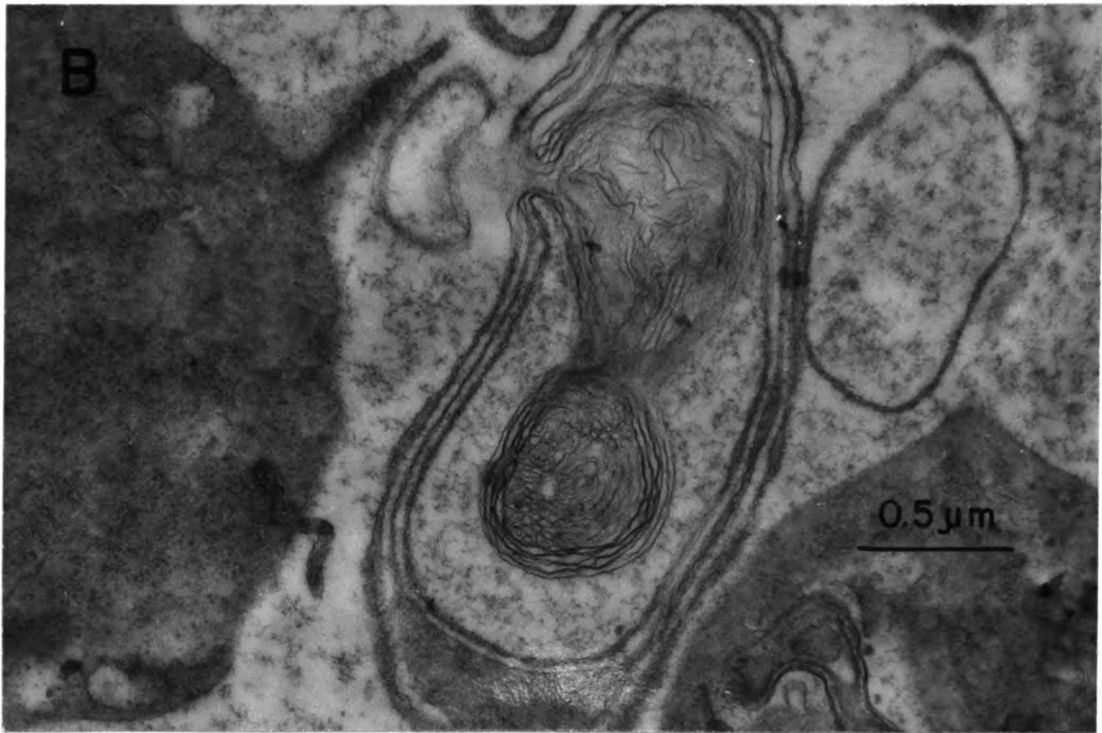
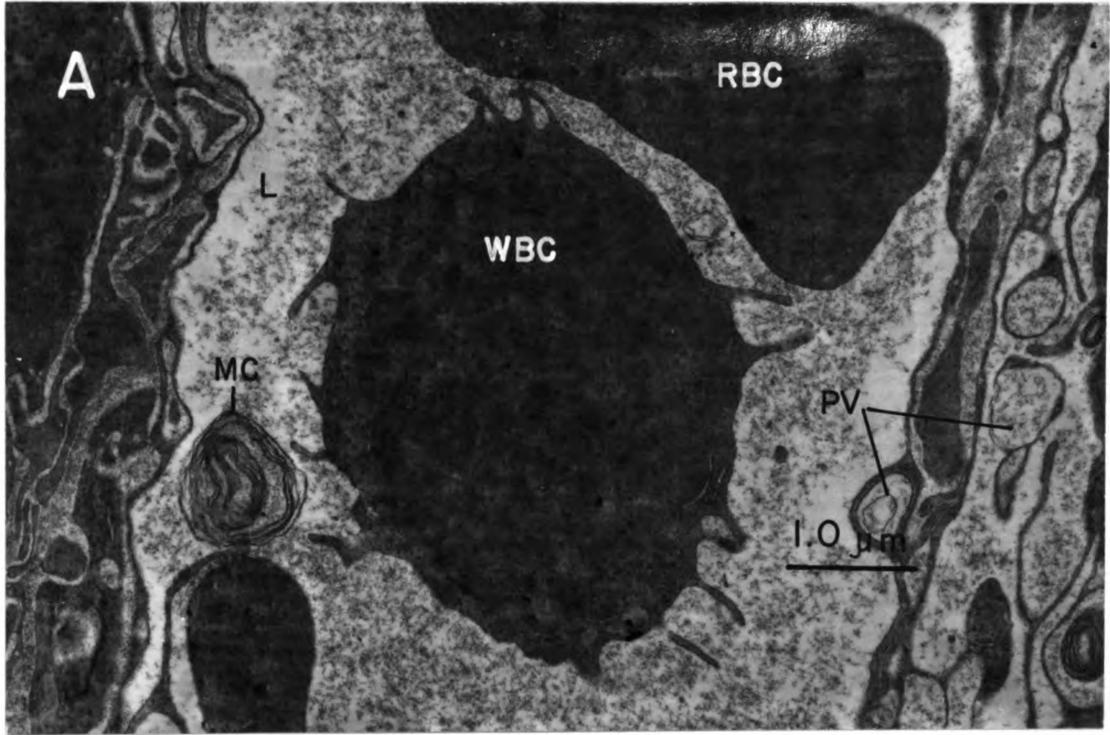


FIGURE 14

FIGURE 15.--Standard immersion-fixed rete: Area with thin-walled vacuoles within the lumen (10,240X).

The distinctive feature in this electron micrograph is the presence of large thin-walled vacuoles (LV) in the vessel lumen. This area is very similar to the one published in the micrographs by Brown, Stalker and Hall (1969) in clotted preparations.

ARV-----Afferent rete vessel
 ERV-----Efferent rete vessel
 LV-----Free luminal vacuole
 PV-----Phagocytic vacuole
 Arrow--Pinocytotic vesicle

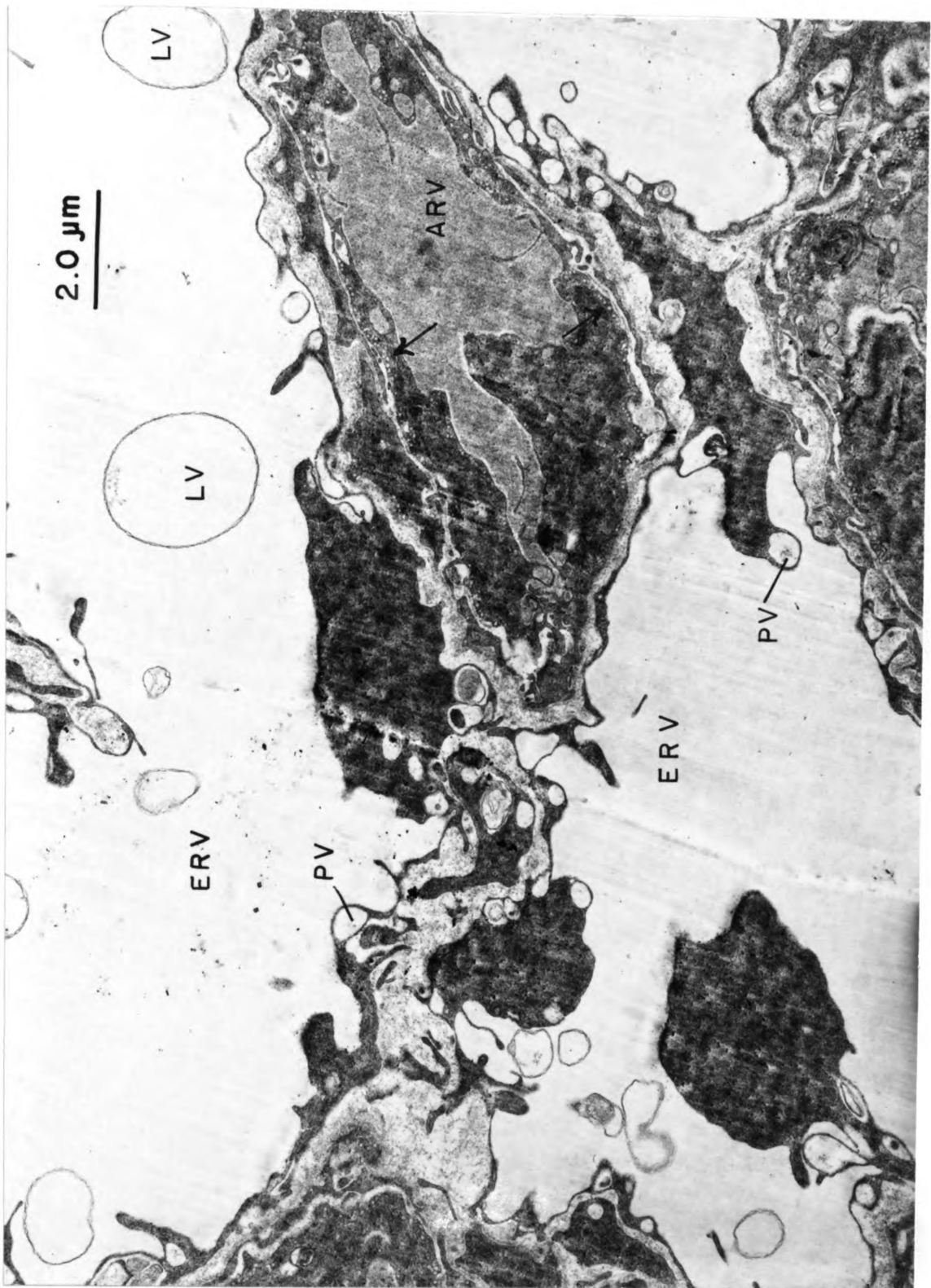


FIGURE 15

FIGURE 16.--Myelinated and non-myelinated neural elements within the arterial manifold wall (26, 250X).

Embedded within the collagenous matrix (C) of the arterial manifold vessel wall are areas through which pass numerous non-myelinated nerve axons (A) with their associated Schwann cells (S). As may be seen here myelinated fibers (MY) are also present. Smooth muscles are present in the arterial manifold wall, and myoneural junctions have been observed. It is not, however, known whether the neural elements seen here are motor or sensory.

- A-----Non-myelinated nerve axon
- C-----Collagenous matrix (collagen fibers in cross-section)
- MY-----Myelinated nerve fibers
- N-----Schwann cell nucleus
- S-----Schwann cell

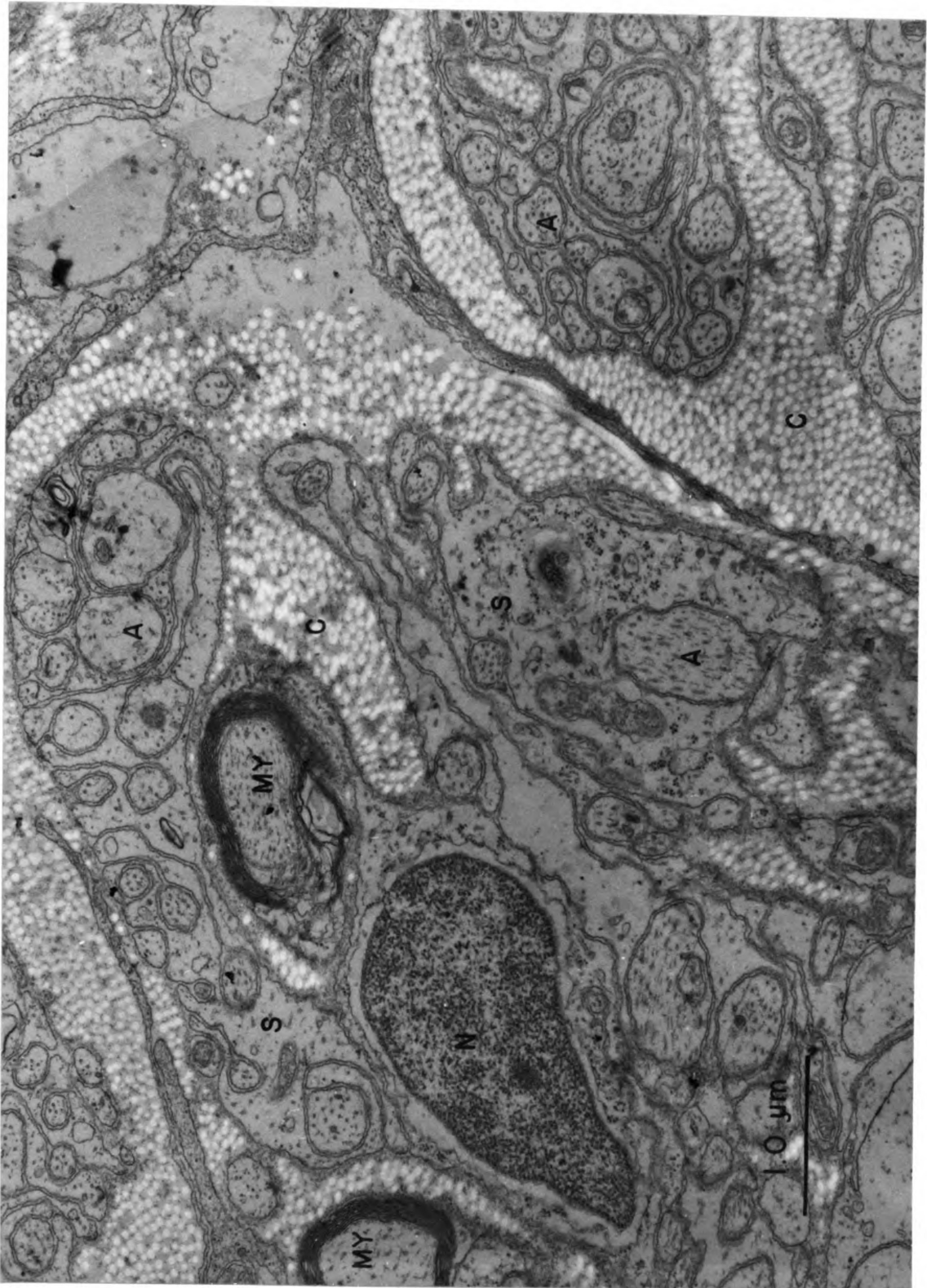


FIGURE 16

FIGURE 17.---Smooth muscle layer underlying the endothelial border of the arterial manifold wall (27,190X).

Underlying the endothelial border (E) within the arterial manifold wall is at least one layer of smooth muscle (SM). Abundant pinocytotic activity (arrows) is seen along the margins of the smooth muscle cell. There are several areas which appear to be points of neural contact (MNJ). The presence of neurons within the arterial manifold wall has been seen in Figure 16. A possible role for the arterial manifold in the regulation of flow through the choroidal rete mirabile is suggested by the presence of these tissues.

A-----Axon
 C-----Collagen
 E-----Endothelial cell
 L-----Lumen
 M-----Myofibril
 MNJ-----Myoneural junction
 N-----Nucleus
 RER-----Rough endoplasmic reticulum
 SM-----Smooth muscle
 Arrow----Pinocytotic vessels

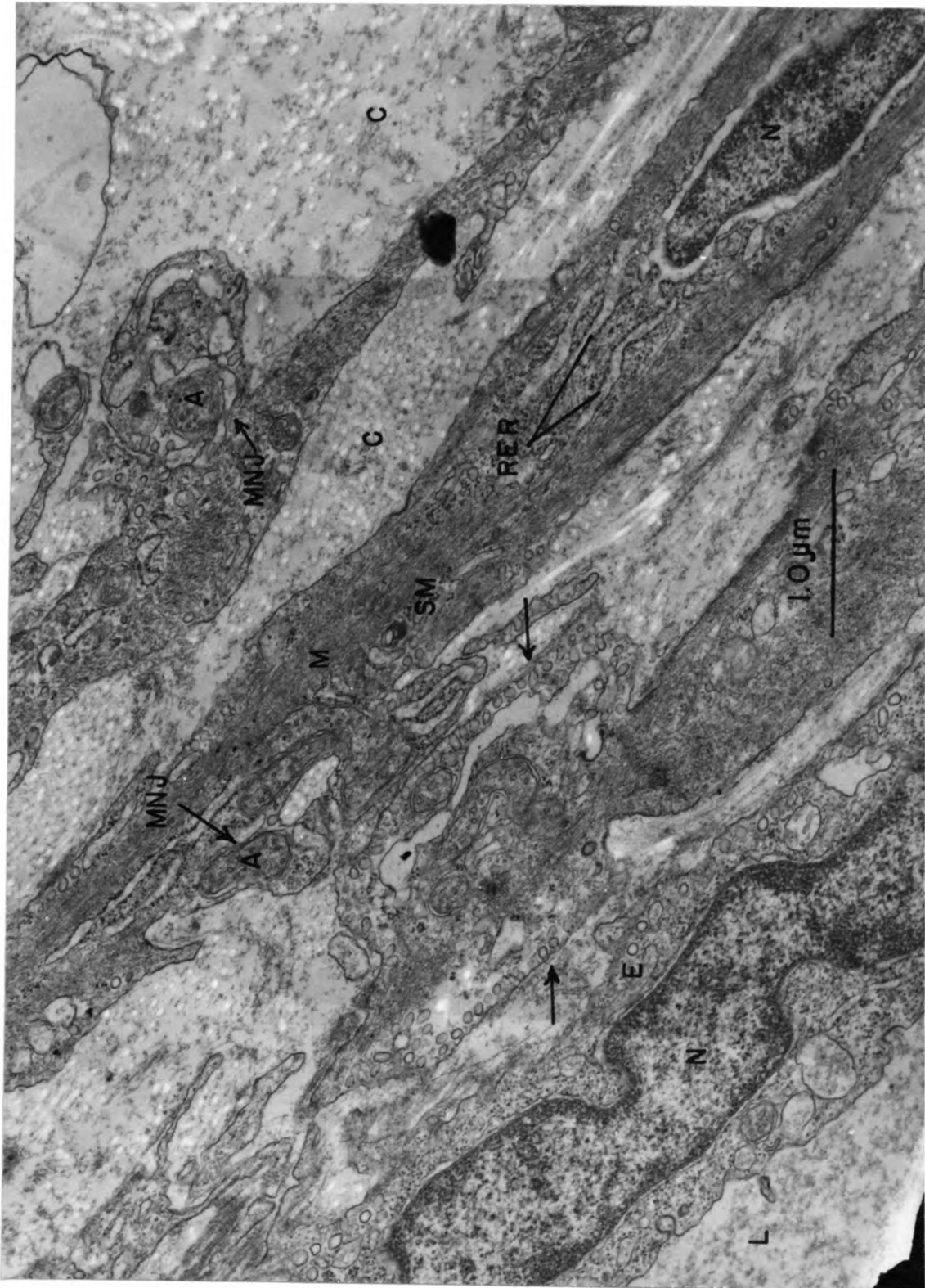


FIGURE 17

FIGURE 18.--Arterial manifold wall displaying an association between pinocytotic activity within the endothelium and smooth muscle (26,250X).

The major point of interest in this electron micrograph is the abundant pinocytotic activity of the smooth muscle cell border adjacent to an area of extensive pinocytotic activity in the endothelial cell. Note that very little pinocytotic activity is occurring along the luminal border of the endothelial cell, so that it may be questionable whether the pinocytosis is active in trans-endothelial transport of macromolecular nutrients and metabolites. The possibility exists that pinocytotic activity within smooth muscle is indicative of active calcium ion uptake or extrusion, replacing the role played by sarcoplasmic reticulum in skeletal muscle. If this is true, then the endothelial cell pinocytotic activity may also operate in conjunction with this goal. This postulate is based upon no empirical evidence, but is merely suggested by the morphological evidence presented here.

C-----Collagenous matrix
E-----Endothelial cell
G-----Golgi apparatus
L-----Lumen
M-----Myofibrils
N-----Endothelial nucleus
SM-----Smooth muscle cell

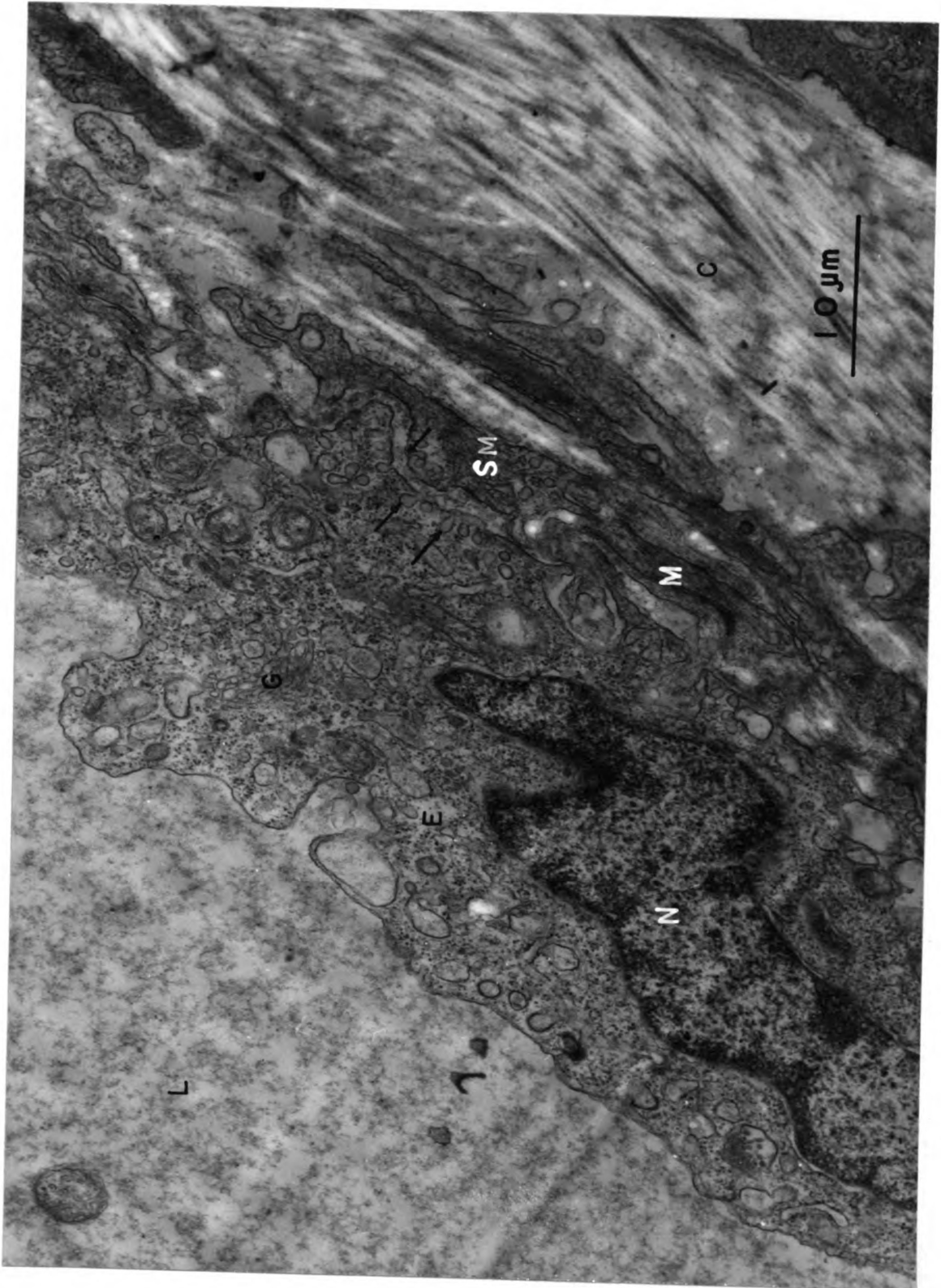


FIGURE 18

FIGURE 19.--Heparinized, immersion-fixed choroidal rete mirabile in cross-section (8,400X).

Upon determining that clotting had occurred in the initial preparations (Figures 13-15), it was found that heparinization prior to fixation resulted in much more typical capillary features as seen here. This area is a cross-section of the choroidal rete mirabile. Unfortunately, due to the lack of experience and to the lack of a good technician, this micrograph is replete with chatter. Through this study it has become obvious that behind every good electron microscopist is a great technician. The chatter, however, does not obscure the general features present here. The most important feature to note is that all afferent rete vessels and their associated pericytes are surrounded by discrete basement membranes. This is not seen with efferent rete vessels.

- ARV-----Afferent rete vessel
- BM-----Basement membrane
- ERV-----Efferent rete vessel
- MF-----Marginal flap
- P-----Pericyte
- RBC-----Erythrocyte



FIGURE 19

FIGURE 20.--Afferent retial vessel in cross-section (20,755X).

At a higher magnification, it is seen that the afferent vessel endothelial cell appears to be a fairly active tissue containing a complete set of cytoplasmic components. Free ribosomes appear dispersed throughout the cytoplasm. Mitochondria are also discernable. The endothelial wall of the adjacent efferent retial vessel shows no apparent difference in its ultrastructural features. The afferent vessel is surrounded by a complete basement membrane. The area within the box is magnified in Figure 21.

BM-----Basement membrane
 ERV-----Efferent retial vessel
 J-----Cell junction
 M-----Mitochondrion
 RBC-----Erythrocyte

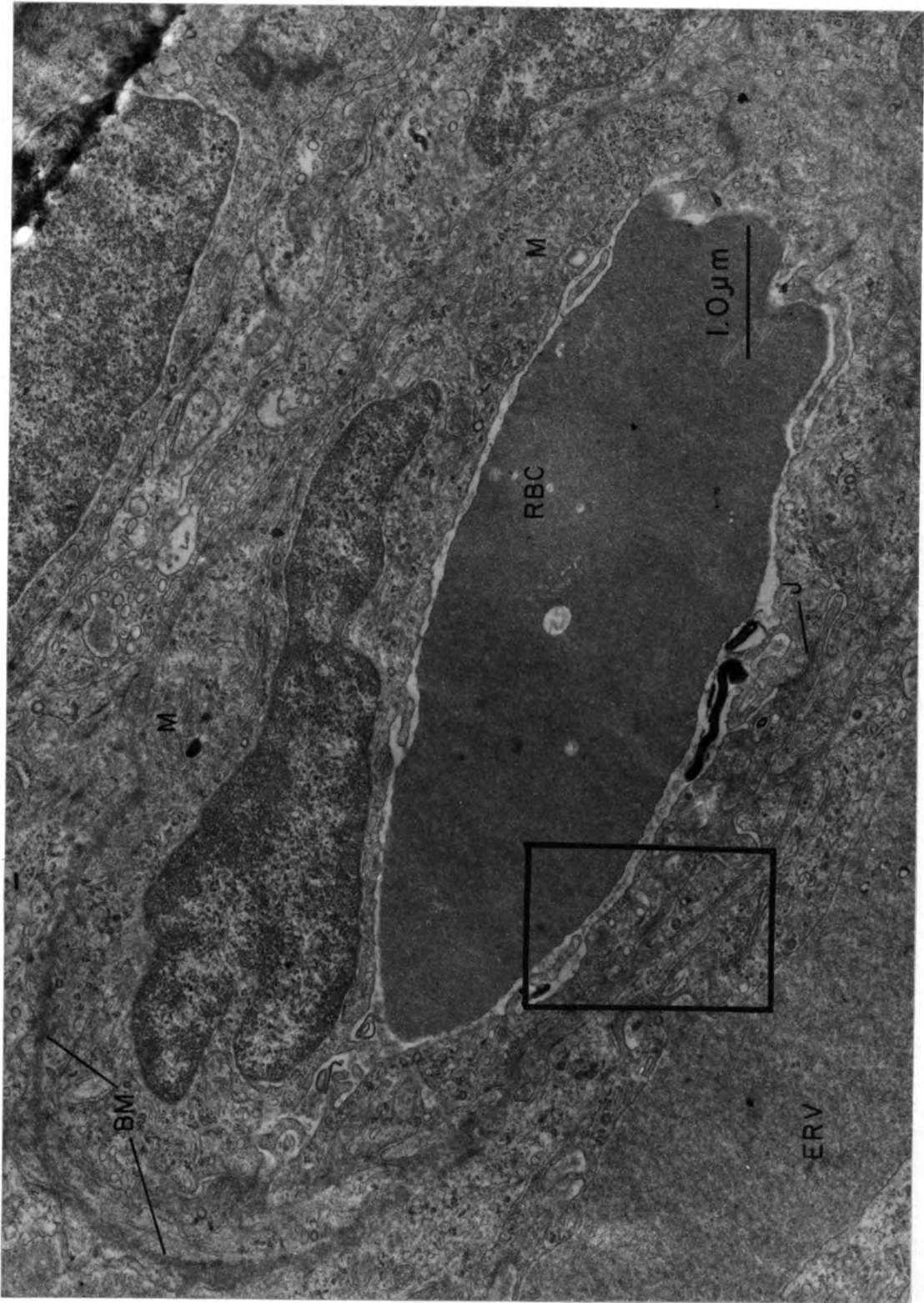


FIGURE 20

FIGURE 21.--Afferent versus efferent rete endothelial ultrastructure (113,750X).

At much higher magnification, no difference is seen between the afferent and efferent rete endothelia. This area is the area enclosed within the box of Figure 20.

- ARV-----Afferent rete vessel lumen
- BW-----Basement membrane
- E-----Endothelium
- ERV-----Efferent rete vessel lumen
- RBC-----Erythrocyte

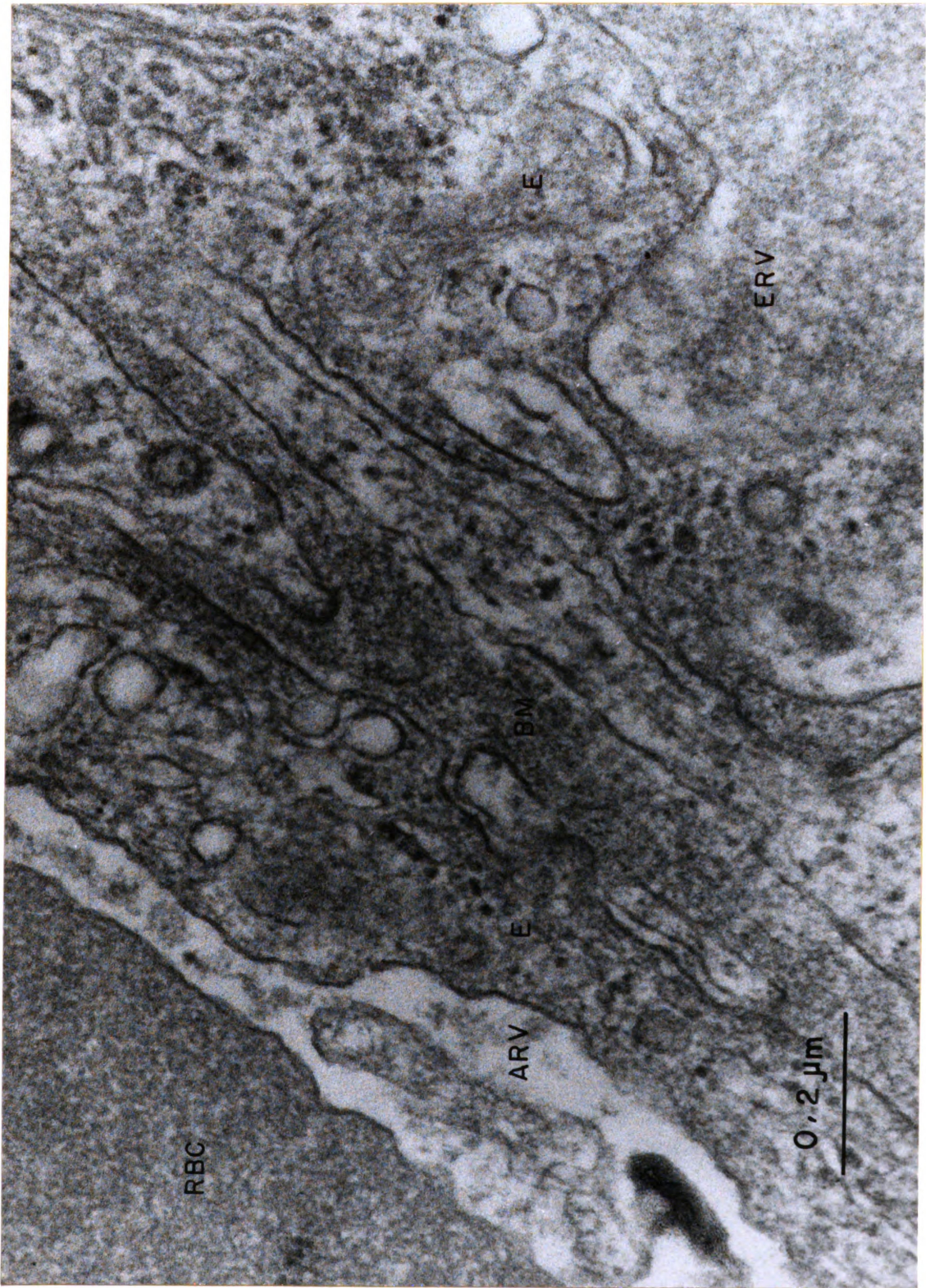


FIGURE 21

FIGURE 22.--Vessels of the peripheral choroidal layer (methylene blue, 925X).

The tissue here has been embedded in EPON 812, sectioned at about 2 um, and stained with methylene blue. This is the condition that the tissue is in for ultrathin sectioning for electron microscopic examination and may be contrasted to a similar area in paraffin embedded tissues of Figures 10 and 11. Note again, the loose stroma surrounding the vessels. Melanocytes are also obvious in this section. Note that they are never seen to surround the vessels entirely.

Arrows---Melanocytes
S-----Stroma

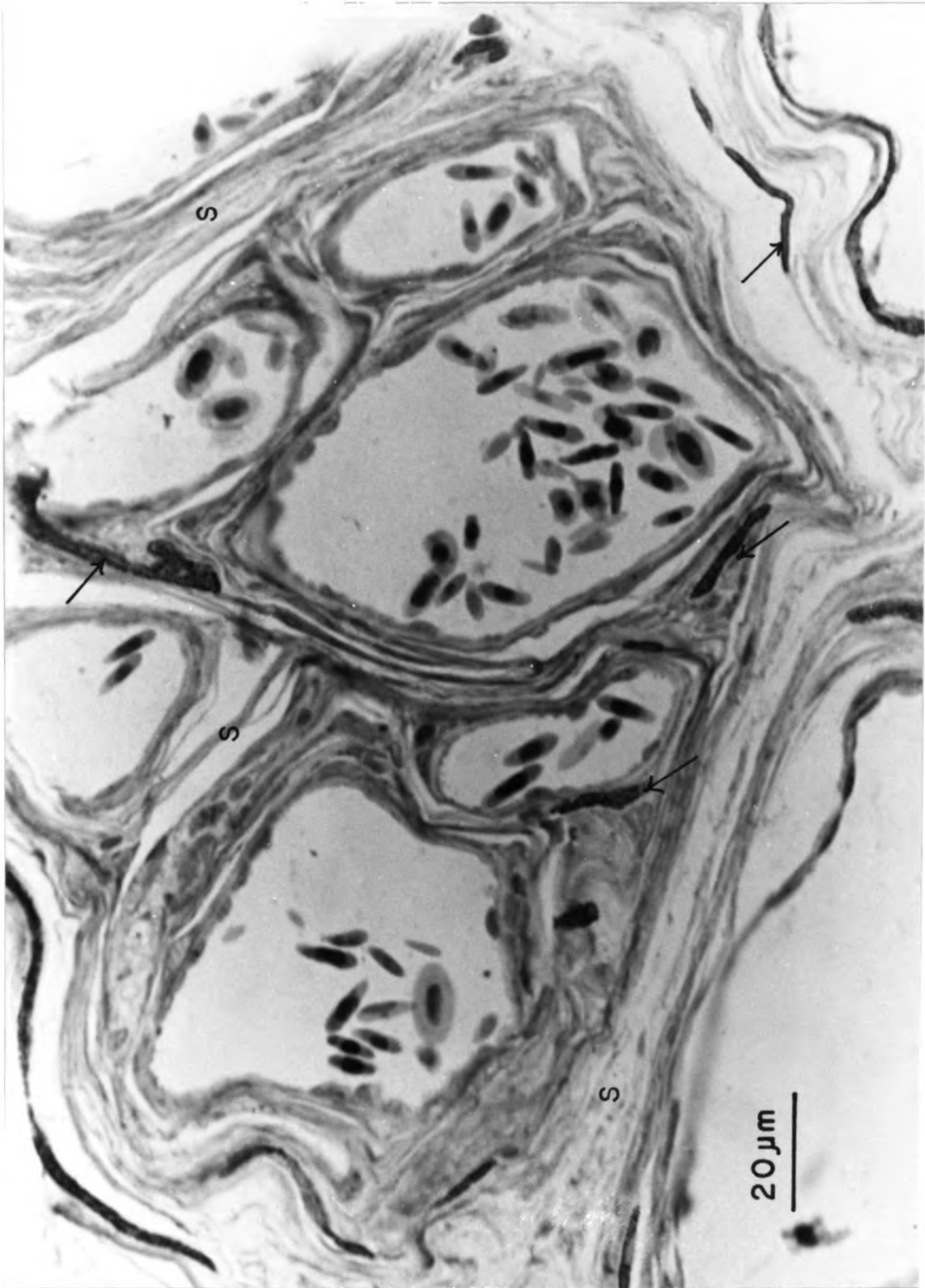


FIGURE 22

FIGURE 23.--Peripheral choroidal vessel ultrastructure (14,175X).

The vessels in this region are seen to possess a single endothelial layer (E) overlain by a thick, collagenous matrix (C) through which fibrocytes (F) are seen to pass. Melanocytes are abundant and are easily recognized as having many dense black, spherical melanin granules. Overlying the melanocytes is a layer of loose, multilaminar membranes comprising the bulk of the stroma through which the collecting and distribution vessels pass.

C-----Collagenous matrix
 E-----Endothelial layer
 F-----Fibroblast

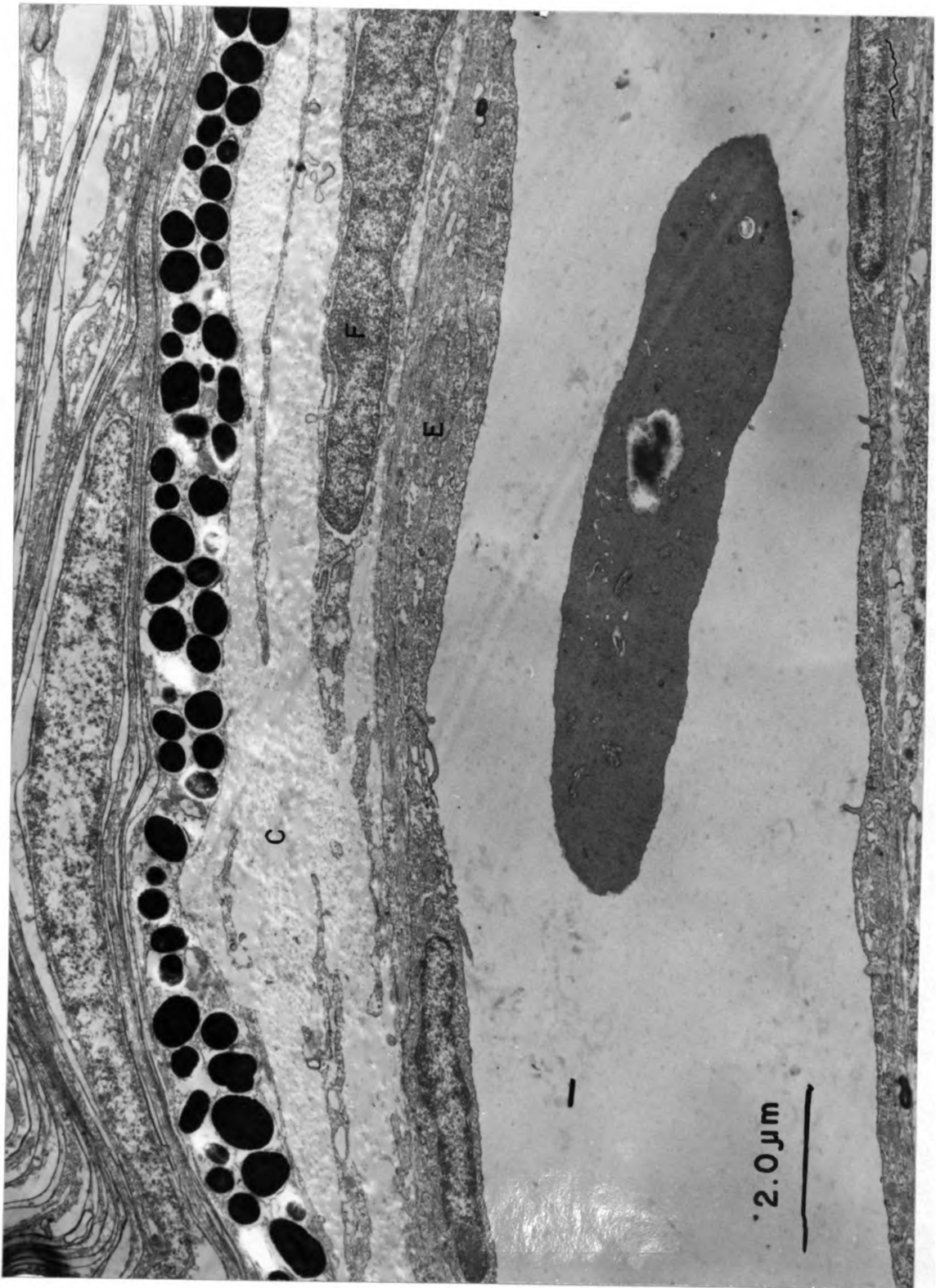


FIGURE 23

FIGURE 24. ---Peripheral vessel wall (25,625X).

This is an enlargement of an area of Figure 23. Note the extensive network of rough endoplasmic reticulum in the cytoplasm of the fibrocyte (F). Fibrocytes are largely responsible for the production of the collagen which is abundant here. The striated layer adjacent to the melanocyte does not at first appear cellular in nature, but the large nucleus (N) present would suggest otherwise.

C-----Collagenous matrix
 E-----Endothelium
 F-----Fibrocyte
 MEL-----Melanocyte
 N-----Stromal nucleus
 RER-----Rough endoplasmic reticulum
 S-----Stroma



FIGURE 24

FIGURE 25.--Choriocapillaris, Bruch's membrane, and pigment epithelium (13,840X).

The choriocapillaris is a vast catacomb of capillary-sized vessels lying adjacent to the entire surface of the retina. It is separated from the pigment epithelium (PE) by Bruch's membrane (BM). The choriocapillaris endothelium is seen to be polarized in that the "central prominence" of the cell containing the nucleus and bulk of the cytoplasmic constituents, without exception lies on the scleral side of the vessel and sends flange-like extensions toward the retina to complete the vessel wall. Unlike the case in mammals, the basal border of the pigment epithelium abutting Bruch's membrane is smooth and lacks involutions.

Arrow---Flange-like extension of the choriocapillaris endothelial cell
 BM-----Bruch's membrane
 CC-----Choriocapillaris
 E-----Endothelium
 PE-----Pigment epithelium
 R-----Reticulocyte
 RBC-----Erythrocyte

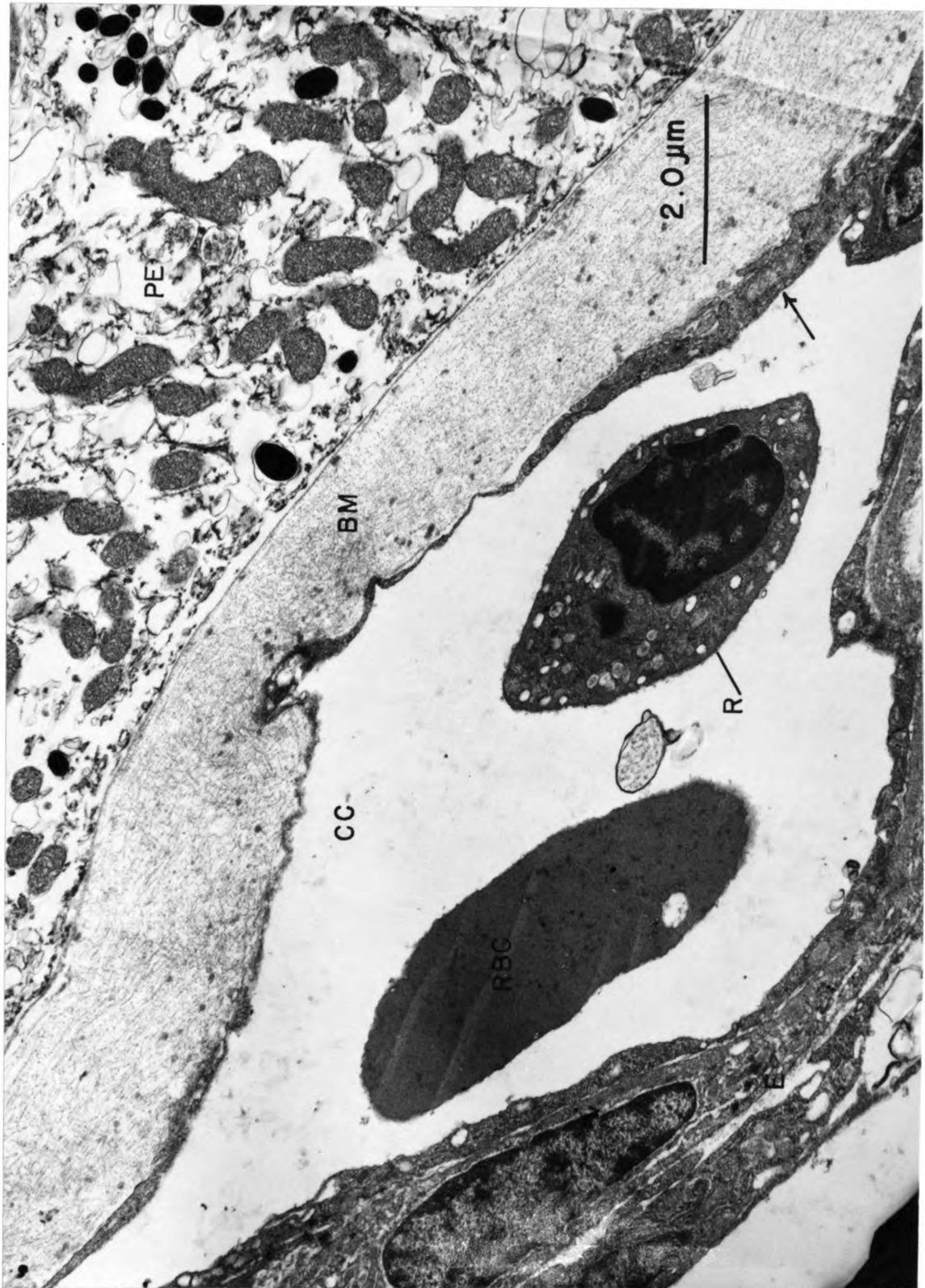


FIGURE 25

FIGURE 26.--Fenestrated choriocapillaris endothelium.

A feature which characterizes the choriocapillaris endothelia of mammals is that diaphragmed fenestrae are very abundant in that portion of the endothelial wall abutting Bruch's membrane. In Salmo gairdneri, it is seen that the endothelia are extremely attenuated in this region and occasional fenestrae are seen but their abundance nowhere approaches that seen in the mammalian choriocapillaris (A--41,405X; B--265,000X).

Arrows--Diaphragmed fenestrae
BM-----Bruch's membrane
CC-----Choriocapillaris

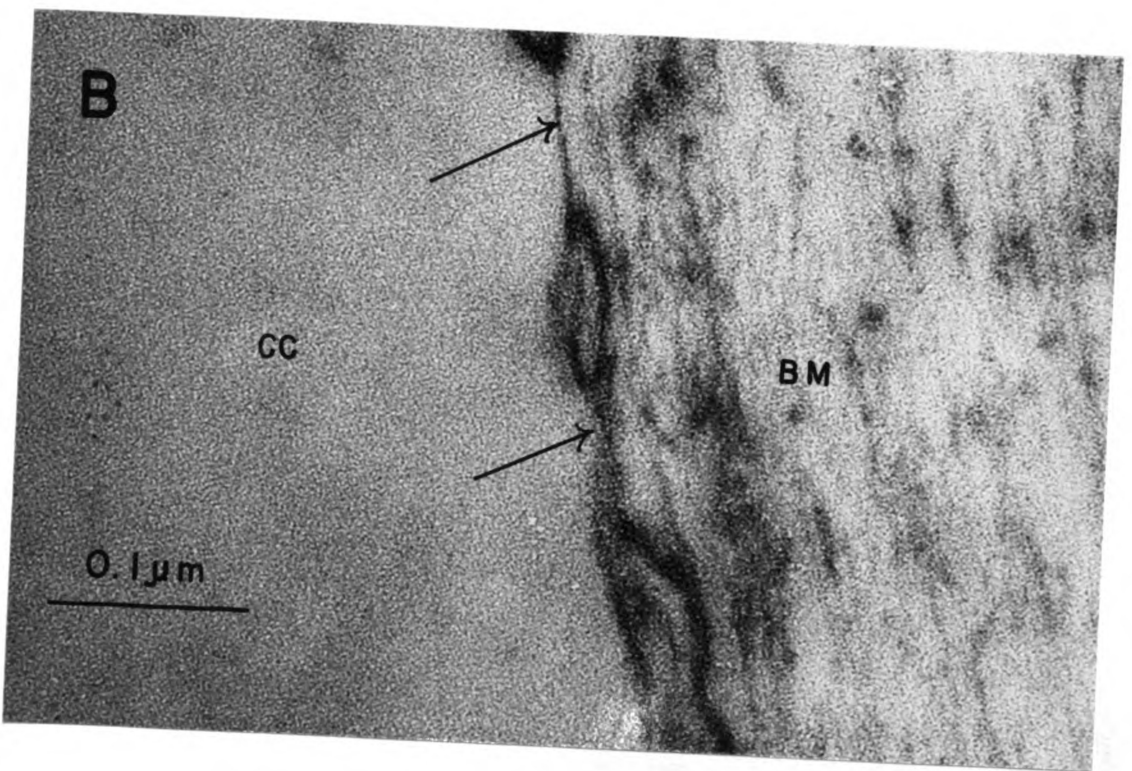
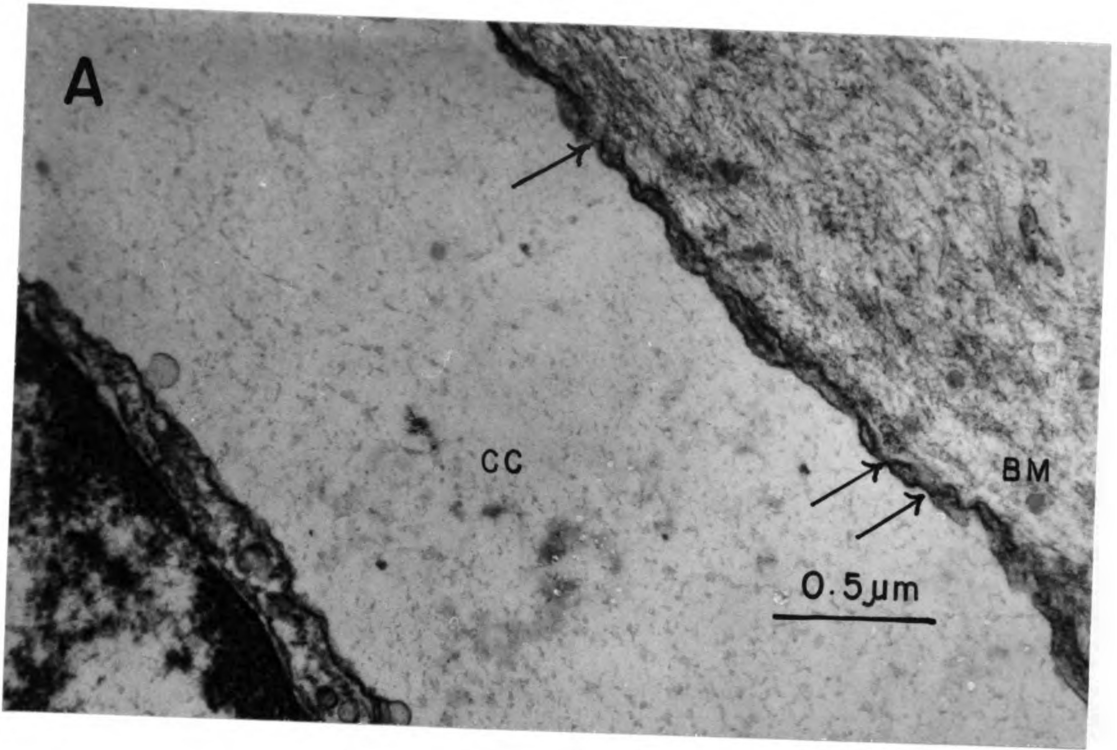


FIGURE 26

FIGURE 27.--Bruch's membrane (41,405X).

Bruch's membrane is seen here to be composed of a network of very fine fibrils embedded in a uniform electron lucent matrix. It is bordered on one side by the choriocapillaris endothelial cell membrane and on the other by the pigment epithelium basement membrane. This arrangement is relatively structureless compared to the mammalian morphology (A--41,405X; B--41,405X).

B-----Basement membrane
CC-----Choriocapillaris
E-----Endothelium
M-----Mitochondrion
PE-----Pigment epithelium

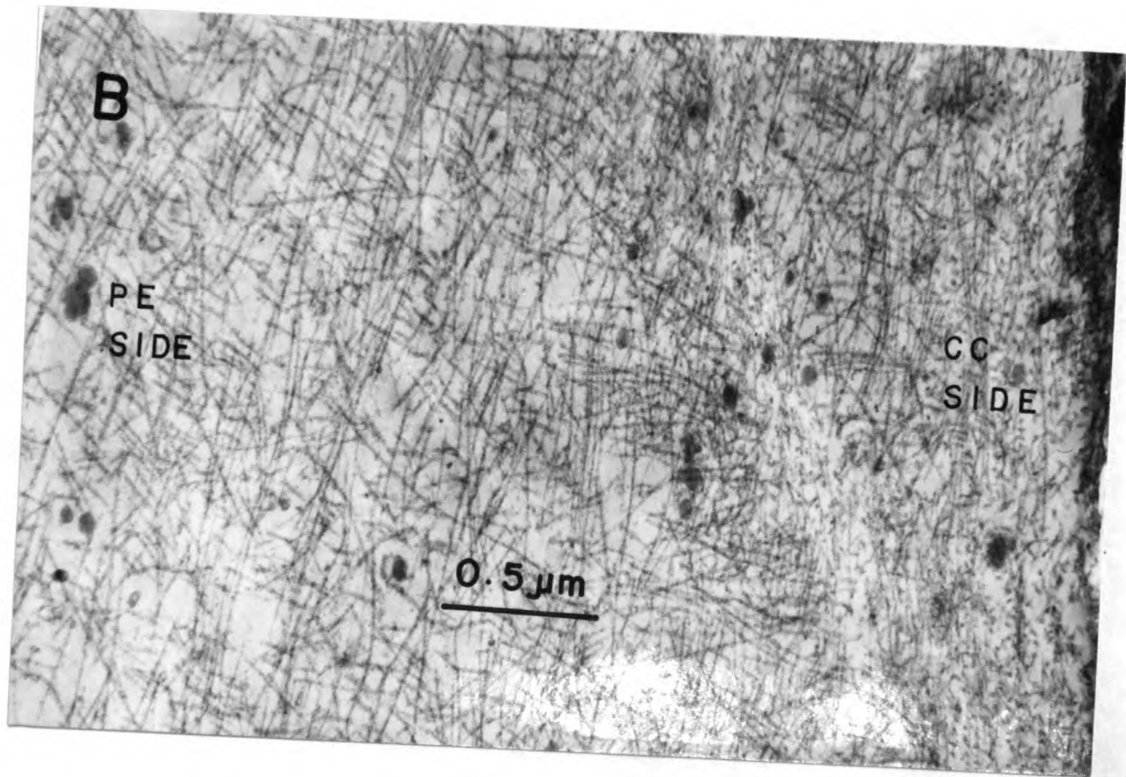
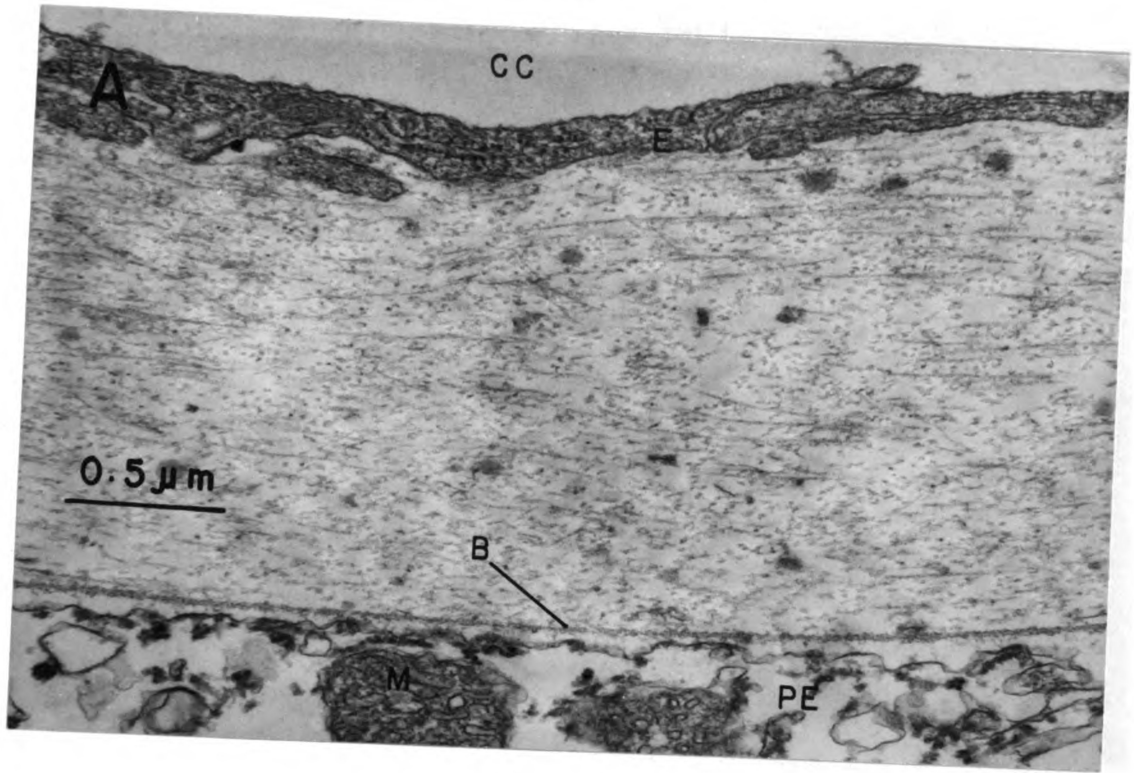


FIGURE 27

FIGURE 28.--Myeloid bodies within the pigment epithelium (16,560X).

As a point of interest, the cellular inclusions of pigment epithelium are unusual in appearance in relation to other tissues. The cell has four prominent inclusions: melanin granules (MG), abundant mitochondria (M), nucleus (N), and myeloid bodies (MB). Note that the pigment granules are rod-shaped as opposed to the prominent spherical shape seen in the melanocytes of the choroid layer. The myeloid bodies have been described in the literature, but until recently, their origin and function have been in debate. It has now been conclusively established (Anderson and Fisher, 1975) that they arise from phagocytosed sections of shed rod and cone outer segments. There is a definite structural similarity between these myeloid bodies and the photoreceptor outer segments (Figure 29). (A--16,560X; B--16,560X).

M-----Mitochondrion
MB-----Myeloid body
MG-----Melanin granules
N-----Nucleus

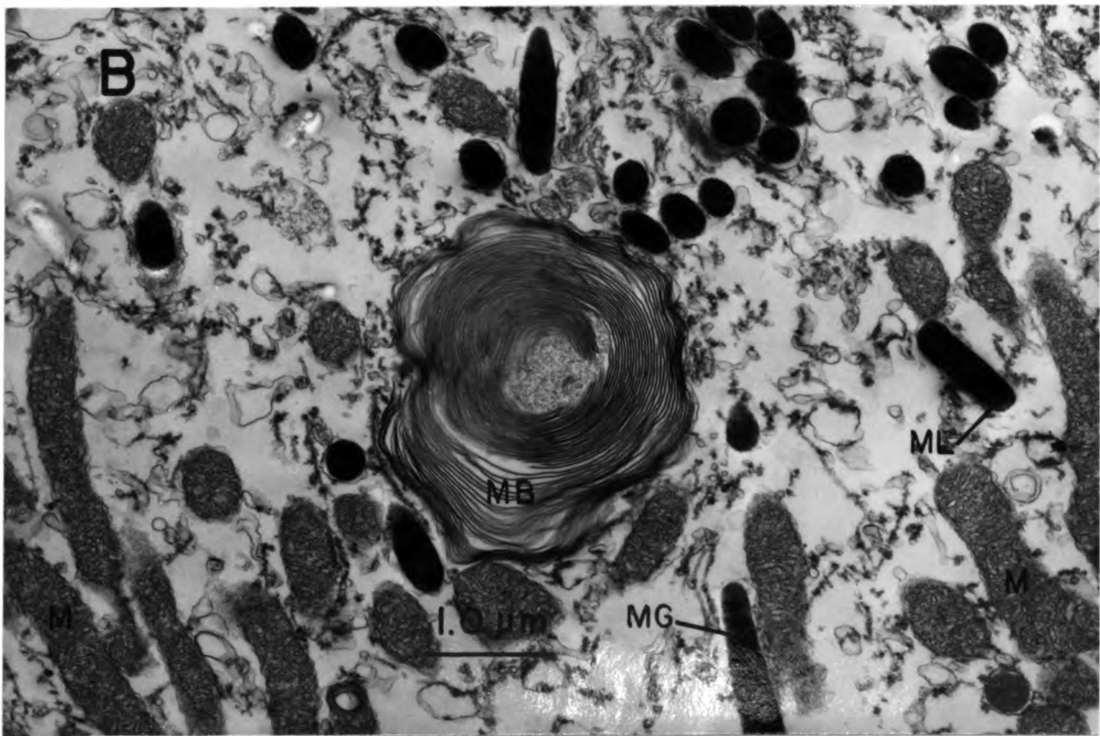
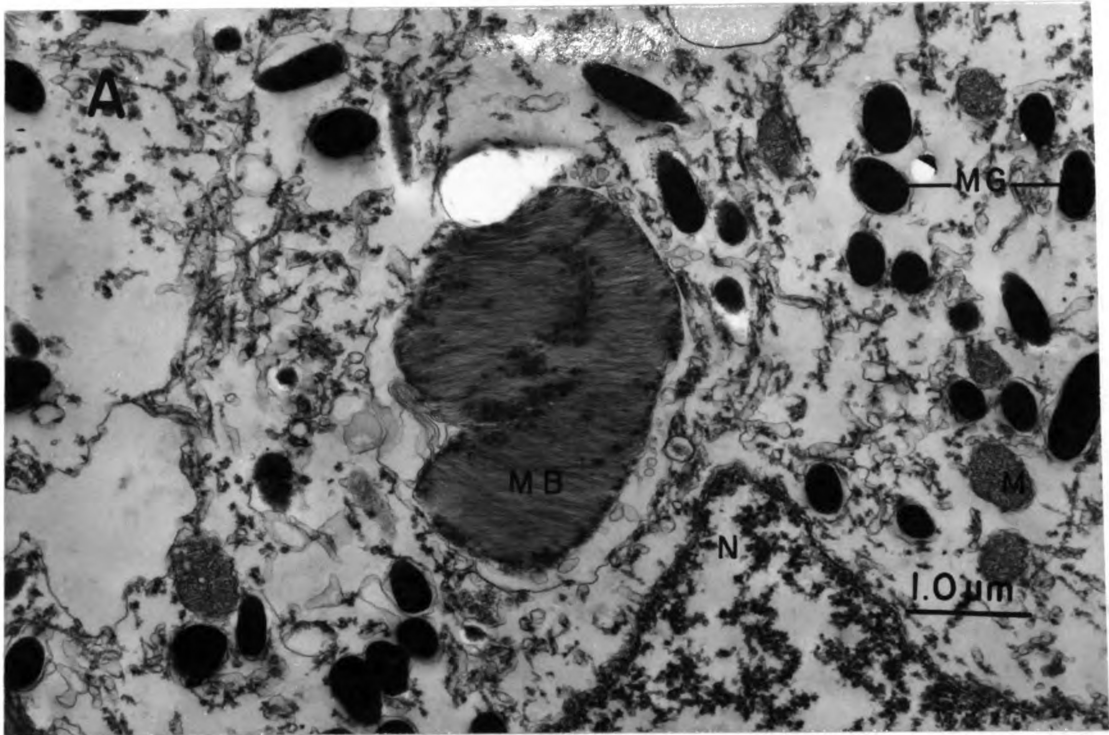


FIGURE 28

FIGURE 29. --Photoreceptor outer segment (20,755X).

The receptor cell outer segment has a very characteristic ultrastructure. The main feature is a highly folded membrane which gives the appearance of stacked discs. The photoreceptor pigments must be membrane bound, and this structure illustrates an adaptation to accommodate as much pigment as possible within the space provided. In the light-adapted state, the pigment epithelium stretches arm-like extensions containing melanin granules normal to the surface of the retina up between the receptor cells. These extensions act as screening pigments during times of abundant illumination. This serves to increase image resolution in the visual process. Such an appendage is seen here running along side this section of receptor cell outer segment. Note the similarity between the membranes here and those in the myeloid bodies of Figure 28.



FIGURE 29

FIGURE 30.--Choroidal rete mirabile carbonic anhydrase stain.

Here, the choroid rete is seen in cross-section to display an intense staining reaction (A) which is totally eliminated by $10^{-5}M$ acetazolamide inhibition (B). No reaction was ever seen in any of the inhibited tissues, whereas any unstained areas of tissue in the uninhibited treatments were believed to have dipped beneath the surface of the incubation medium which was known to eliminate the stain. Thus, it had been believed that the entire choroid rete possessed a high degree of carbonic anhydrase activity. From these light micrographs, however, no localization of the stain to either afferent or efferent vessel type could be made. (A--145X; B--295X).

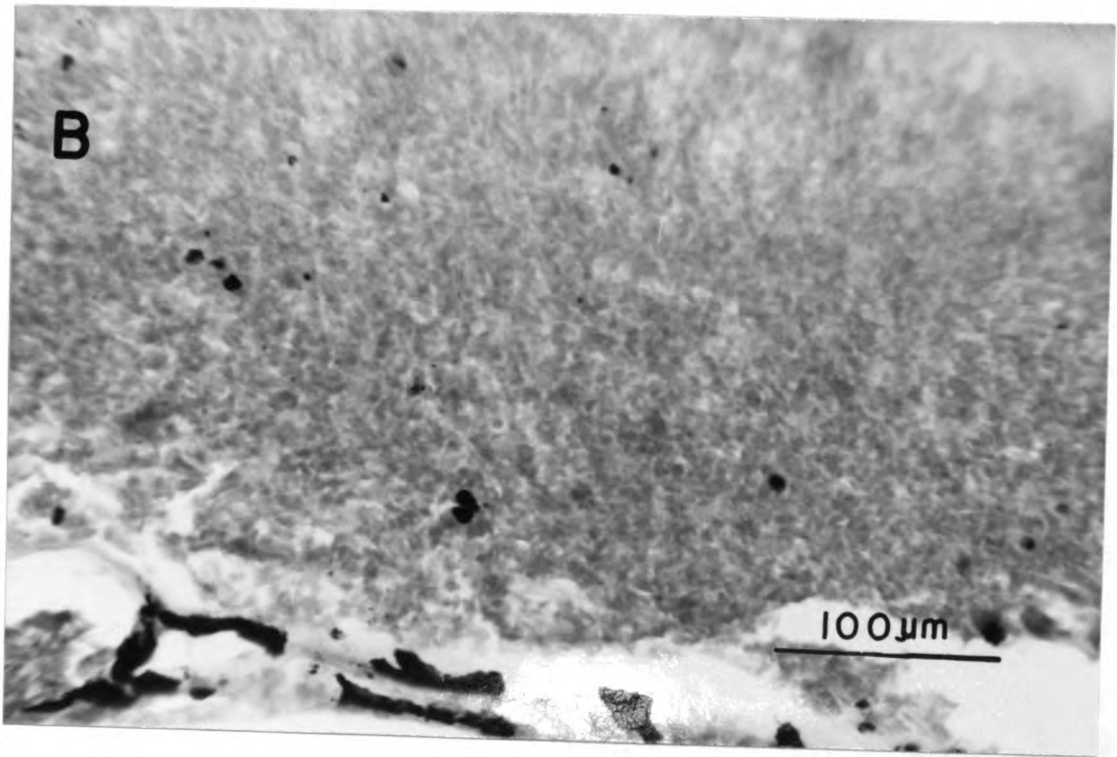
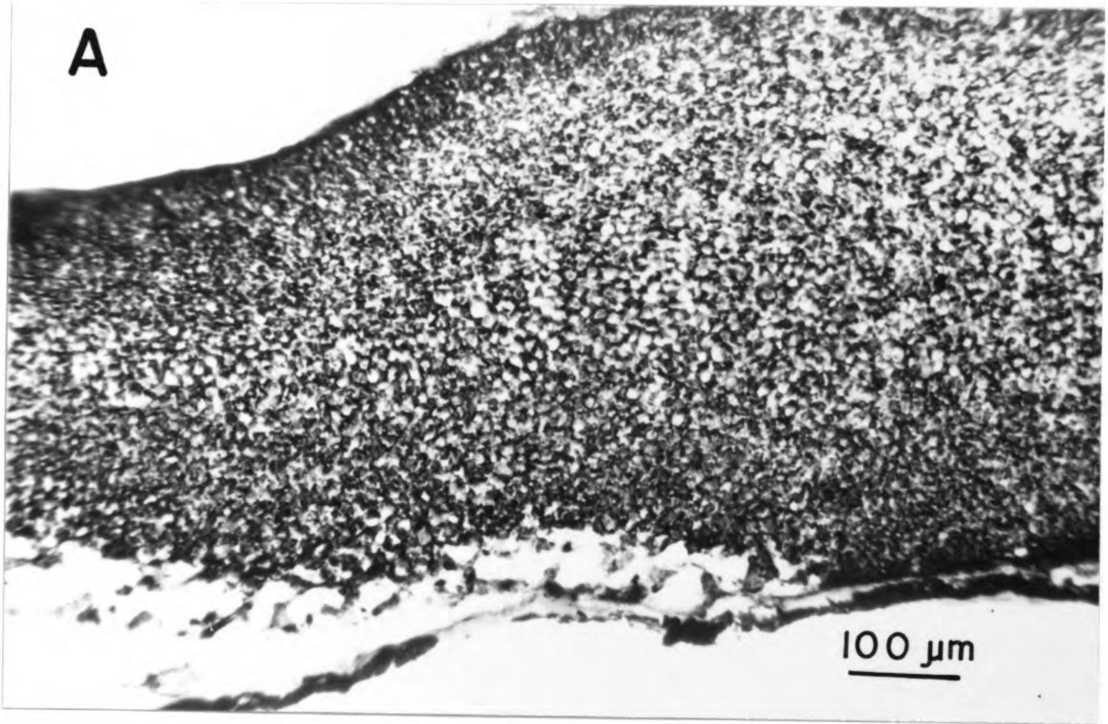


FIGURE 30

FIGURE 31.--Choroid rete mirabile carbonic anhydrase stain (295X).

At higher magnification, the choroid rete is again seen to be intensely active (A). Sodium acetazolamide completely inhibits the staining reaction (B). No conclusions may be reached with regard to the localization of activity to any one particular site at this degree of resolution. (A--295X; B--295X).

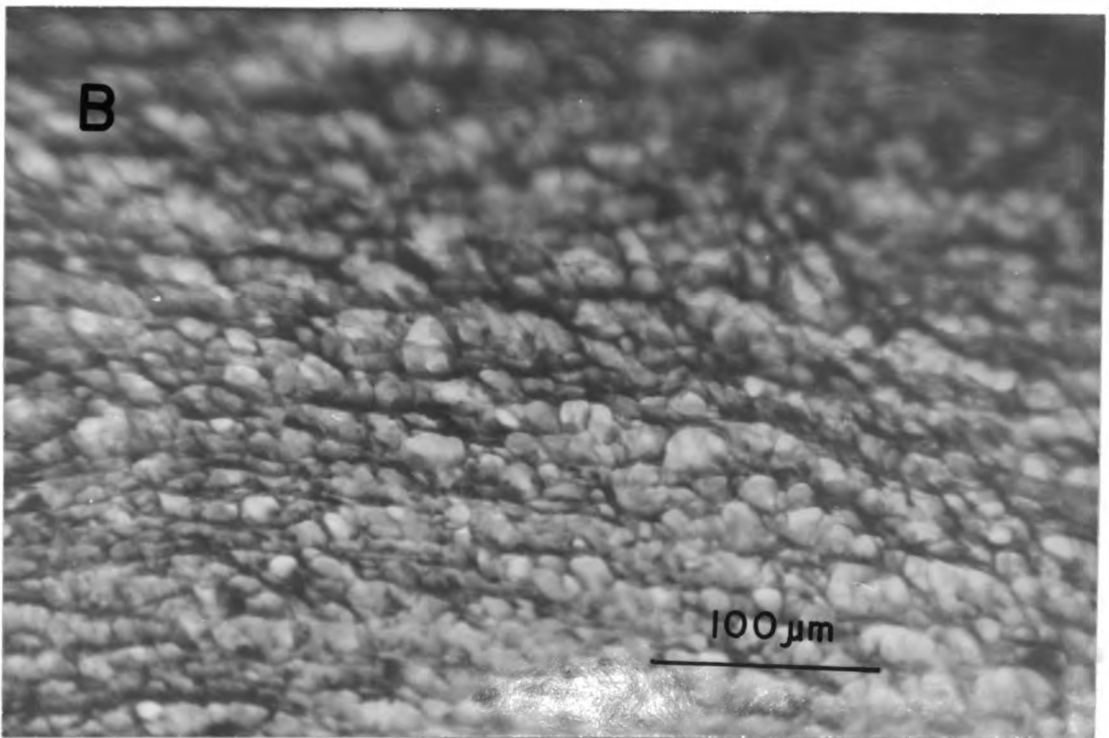
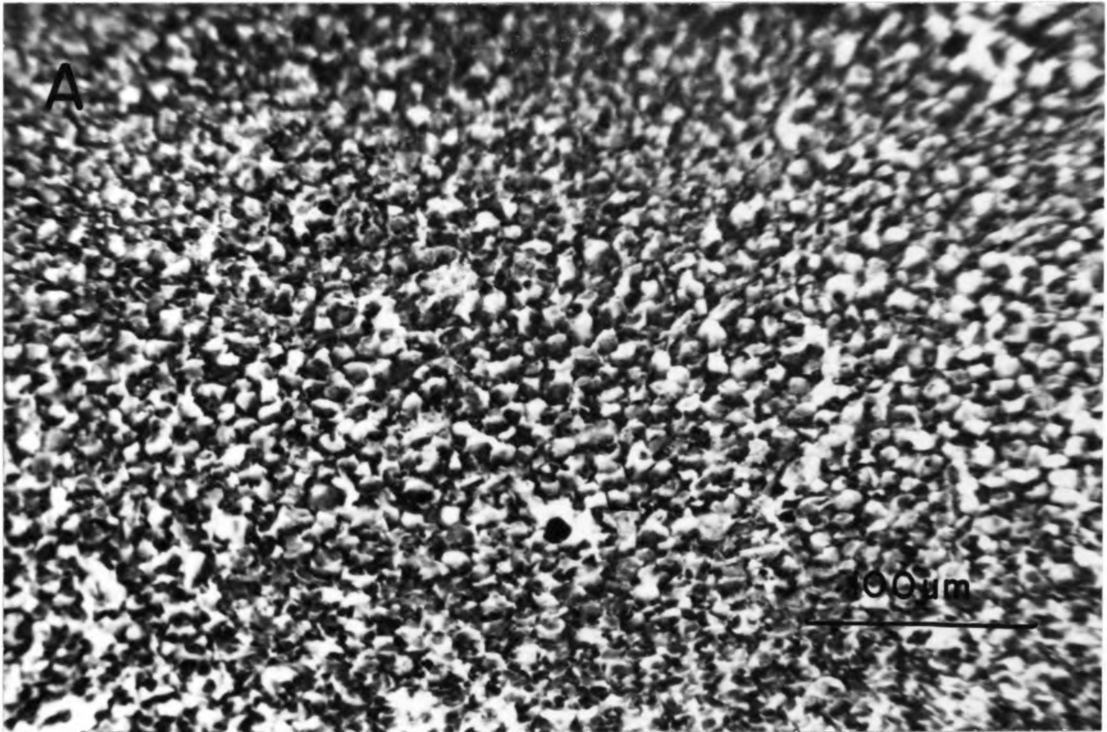


FIGURE 31

FIGURE 32.--Peripheral region of the choroidal rete stained for carbonic anhydrase (145X).

The peripheral end of the rete is notable by the presence of black melanin pigments within the stroma surrounding the collection and distribution vessels. This feature is seen in the acetazolamide inhibited preparation (B). No activity is seen here, even in the erythrocytes which fill the lumen of one of the vessels (arrow). Inhibition is complete. In the uninhibited tissue (A), carbonic anhydrase stain is seen to be intense in the retial vessels and may extend into some of the distribution and collection vessels (arrows). Note that in the inhibited tissues, the pigment is never seen to surround the vessels entirely. (A--145X; B--145X).

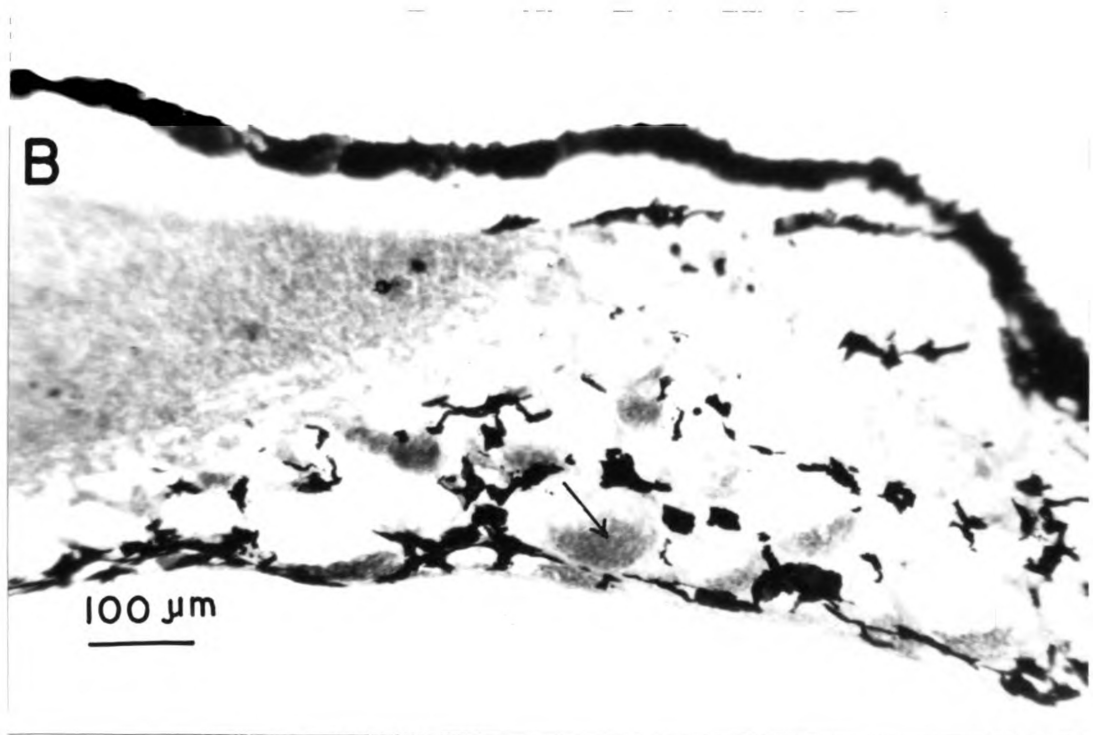
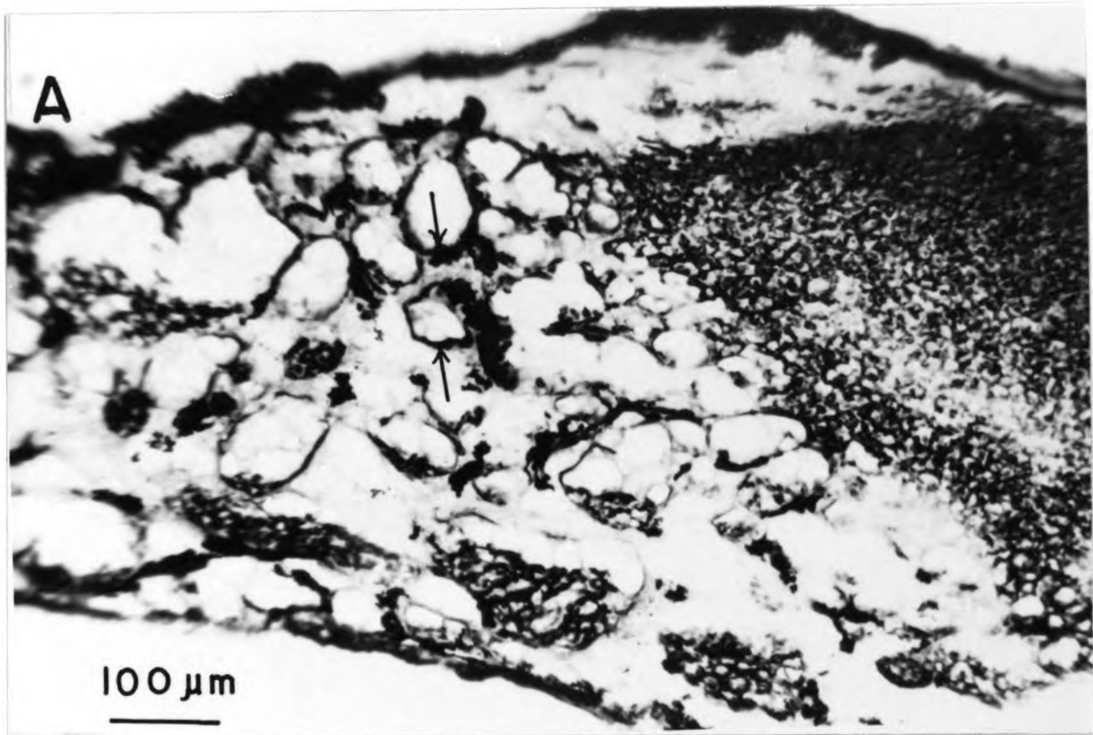


FIGURE 32

FIGURE 33.--Carbonic anhydrase activity within peripheral collection and distribution vessels (295X).

As was seen in the previous micrograph (Figure 32), carbonic anhydrase activity is seen to extend at least partly into the peripheral vessels. Micrograph A displays uninhibited tissue, and the tissue in B is acetazolamide treated. The region displayed in both micrographs is in very close proximity to the rete. The section of tissue in A is relatively thick, and the vessel in the center is seen to be lined with activity. This vessel measures approximately 70 μm in diameter and is definitely beyond retial vessel dimensions. (A--295X; B--295X).

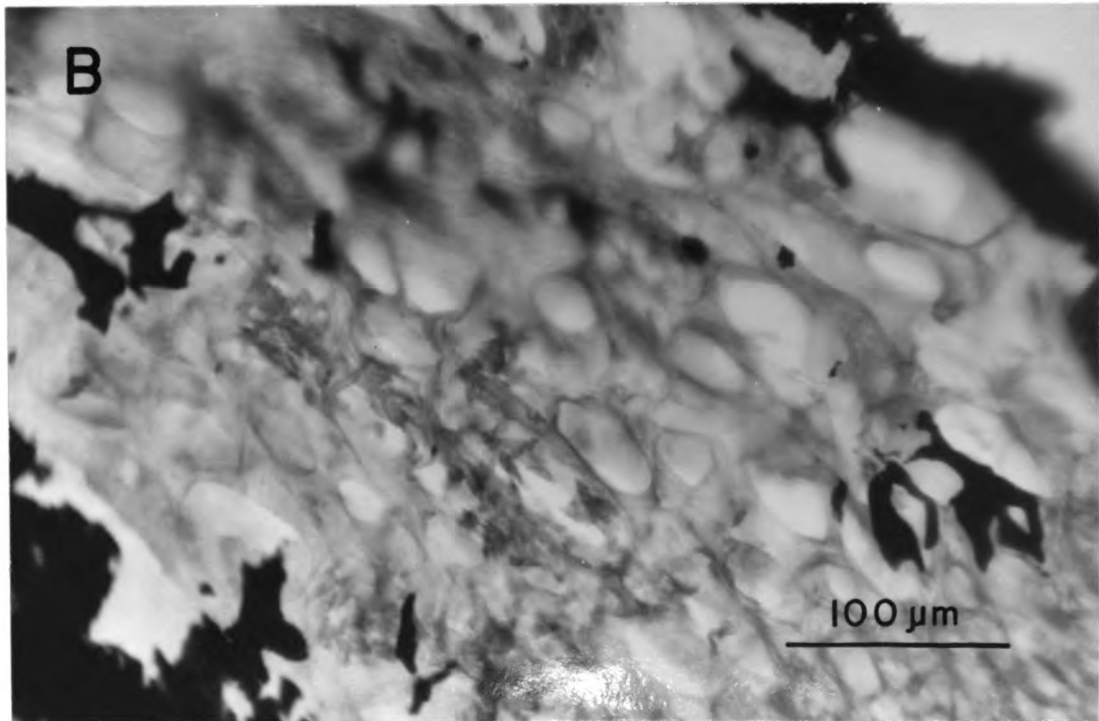
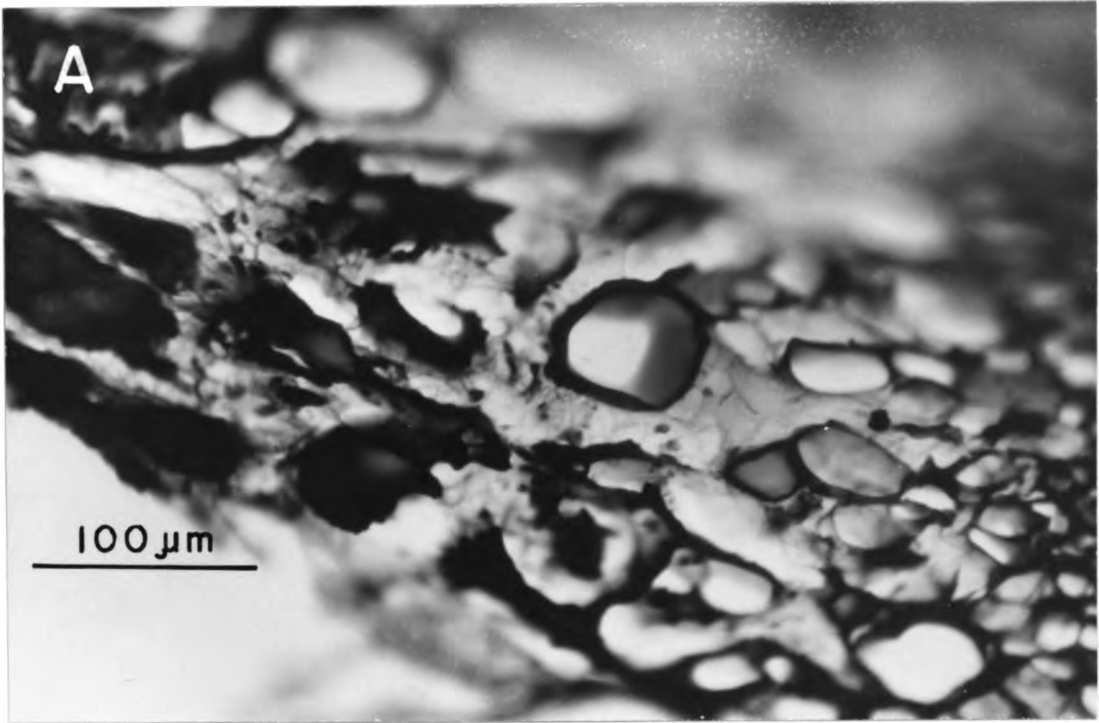


FIGURE 33

FIGURE 34.--Polarization of carbonic anhydrase activity within the choroidal rete vessels (65X).

In tangential section it is seen that there is a definite polarization of carbonic anhydrase activity along the length of the rete. In this section it appears that there is no activity at the central side (i.e., the region of the arterial manifold and venous sinusoid). At approximately one third of the distance along the rete, carbonic anhydrase activity intensifies and continues until reaching the distribution and collection vessels at the peripheral side. This apparent polarization is not due to the central side of the retial tissue having dipped below the surface of the incubation medium which stops the reaction. This is evidenced by the fact that the reaction occurs at a detectable uncatalyzed rate and is seen by a light diffuse stain in the vessels of the central side. A portion of this tissue had, however, folded under the medium and did not show even this diffuse stain (double headed arrows). Finally, it is important to note that this polarization was seen consistently throughout the tissues observed.

AM-----Arterial manifold
VS-----Venous sinusoid

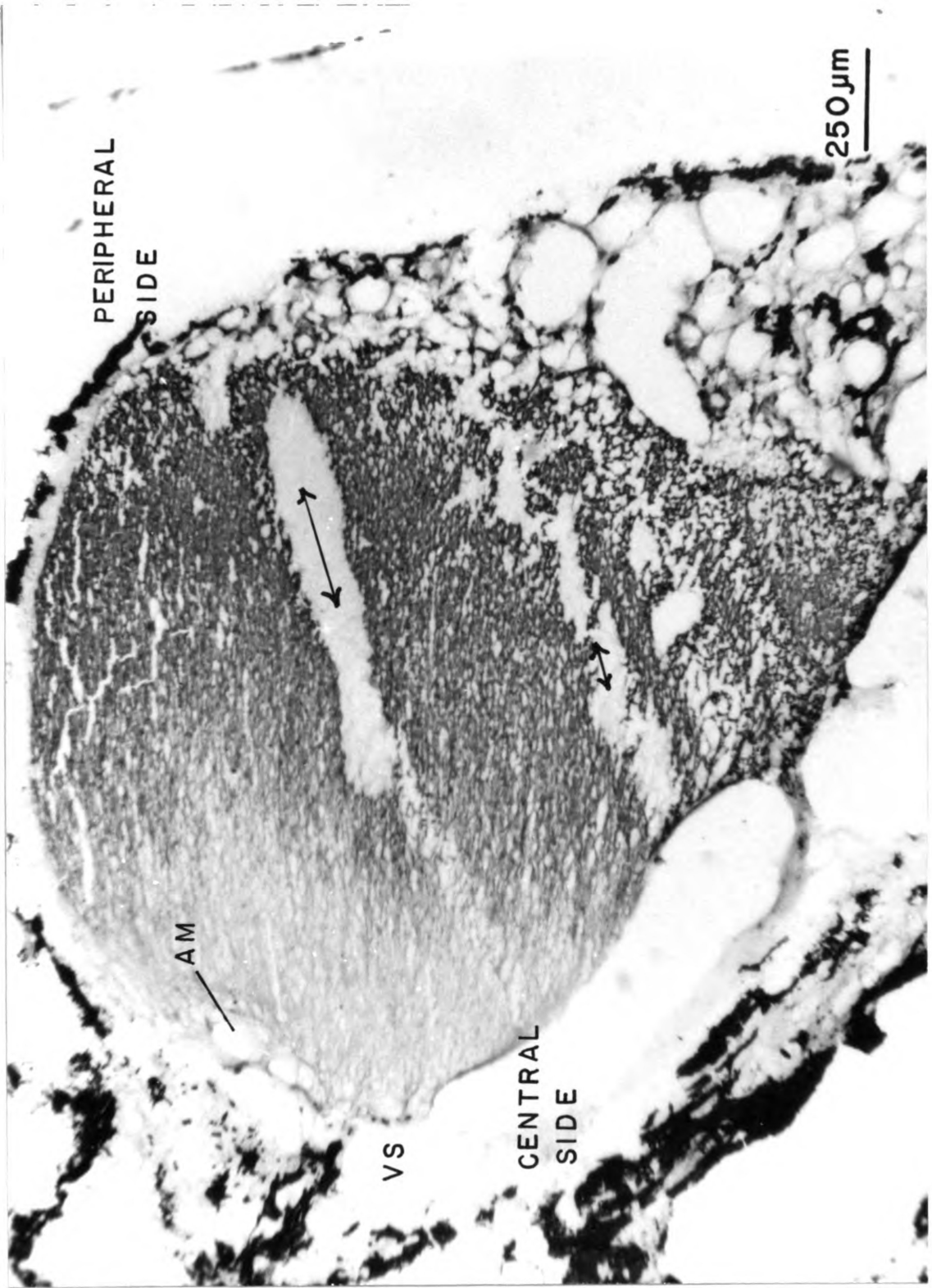


FIGURE 34

FIGURE 35.--General appearance of carbonic anhydrase stained tissues under the electron microscope (25,625X).

Due to the tissue preparatory techniques, the appearance of the ultra-structure of tissues fixed in glutaraldehyde and postfixed in osmium tetroxide (Figures 13-21, 23-29) is quite different from that of the carbonic anhydrase preparations. It is not possible to use osmium tetroxide fixation after the staining procedure due to the fact that the cobalt precipitate has been found to be soluble in this fixative (Rosen, 1974). Lipids are not normally fixed by glutaraldehyde, but they are by osmium tetroxide. As a result, lipids will be extracted during the dehydration process. This means that all membranes will have been extracted and only clear lines or spaces will be seen in the positions that the membranes once occupied. Another point to note is that the carbonic anhydrase stain is said to yield an artifactual nuclear stain which will be evident in many of the micrographs. The cobalt salt should be a fine electron-dense black precipitate (enclosed area). The micrograph here presents a region of retial vascular tissue which serves to illustrate these features.

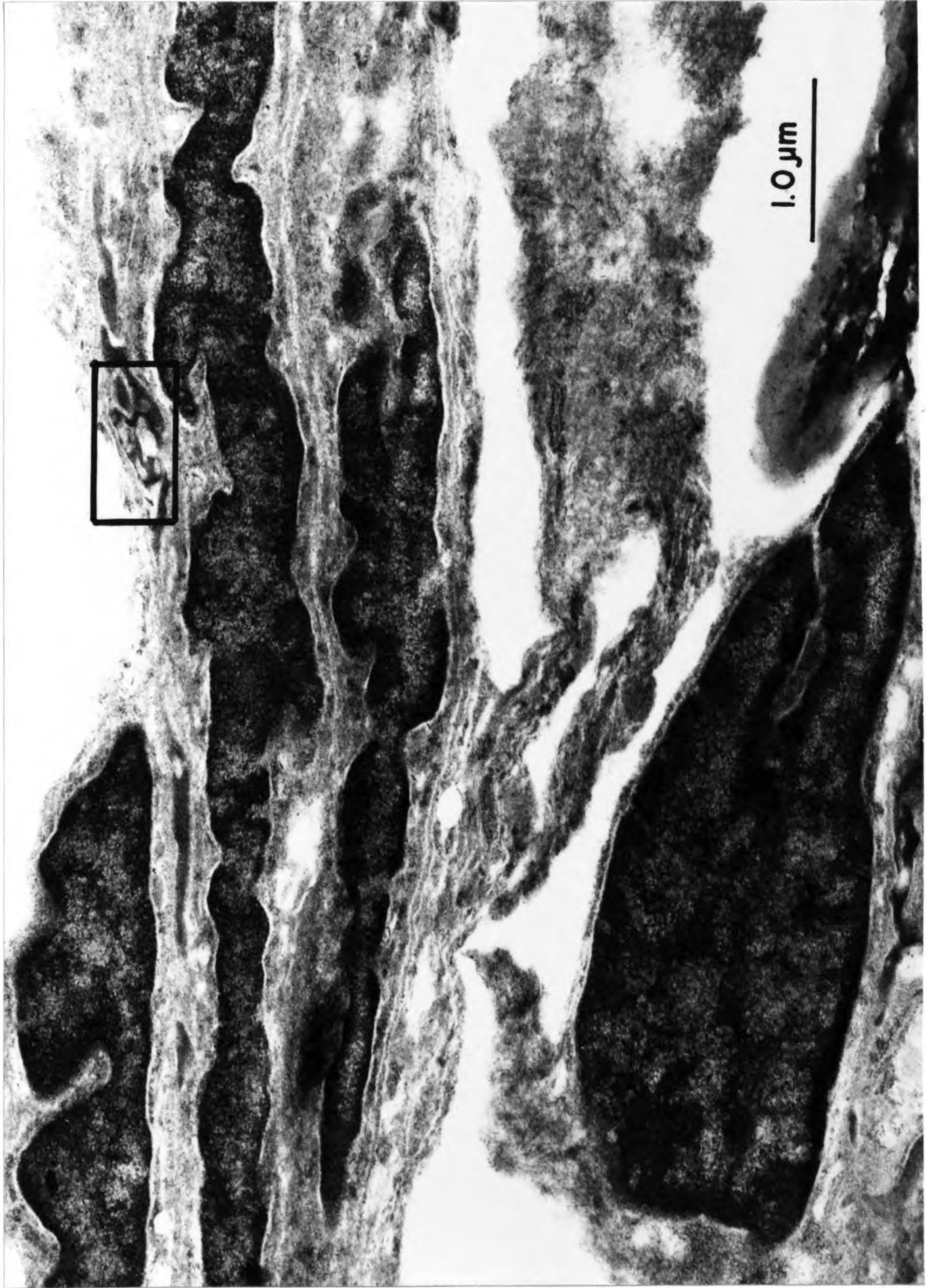


FIGURE 35

FIGURE 36.--Carbonic anhydrase activity within the choroidal rete endothelial cells (66,250X).

- A. Here, the uninhibited carbonic anhydrase reaction has produced dense staining throughout most of the endothelial cell cytoplasm. It is believed that three separate endothelial cells are seen here separated by a distinct interstitial space (double-headed arrows). Numerous tubules, probably representing endoplasmic reticulum (ER) are seen running through the cytoplasm. It appears in places that these tubules have precipitate within them, such that a single tubule appears as two white lines separated by a dense black line. (66,250X).
- B. The tissue has been incubated in medium containing $10^{-5}M$ sodium acetazolamide in order to inhibit the deposition of carbonic anhydrase-catalyzed reaction product. The reaction proceeds at a significant uncatalyzed rate, however, and yields a less dense, ubiquitous background precipitate. The small needle-like crystalline structures seen in this micrograph are dirt of unknown origin. (66,250X).

Arrows--Interstitial space
ER-----Endoplasmic reticulum

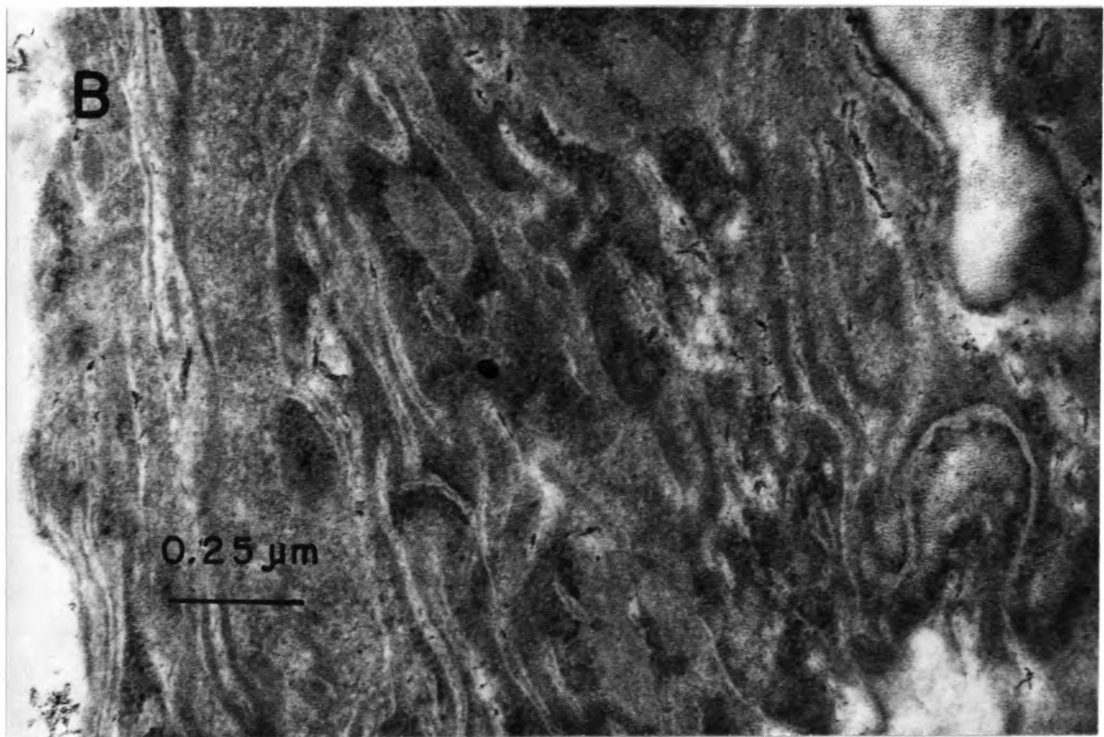
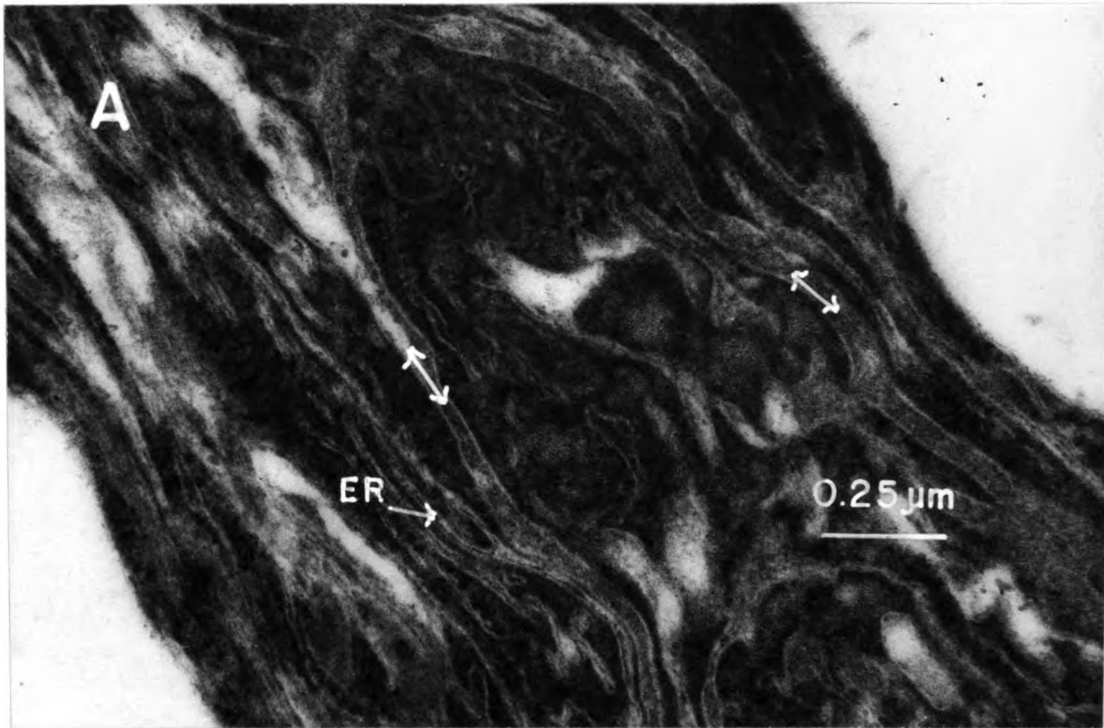


FIGURE 36

FIGURE 37.--Choroid rete endothelial cell carbonic anhydrase activity as compared with erythrocyte carbonic anhydrase activity (102,500X).

At a high magnification, a red blood cell (RBC) with its nucleus (RBCN) is seen lying adjacent to an endothelial cell of the choroid rete. Here the activity of the erythrocyte carbonic anhydrase is seen to be extremely intense as would be expected. The activity within the endothelial cytoplasm seems to be localized in bands not associated with any recognizable subcellular structure, but within the cell cytoplasm itself. An endothelial cell nucleus (EN) is also seen.

EN-----Endothelial cell nucleus
 RBC-----Erythrocyte
 RBCN-----Erythrocyte nucleus



FIGURE 37

FIGURE 38.--Banding pattern of carbonic anhydrase activity within the choroid rete endothelial cell (102,500X).

As was noted in the enclosed area of Figure 35 and in Figure 37, there are regions of dense staining within the endothelial cytoplasm which are not apparently associated with any particular subcellular component, yet are not homogeneously distributed throughout the cytoplasm.



FIGURE 38

FIGURE 39.--A differential carbonic anhydrase activity in afferent versus efferent retial vessels (102,500X).

Previous micrographs had not revealed any distinction between afferent and efferent vessel carbonic anhydrase activity, and indeed, it was not evident from the features of the cells which class of vessels was being observed. This micrograph depicts the junction point of the walls of three vessels separated by a thick, Y-shaped, homogeneous interstitial space. The difference in degree of activity is apparent. This would tend to indicate that the functional roles of afferent versus efferent endothelia may be different. The presence of a basement membrane is the single most characteristic feature of afferent vessels, aside from luminal diameters which were not determinable due to the condition of the tissue. Unfortunately, no basement membrane is seen to follow the cell membranes in the interstitial space in any of the vessels here. Thus, no conclusion may here be reached regarding the specific class of vessel containing the heavy activity on this basis. As discussed in the text, however, there is reason to believe that the more densely stained endothelium is that of an afferent vessel.

IS-----Interstitialium
L-----Lumen
M-----Mitochondrion
N-----Nucleus

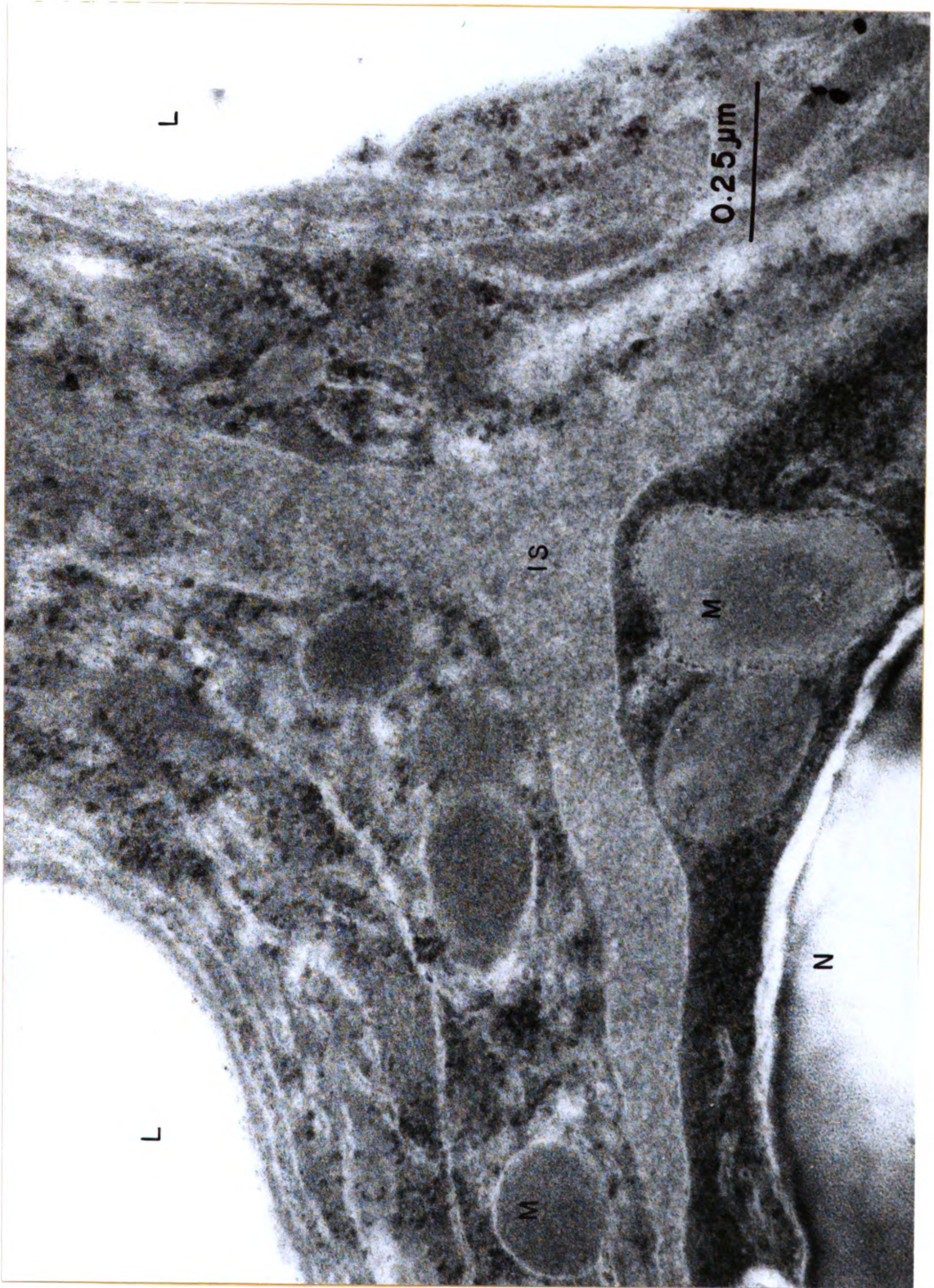


FIGURE 39

FIGURE 40.--The "pseudobranch-type" or acidophilic cell (9,995X).

The pseudobranchial vessels are associated with a large number of very distinct acidophilic or pseudobranch-type cells. These are characterized by having a tightly packed array of mitochondria in association with an extensive network of smooth endoplasmic reticulum originating in the vicinity of the mitochondria and emptying on the basement membrane adjacent to the capillary endothelium. Note that the basement membrane apparently does not surround the pseudobranch cell. It is not seen adjacent to the apical margin. The pseudobranch is known to possess a very large amount of carbonic anhydrase of unknown significance. Although the pseudobranch-type cell appears similar to a chloride cell, they are now believed to be distinctly different cell types. The endothelial cells forming the capillary vessel walls very much resemble the pillar cells seen in the secondary lamellae of the gill filaments. Note that the attenuated portions of the endothelia are non-fenestrated. As a final point of interest, one of the pseudobranch-type cells displays an apparently extreme area of intracellular vacuole formation (NV). A similar condition has been noted in pathologically hypertrophied pseudobranchs in the lake trout, Salvelinus namaycush (Hoffert, Fairbanks, and Fromm, 1971).

A-----Apical margin
 L-----Capillary lumen
 M-----Mitochondrial network
 N-----Nucleus
 NV-----Necrotic vacuole
 P-----Pillar cell-like endothelium
 T-----Smooth endoplasmic reticulum network

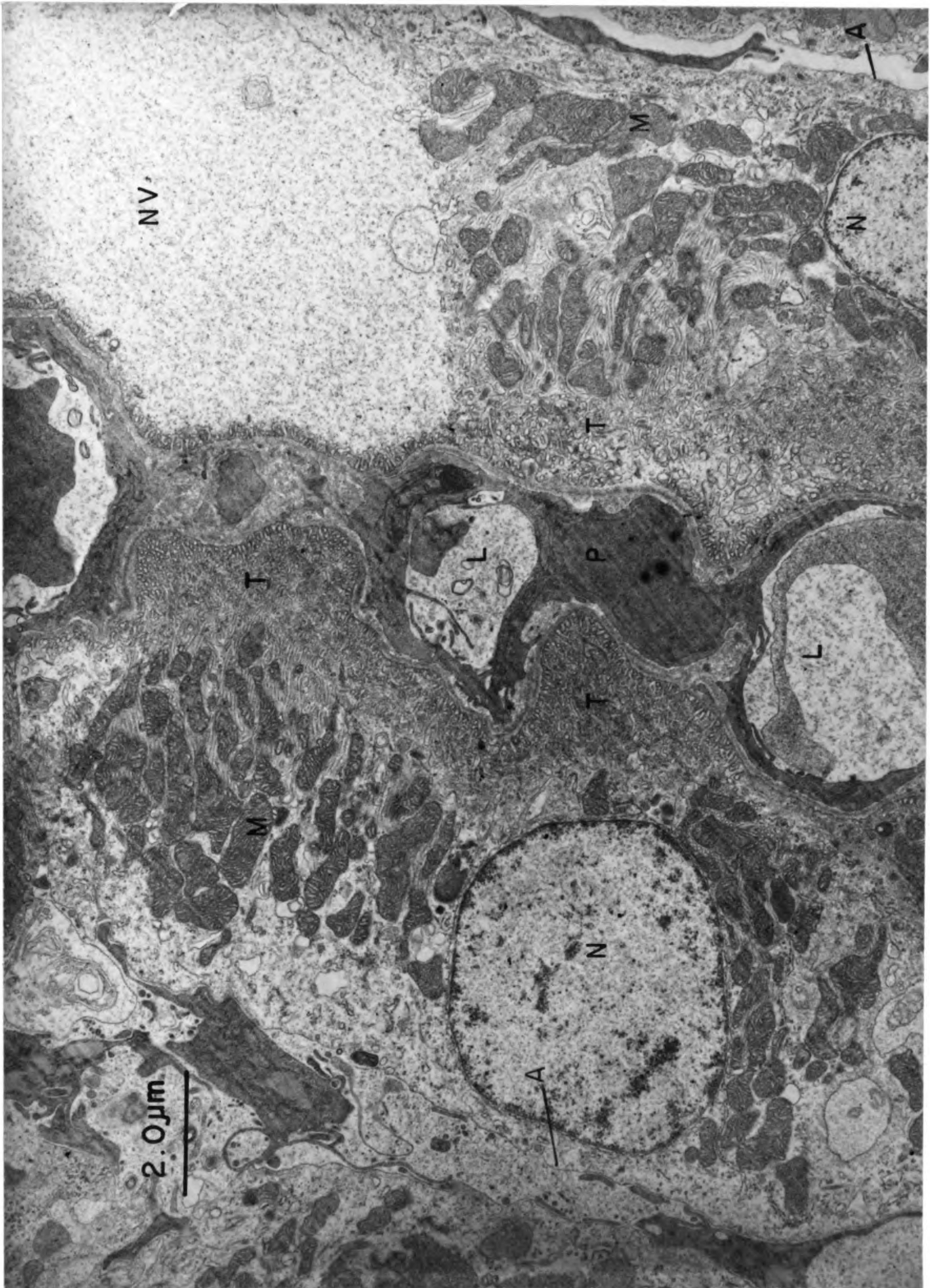


FIGURE 40

FIGURE 41.--The mitochondrial-smooth endoplasmic reticulum network of the pseudobranch-type cell (25,625X).

The mitochondria of the pseudobranch-type cell are seen to be densely packed in a roughly parallel manner perpendicular to the basal border. Between the mitochondria, smooth endoplasmic reticulum are seen to originate and lead down into a complex tubular network.

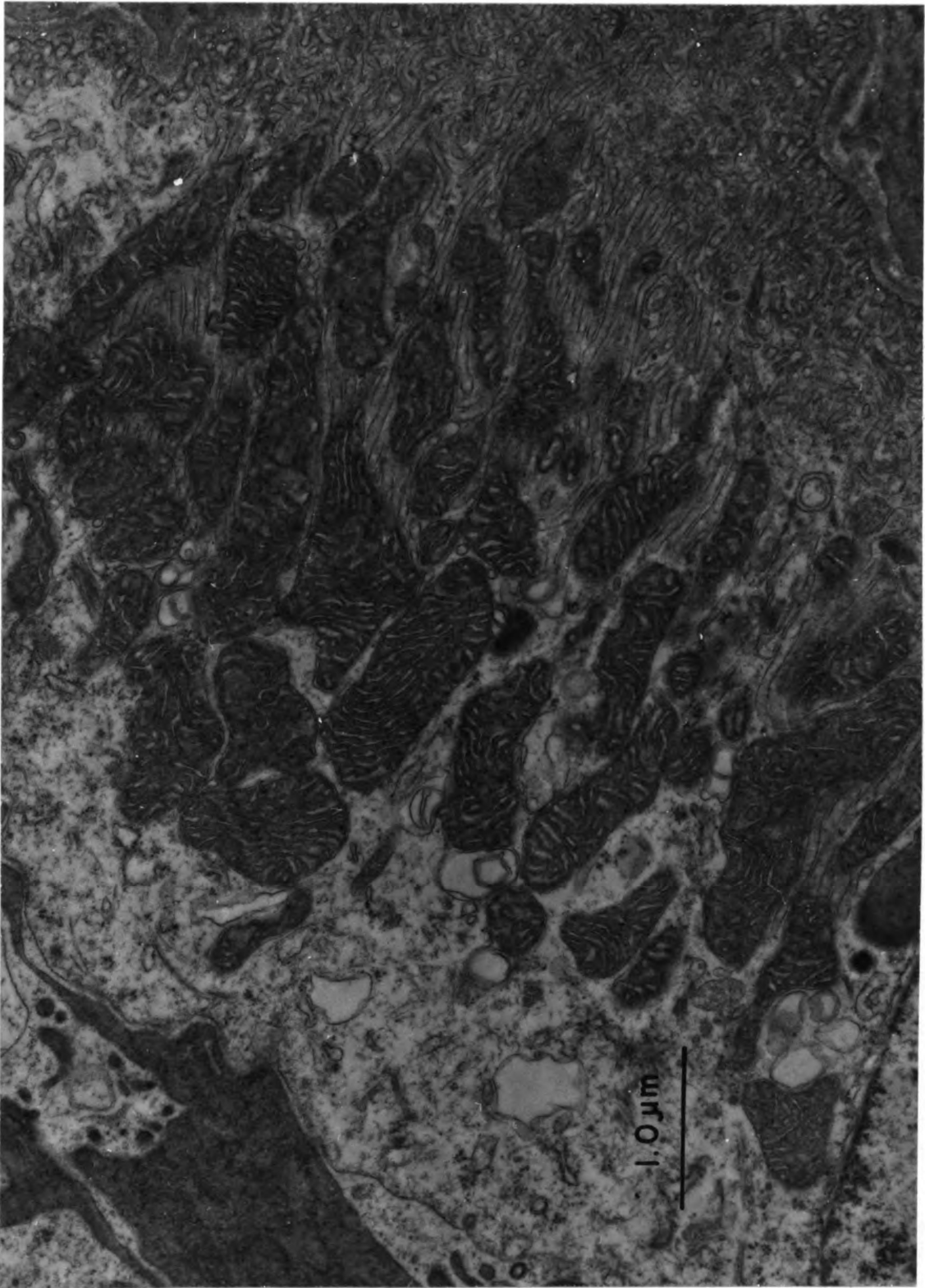


FIGURE 41

FIGURE 42.---Basal border of the pseudobranch-type cell (82,000X).

At the basal border of the pseudobranch-type cell, the tubular network is seen to empty directly into the interstitial space. This border of the pseudobranch-type cell is bounded by a distinct basement membrane. The adjacent endothelial cell lacks any basement membranes.

BM-----Basement membrane
E-----Endothelium
IS-----Interstitial space
L-----Capillary lumen
M-----Mitochondrion
T-----Tubular network

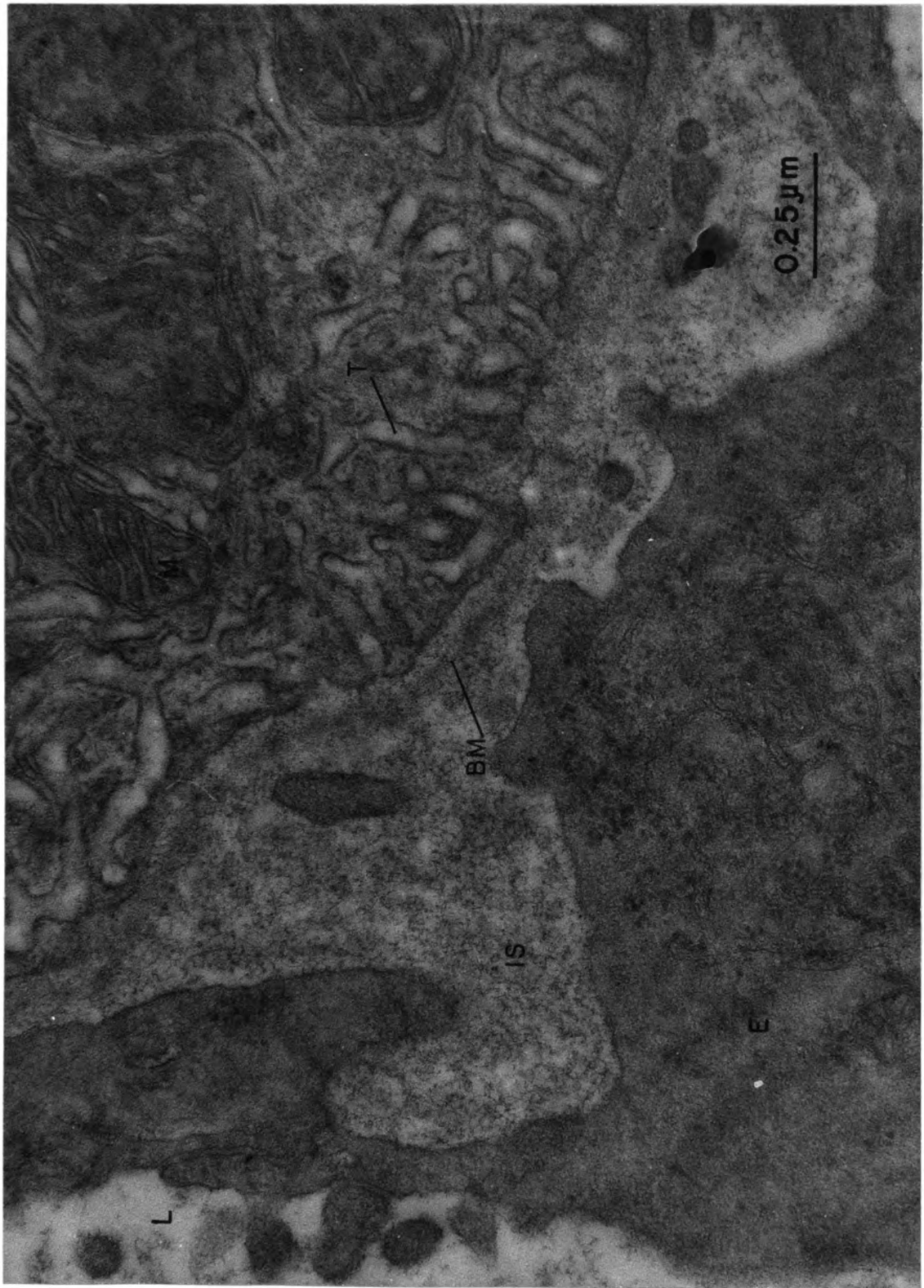


FIGURE 42

FIGURE 43. --Pseudobranch-type cell carbonic anhydrase histochemistry (32,030X).

The nature of the carbonic anhydrase reaction product is not certain in this micrograph. It may be a very fine-grained stain as seen in the choroidal sections, or it may consist of a more dense grainy precipitate seen to be dispersed widely throughout the cytoplasm, but especially clustered closely to the nucleus (arrows). The nucleus has been reported to artifactually stain in this histochemical procedure. Whatever the reaction product, it is apparent that no conclusions may be drawn regarding any carbonic anhydrase secretory activity by this cell.

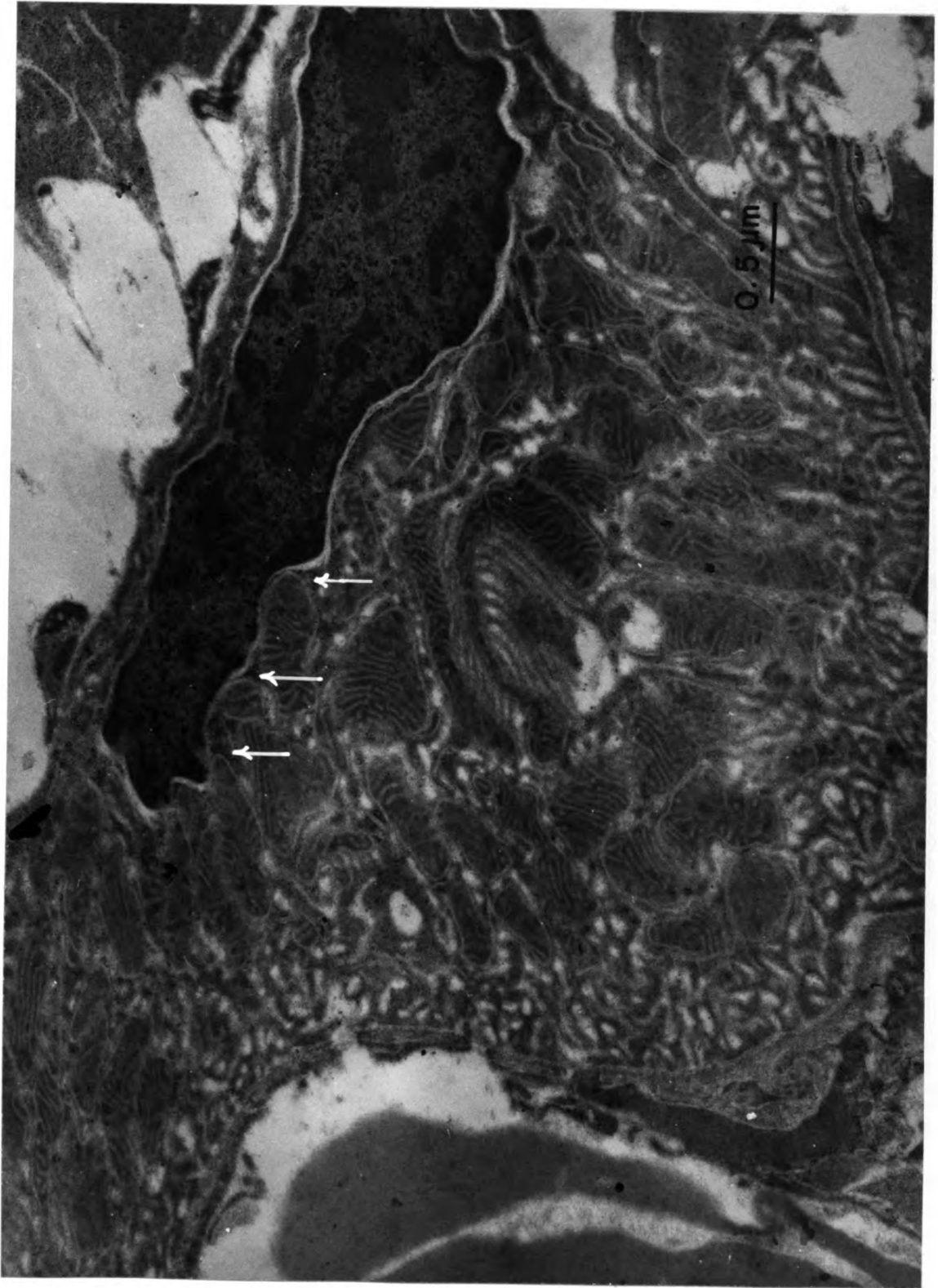


FIGURE 43

FIGURE 44.--Carbonic anhydrase stained pseudobranch-type cell basal border (102,500X).

In a carbonic anhydrase stained section, it is apparent that the tubular network does not show carbonic anhydrase activity.

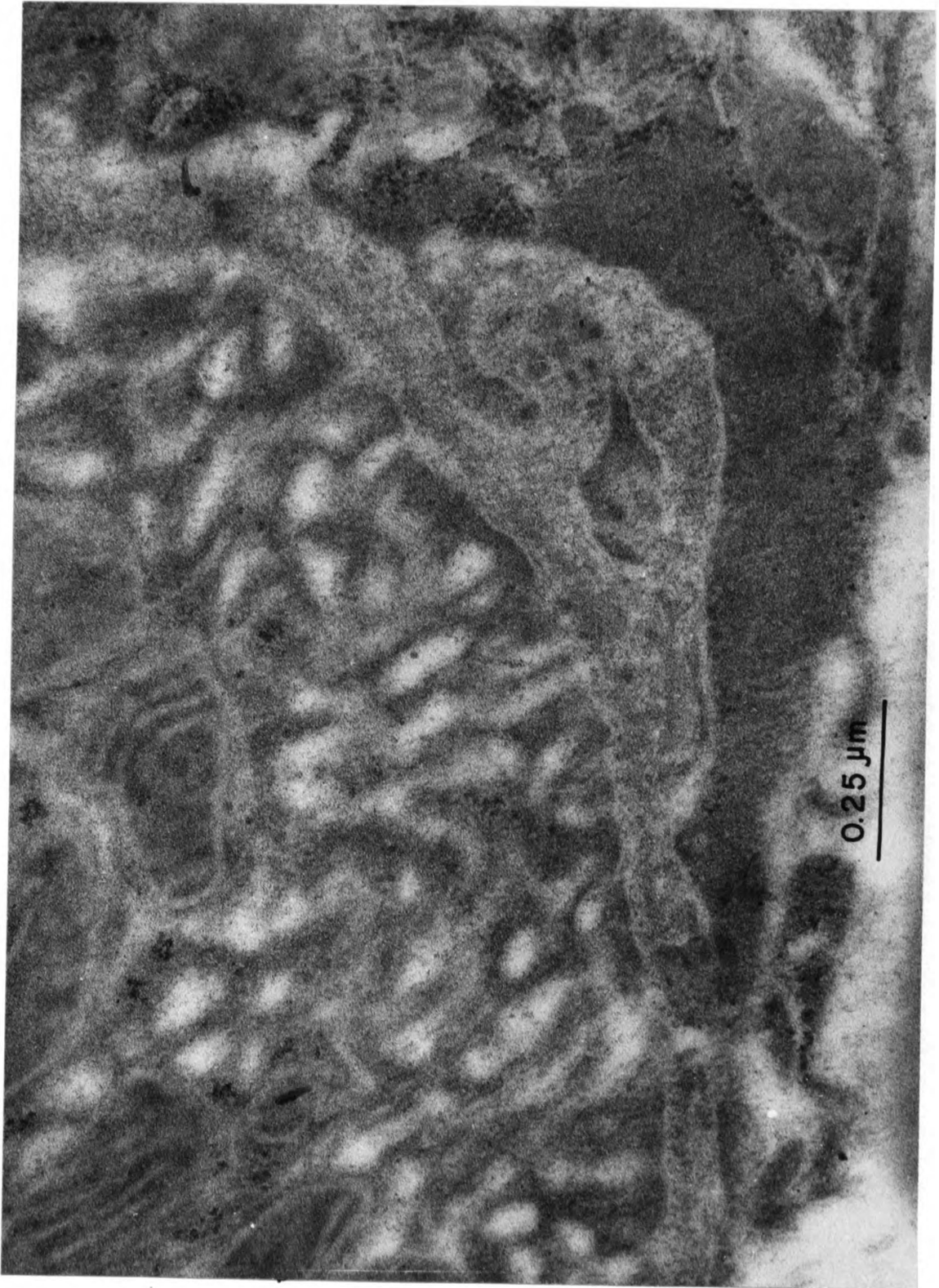


FIGURE 44

FIGURE 45.--"Titres flamboyants final": Carbonic anhydrase stained pseudobranch-type cell mitochondrial-endoplasmic reticulum network (66,250X).

Micrograph A was from a carbonic anhydrase stained tissue, whereas micrograph B represents an acetazolamide-inhibited tissue. Both tissues seen are identical except for the darkness of the background. Also, in the uninhibited section, there are small granular particles which have been suspected of being the true carbonic anhydrase reaction product. The globular black densities in the inhibited micrograph are dirt which had condensed on the section.

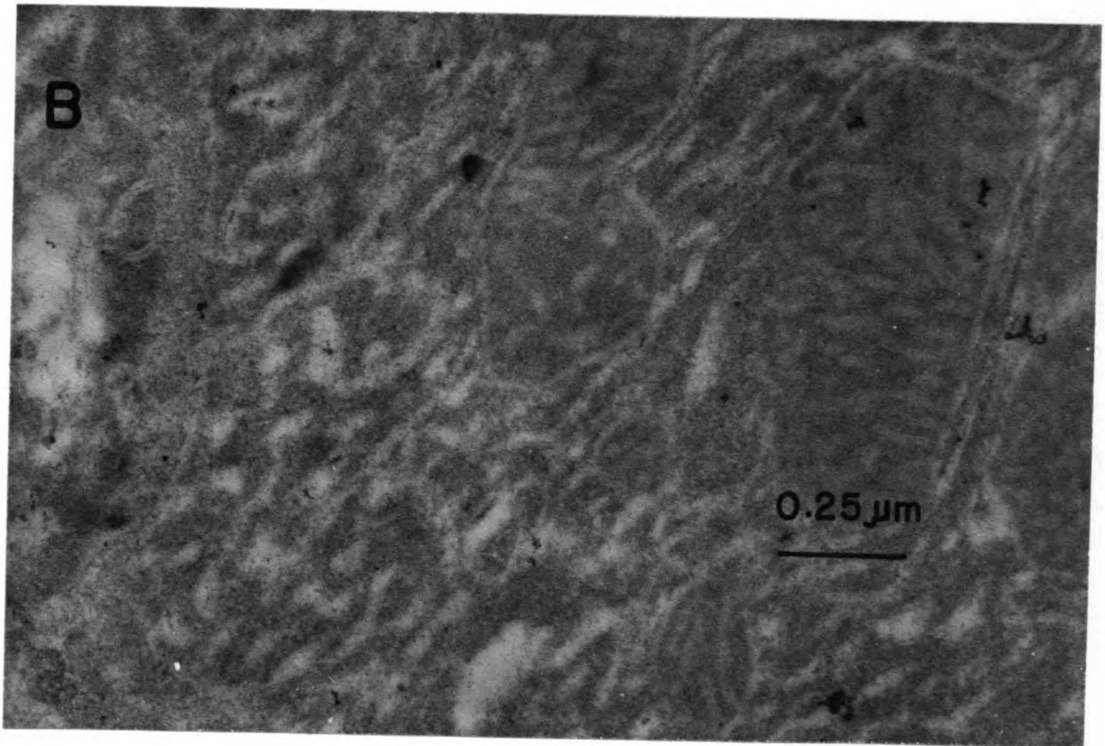
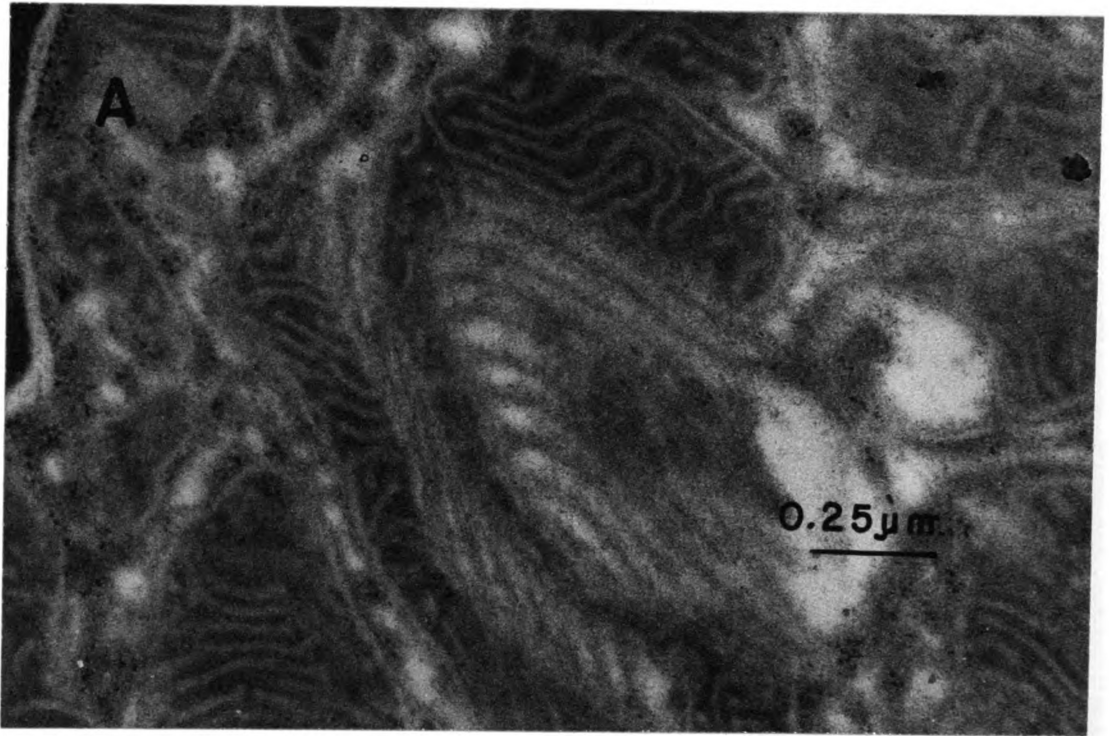


FIGURE 45

MICHIGAN STATE UNIVERSITY LIBRARIES



3 1293 03071 2412